1988

Major and trace element characterization and correlation of the Sentinel Butte Ash/Bentonite (Paleocene), McKenzie County, North Dakota

Richard A. Larsen
University of North Dakota

MAJOR AND TRACE ELEMENT CHARACTERIZATION AND CORRELATION OF THE SENTINEL BUTTE ASH/BENTONITE (PALEOCENE), McKENZIE COUNTY NORTH DAKOTA

by

Richard A. Larsen

Bachelor of Science, University of North Dakota, 1983

A Thesis

Submitted to the Graduate Faculty

of the

University of North Dakota

in partial fulfillment of the requirements

for the degree of

Master of Science

Grand Forks, North Dakota

December

1988

This thesis submitted by Richard A. Larsen in partial fulfillment of the requirements for the degree of Master of Science from the University of North Dakota has been read by the Faculty Advisory Committee under whom the work has been done, and is hearby approved.

_____

(Chairman)

_____

_____

This thesis meets the standards for appearance and conforms to the style and format requirements of the Graduate School of the University of North Dakota, and is hereby approved.

_____

Dean of the Graduate School

Permission

Title Major and Trace Element Characterization and Correlation of the Sentinel Butte Ash/Bentonite (Paleocene), McKenzie County North Dakota

Department Geology

Degree Master of Science

In presenting this thesis in partial fulfillment of the requirements for a graduate degree from the University of North Dakota, I agree that the library of this University shall make it freely available for inspection. I further agree that permission for extensive copying for scholarly purposes may be granted by the professor who supervised my thesis work or, in his absence, by the Dean of the Graduate School. It is understood that any copying or publication or other use of this thesis or part thereof for financial gain shall not be allowed without my written permission. It is also understood that due recognition shall be given to me and the University of North Dakota in any scholarly use which may be made of any material in my thesis.

Signature _____

Date _____

TABLE OF CONTENTS

LIST OF ILLUSTRATIONS

Figure

LIST OF TABLES

Table

ACKNOWLEDGMENTS

I would like to thank my advisory committee chairman, Dr. R. D. LeFever, for his advice and consultation. His expertise in statistical analysis was invaluable. Thanks is also extended to the rest of my advisory committee, Drs. Frank R. Karner, and Alan M. Cvancara, for their critical review of the manuscript.

A special thanks is extended to Dr. Nels Forsman for suggesting this project to me. His knowledge of volcanogenic sediments has been a great asset to this study. The laboratory assistance of Dr. R. J. Stevenson was greatly appreciated, as was his bantering, which took the "edge" off the unproductive days.

Gratitude is extended to the North Dakota Geological Survey for supplying a vehicle for summer field work. Dr. Greg McCarthy of the chemistry department, North Dakota State University, supplied a muffle furnace which greatly facilitated major element analysis. Thanks and appreciation are extended to them. The National Park Service, and especially the employees of the North Unit of Theodore Roosevelt National Park, are appreciated for allowing access and permission to collect samples within the park.

Finally, a very special thanks to Kelly, Erin, and Colin, whose love, understanding and patience, made this thesis possible and worthwhile.

to

Erin Rose and C.J.

ABSTRACT

The Sentinel Butte ash/bentonite has been used for stratigraphic correlation in and around the North Unit of Theodore Roosevelt National Park in western North Dakota primarily by tracing it along the escarpments of the Little Missouri River. The purpose of this study was to determine the geochemical fingerprint for the Sentinel Butte ash/bentonite, and use this fingerprint to assess the correlation value of this and other terrestrial bentonites. Mapping enlarged the known geographic distribution of this unit and provided an insight into its diagenetic history.

Samples from thirty randomly chosen sites and fifteen grab sites were used to evaluate the geologic and geographic variability of the Sentinel Butte ash/bentonite. Cluster and discriminant analysis were used to categorize and differentiate the upper and lower bentonites, and the ash, on the basis of their elemental concentrations. Factor analysis was used to determine which trace elements had the lowest variability associated with them, and to use those elements as a geochemical fingerprint.

The geographic and geological variability of the Sentinel Butte ash/bentonite can be attributed to leaching of the soluble elements during the glass to bentonite alteration, introduction of cations via ion-rich groundwater, and syndepositional and post-depositional contamination. The leached elements include Na_2O, K_2O, MnO, Ba, Pb, Rb, Sr, and Nb and are found in higher concentrations in the parent ash. A silica enriched zone at the top of the underlying unit also suggest that SiO_2 was leached from the parent ash during the alteration

process. Elements that were introduced into the ash/bentonite by ion-rich groundwater or as detrital contaminants include Fe_2O_3, MgO, TiO_2, Cr, and Cu. Aluminum concentration values also tend to be slightly higher in the bentonites compared to the ash. The upper bentonite exhibits higher concentrations of CaO and Zr, which is interpreted as post depositional contamination. Those elements that remained immobile during the alteration process include P_2O_5, Co, Y, Ga, Zn, and Ni.

The elements that were found to be useful for correlating the Sentinel Butte ash/bentonite and provided a geochemical fingerprint for this deposit include Fe_2O_3, TiO_2, Cu, Zn, Ga, Y, and Zr. Using these fingerprint elements samples collected outside of the random sampling area were correlated with the Sentinel Butte ash/bentonite. All but three of those samples were found to be correlative with the unknown ash/bentonite, expanding the known areal extent of the unit.

INTRODUCTION

General Statement

This study assesses the geochemical fingerprint of the terrestrial Sentinel Butte ash/bentonite in McKenzie County, North Dakota. Bentonites and volcanic ashes can be invaluable in the correlation of strata and in establishing the age equivalence of regionally separated geologic units. Some of the authigenic minerals found in volcanic ashes can also be useful in determining an absolute date for these units. Furthermore, dating isochronous beds can be helpful in establishing a time-stratigraphic framework and sedimentation rates for the surrounding strata. The purpose of this study is to evaluate the geochemical fingerprint of the Sentinel Butte ash/bentonite and assess whether terrestrially-formed bentonites and can be correlated over great distances. Differences in diagenesis and detrital input along the lateral extent of a tephra unit may alter the geochemical signature and make correlation difficult. These differences are more of a potential problem in the case of terrestrial bentonites than of marine tephra deposits. This study evaluates the use of geochemical fingerprints in correlating terrestrially-formed bentonites.

Utility of Terrestrial Bentonites for Correlation

The sandwiched nature of the Sentinel Butte ash/bentonite provides the opportunity to compare the geochemical signature of bentonites to that of the progenitor ash. In this way the geochemical variability

can be ascribed to processes that control the distribution of elements. Factors such as detrital contamination, specifically post-depositional contamination, varying degrees of alteration, cation exchange, and microenvironments which may concentrate a given cation, all affect the usefulness of a given geologic unit to be used effectively for correlation purposes. The uncertainty about detrital contamination and alteration effects does not obviate the use of composition as a correlation and stratigraphic tool, provided that the existing compositional variations can be documented. A large range of compositional variation may be caused by differences in detrital input or diagenesis. Establishing a narrow compositional range would suggest a lack of such differences along the course of a pyroclastic unit. Establishing a geochemical fingerprint for the Sentinel Butte ash would be beneficial, for correlation purposes although its geographic distribution is limited. The upper and lower bentonites have a larger geographic distribution, and are more useful for correlation.

General Geology and Geologic Setting

Sentinel Butte Formation

The term Sentinel Butte Group was introduced by Leonard (1908, pl. XII) for the lignite-bearing strata in the upper portion of the Fort Union Formation. He noticed a color change within the Upper Fort Union strata, and referred to the beds above this color change as the Upper Fort Union. Other workers have subsequently recognized this same color contact and the mappability of the Upper Fort Union strata (Royse,

1967b; Jacob, 1975). The current terminology applied to the Upper Fort Union strata, and favored by the North Dakota Geological Survey, is the Sentinel Butte Formation.

The Sentinel Butte Formation is exposed primarily in the badlands along the Little Missouri River in southwestern North Dakota. It is a lignite-bearing, nonmarine formation that is 380 to 620 feet (116 to 189 meters) thick (Jacob, 1976). In the area of the Theodore Roosevelt National Memorial Park a thickness of nearly 600 feet (183 meters) of Sentinel Butte strata is continuously exposed (Carlson, 1985, p. 21). Good exposures can also be observed along Lake Sakakawea, along the slopes of many buttes (e.g., Sentinel Butte, Bullion Butte), and in some river valleys (e.g., Knife River Valley) (Fig. 1). The upper portions of the Sentinel Butte Formation have been widely removed by erosion and can be observed only in a few isolated localities.

The age of the Sentinel Butte Formation has been established by paleobotanical evidence as Paleocene (Brown, 1948). The Sentinel Butte Formation consists of interbedded sandstone, siltstone, mudstone, carbonaceous shale, and lignite, which characteristically weather to somber shades of grays and browns. Individual beds of the Sentinel Butte Formation generally lack lateral continuity, although some useful marker beds are present in areas of good exposures. The marker beds include a basal sand, the "blue bed" (Sentinel Butte ash/bentonite), a lower and upper "yellow bed", and an upper sand (Fig. 2).

The Sentinel Butte Formation conformably overlies the Bullion Creek Formation. The lower contact is placed at the color change from the buff yellows or light grays of the underlying formation to the

Figure 1. Distribution of surface exposures of the Sentinel Butte Formation in southwestern North Dakota (modified after Bluemle, 1977). TRNP (NU) = Theodore Roosevelt National Park (North Unit).

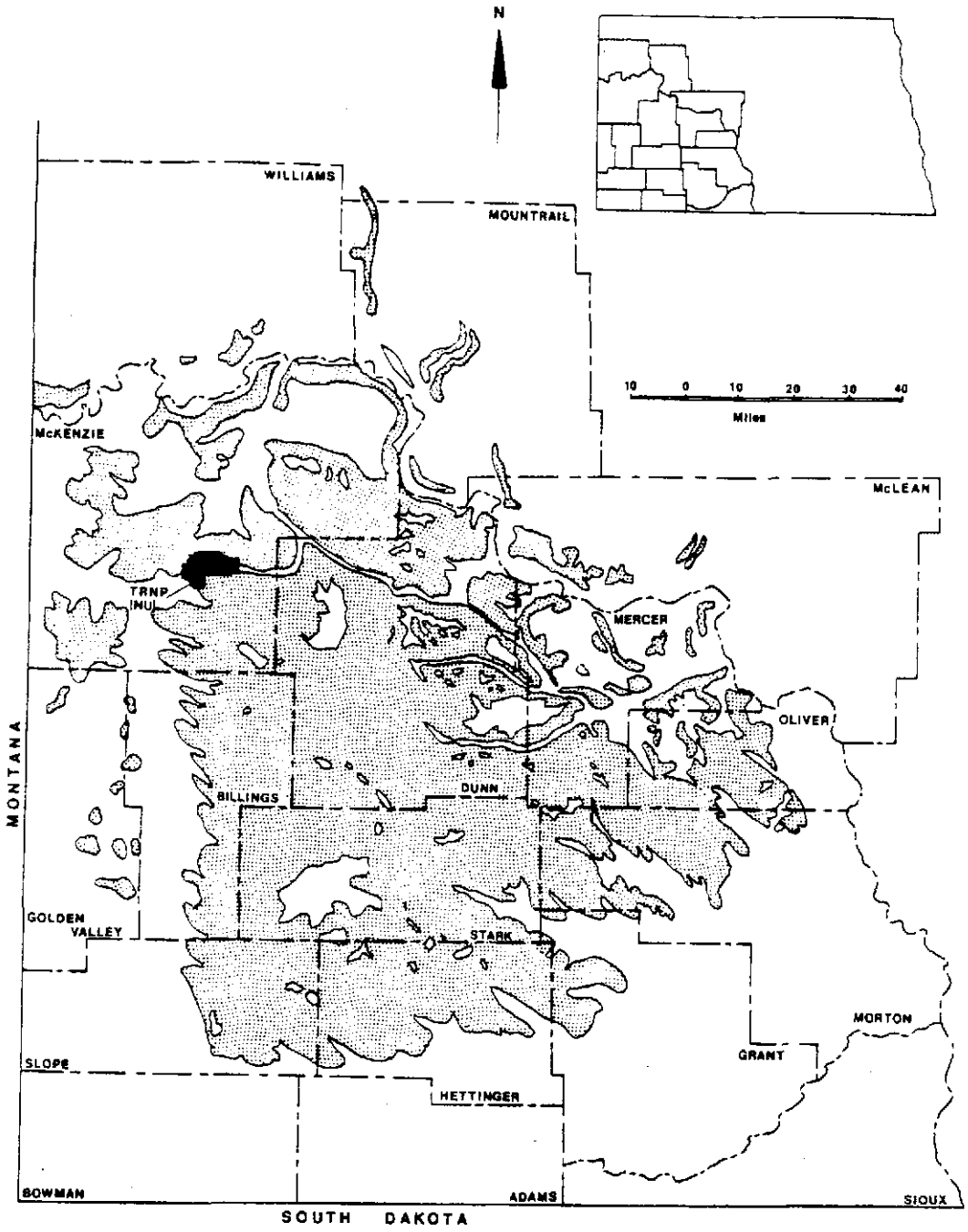
N
WILLIAMS
MOUNTRAIL
McKENZIE
McLEAN
TRNP
MERCER
OLIVER
MONTANA
BILLINGS
DUNN
GOLDEN
VALLEY
STARK
MORTON
GRANT
SLOPE
HETTINGER
BOWMAN
ADAMS
SIOUX
SOUTH DAKOTA
10 0 10 20 30 40
Miles

Figure 2. Simplified stratigraphic column showing positions of key marker beds within the Sentinel Butte Formation (modified after Forsman, 1985, p.18).

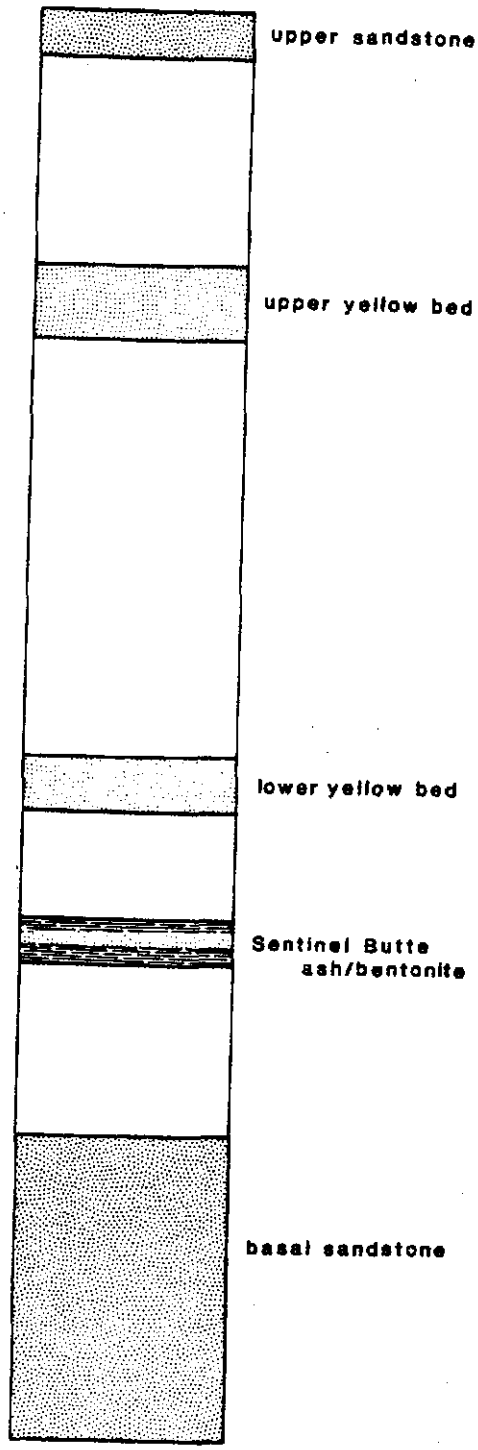
upper sandstone
upper yellow bed
lower yellow bed
Sentinel Butte
ash/bentonite
basal sandstone

somber, darker grays and browns of the overlying Sentinel Butte Formation. The upper contact is disconformable; the Eocene Golden Valley and Oligocene White River Formations and Pleistocene glacial tills overlie the Sentinel Butte Formation at various locations.

The Sentinel Butte Formation is characterized by fine-grained sediments deposited by low-energy alluvial processes. Depositional settings of the Sentinel Butte Formation have been interpreted to represent fluvial channel, floodbasin, lacustrine and backswamp environments (Royse, 1970, 1972; Jacob, 1976). Paleoenvironmental interpretations for the Sentinel Butte Formation have generally been modeled after a prograding deltaic plain.

Sentinel Butte Ash/bentonite

The Sentinel Butte ash/bentonite occurs over an area of approximately 155 square miles (400 square kilometers) in central McKenzie County, North Dakota. The unit is 1 to 30 feet (0.3 to 9.1 meters) thick and the most extensive exposures occur in the North Unit of Theodore Roosevelt National Park. The ash/bentonite is easily traced north and west, but the unit thins eastward from Squaw Creek and is not visible at the east entrance to the park. Approximately 1.5 miles (2.4 kilometers) east of Squaw Creek, the entire deposit is 2 feet (0.6 meters) thick. Eastward from this location, the ash continues to thin and disappears completely within 2 miles (3.2 kilometers). Southeast of the park entrance and south of the Little Missouri River a small isolated exposure of the Sentinel Butte bentonite occurs on a prominent

bench. This exposure represents the easternmost known extent of the Sentinel Butte ash/bentonite.

Westward, the bentonite also thins and appears to split into two distinct tongues. The location where the bentonite splits is extremely difficult to place due to the paucity of exposures. Chemical analysis, provided by this study, will determine if in fact these two tongues are related.

In the park area the ash/bentonite caps prominent benches, while northward it occurs in small coulees and on erosion-resistant remnants. The ash/bentonite is a distinctive bed that can be traced visually for 5 to 6 miles (8 to 10 kilometers) along Squaw Creek and the Little Missouri River. The colors of the Sentinel Butte ash/bentonite are in direct contrast to the somber gray, brown, and pale yellow shades of the surrounding sediments. Its conspicuous field expression is accentuated by upper and lower gray to dark-blue gray bentonites sandwiching a gray-white tuff. The upper and lower bentonites turn very dark gray to black when they are wet.

The Sentinel Butte ash/bentonite is a homogeneous unit throughout the study area. The upper and lower bentonites are massive units of swelling clays, and the tuff is a finely laminated siltstone. However, several locations display diagenetic or other structures that interrupt this homogeneity. The general field expression and the other irregularities will be described more completely below.

The upper and lower bentonites commonly form separate "popcorn-covered" benches, although the lower bentonite is usually much more prominent. The lower bentonite is 2 to 16 feet (0.6 to 4.9 meters)

thick and is found throughout the study area. The upper bentonite is 1.5 to 9 feet (0.4 to 2.8 meters) thick and is not exposed everywhere. The lower bentonite flows when wet and often drapes the underlying sediments. The lower bentonite is also a darker shade of gray than the upper bentonite. Where the ash is not present the upper and lower bentonites can be distinguished by this color difference.

Approximately 0.5 miles (1 kilometer) south of Zoar Church (149-100-14bb) large calcareous concretions occur in the upper portion of the lower bentonite. This is the only location where the these concretions were observed. The concretions are 4 to 36 inches (10 to 91 centimeters) in diameter and occur beneath an unusually thick section of ash. Authigenic barite crystals are found exclusively on the lower bentonite, and occur at fourteen of the thirty sample sites (Appendix A). They occur as prismatic crystal masses, which are brownish-red to dark brown on a weathered surface. Authigenic cristobalite also occurs exclusively near the base of the lower bentonite, at one of the thirty randomized sample sites, and at one other location. The cristobalite occurs as small (2-3 centimeter) prismatic crystal masses that are white to dark gray in color, although one crystal mass is approximately 10 centimeters in diameter. The crystals are composed of 2- to 8-micron size "rosettes" clustered together in elongated masses (Fig. 3).

Forsman (1985, p. 86) determined that the Sentinel Butte ash consists of 91 percent silt-sized particles. The silt fraction is dominated by volcanic glass shards (75 percent). The remaining 25 percent of the silt fraction consists of phenocrysts, probable phenocrysts, and detrital components. The detrital constituents

Figure 3. Authigenic cristobalite crystals from the base of the lower bentonite: A) SEM view of elongated prismatic crystals, bar = 10 micrometers B) SEM view of clusters of rosettes which form the prismatic crystals, bar = 1 micrometer.

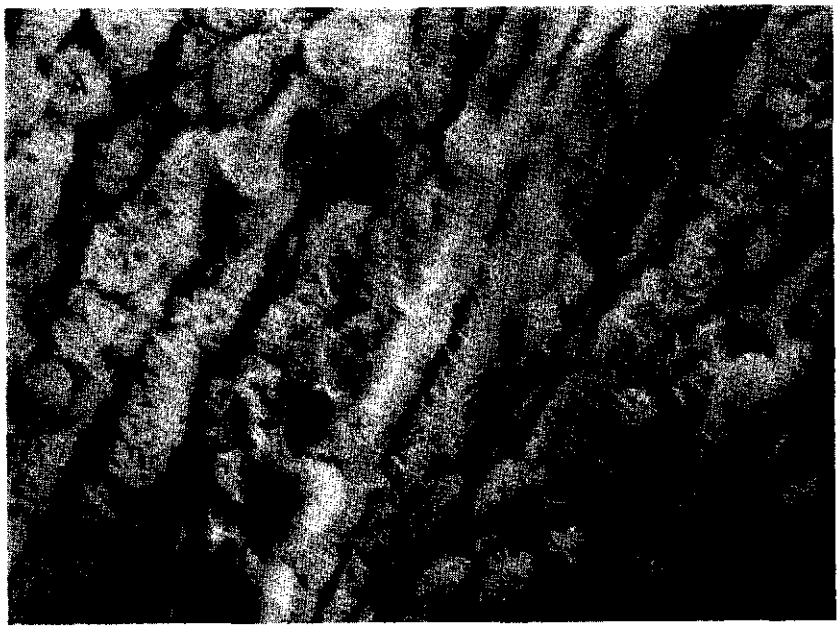


B

comprise a relatively small percentage of the silt fraction; therefore, the Sentinel Butte ash will be considered a tuff or a "dust tuff" throughout this report. However, according to the recommendations of the International Union of Geological Sciences (IUGS), (Schmid, 1981, p. 43) the Sentinel Butte ash should be classified as a tuffaceous siltstone, due to the detrital constituents.

The Sentinel Butte ash is finely laminated and is light gray to gray, although it appears white from a distance. The tuff is 1 to 6.5 feet (0.3 to 2.0 meters) thick and is not continuously exposed throughout the study area. The surface expression of the tuff is remarkably consistent and varies only locally. At two locations, carbonized plant fragments separate the laminations of the ash. At two other locations, an opaline silica sand is present where the ash is normally found. The field expression of the opaline silica is quite different from that of the tuff. The grain size is medium to coarse sand and the silica has a "salt and pepper" texture.

The color of the Sentinel Butte ash/bentonite is in such contrast to that of the surrounding sediments that the upper and lower contacts are often readily discernible at a distance. However, upon closer examination, the contacts are more difficult to place. The base of the ash/bentonite is sharp, although it is often not exposed due to plastic flowing of the smectite clay. The contact is placed at the boundary between swelling clay and an underlying silty mudstone. At many locations a silica-enriched zone is present at the top of the underlying unit. The silicification, which resulted from the release of silica during the alteration of the ash to a bentonite, has preserved in at

least seven different locations a water-rippled surface on a mudstone. The majority of these ripple crests trend northwest with a mean direction of N33W. In the southwestern area of exposure the ripple crests trend approximately N28E. Other areas have silica-enriched zones that have been extensively fractured, hindering conclusive identification of ripples.

The upper contact of the Sentinel Butte ash/bentonite is gradational, and up close it is often difficult to place. The overlying sediments, where exposed, are light to dark gray claystones (non-swelling) or, at many locations, are carbonaceous. Throughout this study, the upper boundary of the ash/bentonite was placed where the swelling clay was no longer pervasive. The upper and lower contacts of the sandwiched tuff are horizontal and transitional. This transitional boundary occurs over a distance of approximately 0.8 to 8 inches (2 to 20 centimeters).

Previous Investigations

The earliest descriptions of the Sentinel Butte Formation were the result of reconnaissance expeditions (Leonard and Smith, 1907; Leonard, 1908). Because these expeditions were primarily concerned with the coal reserves of the Fort Union strata, little mention of bentonites is given. The term Sentinel Butte ash/bentonite was used herein to distinguish it from other bentonites and ashes in the Paleocene strata in southwestern North Dakota and surrounding areas.

Sentinel Butte ash/bentonite

The Sentinel Butte bentonite was informally named "the blue" by Fisher (1953, pl. IV). According to Fisher, "the blue", along with two overlying beds, can be continuously traced from the vicinity of Sheep Butte eastward approximately 45 miles, and from the southern boundary of the North Unit of Theodore Roosevelt National Park to 7 miles north and east of Watford City, North Dakota. Laird (1956, p. 13, 15) modified Fisher's informal name "the blue" to the "Big Blue Bed." He described it as "the most spectacular bed in the park, which can be traced for miles up and down the Little Missouri River and for some distance to the north." Laird also noticed that the lower bentonite was more persistent than the upper bentonite in the vicinity of the park (personal communication to Hanson, 1954).

Bentonitic clay has been described in many areas of the badlands of southwestern North Dakota. Hanson (1955) and Meldahl (1956) described bentonites in the Elkhorn Ranch and the Grassy Butte areas respectively, although no attempt was made by either author to correlate these clays with known Sentinel Butte bentonite deposits. Carlson (1985) also reported "bentonitic" clays approximately 50 feet above the base of the Sentinel Butte Formation. Many of the clay beds in the Fort Union Group are blue-gray. Hence, there is a potential to misidentify a "blue" clay bed as a true bentonite or as correlative with the Sentinel Butte ash/bentonite (e.g., Brekke, 1979; Nesemeier, 1981; Royse, 1967b). To avoid confusion Forsman (1985) advocated the use of the names "Sentinel Butte bentonite," "Sentinel Butte ash," or, if both are present, "Sentinel Butte bentonite/ash", instead of

using the term "blue bed", when identifying these deposits in the field.

The clay mineralogy of the Sentinel Butte bentonite has been identified by x-ray diffraction techniques (Clark, 1966; Metzger, 1969; Forsman, 1982; 1985). Metzger (1969) identified the dominant clay mineral as a sodium montmorillonite. In more detailed petrographic studies, Forsman (1982; 1985) identified the Sentinel Butte bentonite as an iron-rich montmorillonite.

The prominent outcrop expression of the lower bentonite in and near the North Unit of Theodore Roosevelt National Park has been used for correlation purposes by several authors. The Sentinel Butte bentonite was found to be useful for mapping surficial structures (Benson, 1954) and for correlating the beds of the Sentinel Butte Formation in the Sperati Point Quadrangle (Clark, 1966). In attempting to trace the contact of the Bullion Creek and Sentinel Butte Formations in the subsurface, Royse (1967b) used the Sentinel Butte bentonite and the "lower yellow bed" as key marker beds for correlation. Other authors briefly mentioned key marker beds in the Sentinel Butte Formation, including the Sentinel Butte bentonite (Steiner, 1978; Carlson, 1985).

The Sentinel Butte bentonite has been recognized for most of this century (Forsman, 1982, p. 323), although the tuff has gone largely unnoticed. Royse (1967a, p. 12) described the entire unit as having a "tri-partite" character and Metzger (1967, p. 214) wrote of "alternating blue and light gray layers." Meldahl (1956) attempted to find evidence in the form of glass shards, of a volcanic origin for the Sentinel Butte

bentonite. Finding no volcanic glass, he concluded that the origin of the Sentinel Butte bentonite may be related to that of lignite. Hickey (1977, p. 10) also questioned the volcanic origin of the Sentinel Butte bentonite and suggested that it may have formed through chemical reactions in poorly drained swamps.

The first report of the presence of glass in the Sentinel Butte Formation and the Sentinel Butte bentonite was by Clark (1966, p. 22). He stated "microscopic studies reveal the presence of volcanic ash in the form of glass shards throughout much of the Sentinel Butte Member." However, Forsman (1985, p.102) found no volcanic glass shards in any Sentinel Butte samples except the Sentinel Butte ash/bentonite. The glass shards that Clark (1966) reported were very likely silicified plant fragments (Forsman, 1985).

A volcanic origin for the Sentinel Butte bentonite was first documented by Forsman and Karner (1975). The volcanic glass grains were found to consist of three morphologic types, all rhyolitic in composition. The presence of a laminated volcanic ash, sandwiched between the two Sentinel Butte bentonites, was also documented by Forsman (1982). Forsman (1984; 1985, p. 141, 142) hypothesized that the original tuff altered inward from its contact with the surrounding sediments, leaving the middle portion of the ash unaltered and fresh.

Correlation of Volcanic Deposits

Upper Cenozoic tephra deposits have been successfully correlated using geochemical fingerprinting techniques, including x-ray

fluorescence (Bowles et al., 1973), neutron activation analysis (Borchardt et al., 1971; Randle et al., 1971), and spark source mass spectrometry (Howorth and Rankin, 1975). Other authors have combined analytical techniques to compare the different geochemical methods and to characterize a particular tephra unit more thoroughly. To characterize volcanic ashes, Sarna-Wojcicki et al. (1979) utilized both x-ray fluorescence and neutron activation analysis, and Smith and Nash (1976) used x-ray fluorescence, electron microprobe and wet chemical techniques.

Geochemical fingerprinting techniques have also been applied to other volcanic deposits. Jack and Carmicheal (1968) chemically fingerprinted rhyolites and dacites using x-ray fluorescence spectrometry. Hahn et al. (1979) utilized both neutron activation analysis and x-ray fluorescence to fingerprint rhyolitic ash-flows and air-fall ashes. The provenance of rhyolitic conglomerates was successfully determined by Abbott and Smith (1978) with x-ray fluorescence methods.

Since the eruption of Mount St. Helens, in May 1980, the U.S. Geological Survey has been monitoring the major, minor and trace element composition of the air-fall material. Major element chemistry has been determined by x-ray fluorescence techniques and minor and trace elements were determined with the aid of Inverted Coupled Plasmon Spectroscopy (ICP) (Taggart, et al. 1981).

Geochemical fingerprinting techniques have only recently been applied to bentonites. Huff (1983) found that a significant chemical fingerprint remained after a volcanic ash had altered to bentonite.

He successfully correlated a Middle Ordovician bentonite unit over 300 km utilizing x-ray fluorescence techniques. Linares et al. (1973) determined that the color of a bentonite is related to the trace element chemistry of its volcanic precursor. Those volcanic rocks (e.g. rhyolites and dacites) richer in metallic ions produced a colored bentonite upon alteration.

METHODS

Field Procedures

The study area is located in central McKenzie County, North Dakota (Fig. 4). The known extent of the Sentinel Butte ash/bentonite occurs in townships 99N and 100N, and in Ranges 147W through 150W. Other areas, described by previous workers as having "blue bed" deposits, were also sampled in an attempt to delimit the full extent of the Sentinel Butte ash/bentonite. The sample locations were labeled by Township, Range, Section, and quarter - quarter section, e.g., 149-99-33ab. The quarter -quarter section was identified by the U.S. Geological Survey lettering system. Sample locations are listed and summarized in Table 1.

The Sentinel Butte ash/bentonite was mapped at a scale of 1:24000, using 7.5" quadrangle maps (Plate 1). The ash and the bentonite were positioned on the topographic maps by measuring their vertical distance above the Little Missouri River with a Jacob staff and a Brunton compass, and by the prominence of the lower bench.

Samples were collected from surface exposures of the Sentinel Butte ash/bentonite using a multistage sampling technique described by Krumbein and Graybill (1965, p. 158-159). Thirty sample sites were located randomly over the entire extent of exposure. At each collection site three samples were obtained from each of the three layers of the ash/bentonite, with a lateral distance of approximately 15 feet between samples in the same layer. All samples were collected from the middle portion of each unit and directly above or below the sample site from the neighboring units. Fifteen grab samples were also collected from

Figure 4. Location of the study area and randomly chosen sample sites (numbers) and a partial listing of the "grab" samples (lettered).

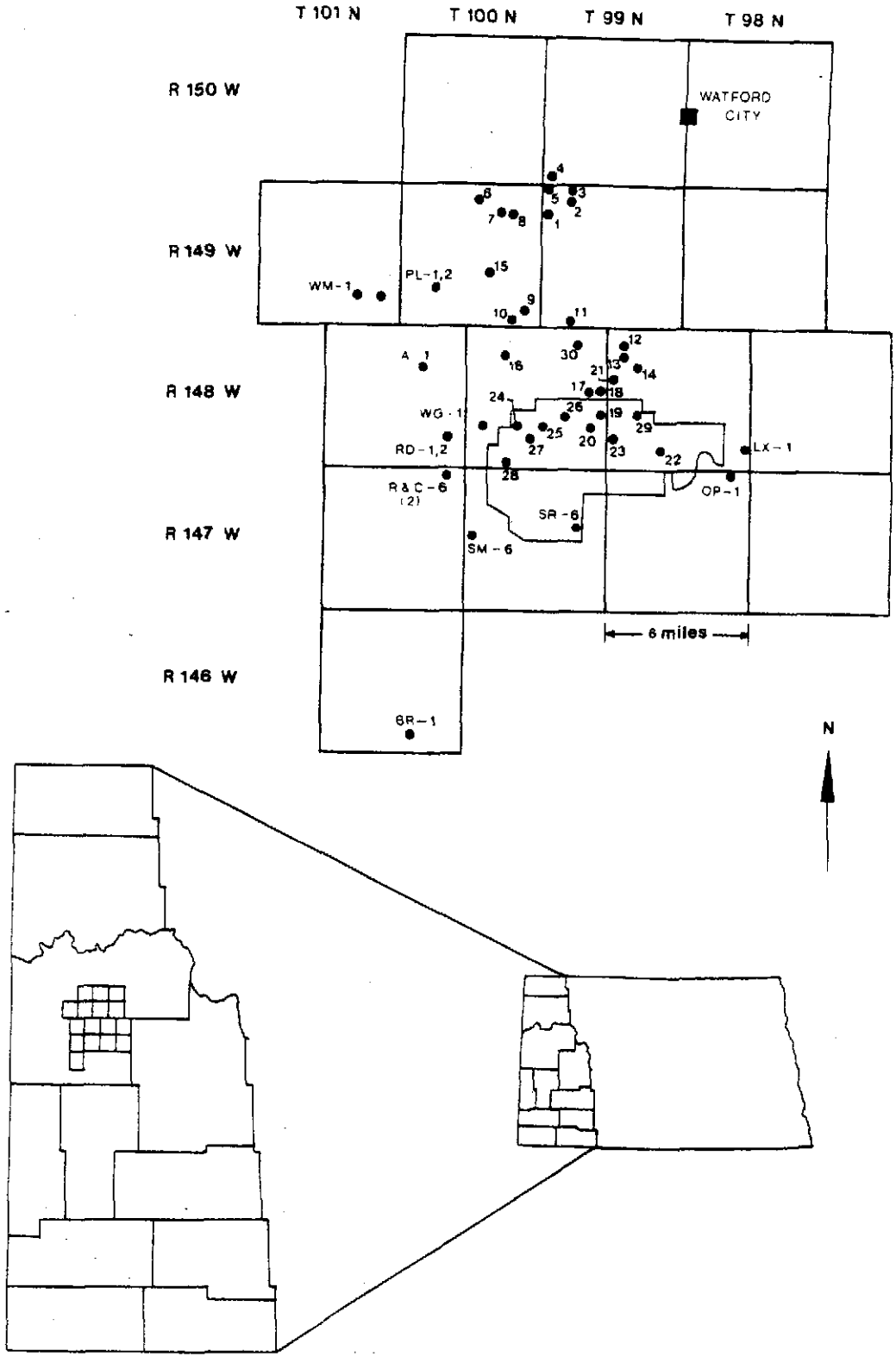
T 101 N
T 100 N
T 99 N
T 98 N
R 150 W
R 149 W
R 148 W
R 147 W
R 146 W
WATFORD CITY
WM-1
PL-1,2
WG-1
RD-1,2
R&C-6 (2)
SM-6
SR-6
OP-1
LX-1
6R-1
A 1
6 miles
N

Table 1. Location and summary of randomly chosen sample sites. The sample designations which begin with a letter are those samples which were obtained as "grab" samples. The asterisk designates the samples used in the chemical analyses. The thickness of each unit is given in meters and are listed as follows: A) upper bentonite, B) middle ash, C) lower bentonite. The presence of silica enrichment or preserved ripple structures at the lower boundary of the deposit is also indicated.

Table 1

Sample	Location	A	B	C	Silica Zone	Preserved Ripples
*1	149-99-7ba	1.70	1.01	1.83	---	---
*2	149-99-5cc	1.73	0.30	3.25	---	---
*3	149-99-5bc	0.43	0.74	3.05	---	---
4	150-99-31cc	1.83	1.12	1.12	not exposed	
*5	149-100-1aa	2.34	1.68	3.35	---	---
*6	149-100-3cd	1.73	0.61	1.27	yes	yes
7	149-100-11ba	(4.92)			yes	---
*8	149-100-11ad	1.12	1.27	1.12	not exposed	
9	149-100-36cd	2.03	1.80	1.93	yes	---
10	149-100-35dd	----	0.81	2.34	yes	yes
11	149-99-32cc	2.18	0.76	3.45	yes	---
*12	148-99-6db	1.73	0.69	4.11	---	---
13	148-99-7ab	(5.23)	----		---	---
14	148-99-8bc	1.73	0.35	4.88	---	---
15	149-100-22db	----	----	1.73	yes	yes
16	148-100-18ab	1.63	0.58	1.12	yes	yes
*17	148-100-13ca	2.84	2.03	3.45	yes	---
*18	148-100-13dd	2.67	0.97	4.42	---	---
19	148-100-24dd	----	----	1.88	---	---
*20	148-100-25bc	1.57	1.47	4.93	---	---
*21	148-99-18ba	1.78	1.37	2.84	---	---
22	148-99-33bb	----	----	0.61	---	---
23	148-99-31ba	----	----	4.57	---	---
*24	148-100-28bd	1.52	0.92	1.07	yes	yes
*25	148-100-27ba	1.96	1.38	2.03	yes	---
*26	148-100-23cb	2.84	0.76	3.66	yes	---
*27	148-100-28da	1.30	1.37	2.03	yes	yes
28	148-100-32dc	----	----	2.08	yes	---
29	148-99-20cb	----	----	2.13	---	---
30	148-100-2dd	----	----	1.88	---	---
*OP-1	147-99-1bc	----	----	1.37	---	---
*BR-1	146-101-34ba	----	----	2.08	---	---
*WG-1	148-101-29bd	----	----	2.90	---	---
*RD-1	148-100-24cd	----	----	1.02	---	---
*RD-2	148-100-25ba	----	----	0.69	---	---
*A-1	148-100-11cc	----	----	1.98	yes	yes
*WM-1	149-101-26cb	----	----	0.41	---	---
*LB-6	148-95-27cb	----	----	0.81	---	---
*C-6	147-101-1bd	----	----	0.61	---	---
*R-6	147-101-1bd	----	----	1.07	yes	yes
*SM-6	147-100-18cc	----	----	0.46	---	---
*LX-1	148-99-36aa	----	----	0.71	---	---
*SR-6	148-100-36cc	----	----	1.22	---	---
*PL-1	149-100-29bc	----	----	1.93	---	---
*PL-2	149-100-29bc	----	----	2.39	---	---

Values in parenthesis represent total thickness

bentonitic deposits located outside the random sample area. One sample was collected from each of the grab locations. The sampling strategy chosen produced a total of 228 samples, which was beyond the scope of this study. To reduce the number of samples to a manageable number, fifteen locations were chosen at random from the 30 original sites. One sample from each site within the upper and lower bentonites, and all three collection sites within the ash were utilized for chemical analysis. A complete description of each sample site is given in Appendix A.

Laboratory Procedures

Throughout each step of sample preparation the samples were prepared one unit at a time, i.e., lower bentonite, middle ash, and upper bentonite, so as to minimize between-sample contamination. Utilizing a large pestle, the samples were disaggregated, and crushed in one gallon plastic freezer bags to particles less than 10 millimeters in diameter. The samples were split to 8- to 12-gram aliquots, using a riffle splitter, for clay and ash major element analysis. A separate split of 20 - 25 grams was obtained for trace element analyses. Two separate aliquots were obtained for the two different specimen preparation techniques used. Glass fusion beads, which required 1 gram of material, were used for major element analysis, and a briquetting technique, which utilized 7 grams of material, was used for trace element analysis. All the sample aliquots were dried at 25-27^{o} C before further preparation.

To accurately assess the chemical variability over the extent of the Sentinel Butte ash/bentonite, glass and clay separates would be invaluable (Randle et al. 1971; Sarna-Wojcicki et al. 1979). However, the small particle size of the ash (average size of 50 to 60 micrometers) and the small difference in specific gravities of the glass and paramagnetic minerals did not allow for an efficient method of separation. The glass fraction could be separated from the mineral fraction by magnetic and density separation techniques, but that was very time-consuming. The clay separates were much easier to obtain. Centrifuging the diluted bentonite samples for approximately 40 minutes at 2000 RPM produced a "purified" authigenic clay separate. However, neither the glass nor the clays could be cleaned completely and a small amount of $CaCO_3$ remained in the clay separate after centrifuging. Therefore, the chemical data presented in this report represent analyses of whole rock samples.

Major Element Specimen Preparation

The 8- to 12-gram aliquots for major element analysis were ground for 7 minutes in a Spex porcelain ball mill. A porcelain ball mill was used to minimize the titanium contamination from the tungsten carbide ball mill. A modification of Norrish and Hutton's (1969) glass fusion technique was used to prepare the samples for major elemental analysis. A predetermined sample weight was ignited to 750°C for 12 - 18 hours. This eliminated any absorbed moisture and oxidized any ferrous iron (FeO) to ferric iron (Fe_2O_3). The weight loss (or gain) of the samples

during ignition is reported as loss on ignition (LOI). Batches of lithium tetraborate (90 -100 grams) were also ignited under the same conditions. This allowed the lithium tetraborate to be weighed out directly, instead of utilizing a correction factor for water present in the flux. The samples were carefully weighed out to a 10:1 flux to sample ratio, and homogenized thoroughly. These charges were placed in carbon crucibles and fused at 1120°C in a Lindberg muffle furnace for 15 to 20 minutes. The carbon crucibles were prepared for fusion by polishing the inside of the crucible with a paper towel, using two fingers and a swirling action. After being used once the sides of the crucible cavity were scraped clean and re-beveled. The carbon crucibles were used 4 to 6 times before being discarded. Before a sample charge was placed in a crucible any carbon residue was blown out with laboratory air. To ensure bead homogeneity the crucibles were stirred once while in the molten state. After stirring, the temperature of the furnace was re-established to 1120°C. Upon completion of the fusion, the crucibles were gently stirred and allowed to cool. When the samples were sufficiently cooled the crucibles were turned upside down and tapped lightly. This freed the glass bead from the crucible. For presentation to the spectrometer the bottom surface of the glass bead was polished with a 5-micron aluminum oxide polishing compound.

Trace and Minor Element Specimen Preparation

Sample preparation procedures are not as detailed for trace elements as they are for major elements. The short wavelength (high

energy) of trace elements is not easily absorbed in a low atomic number matrix. Therefore, the matrix and absorption corrections necessary for low atomic number elements are not a requirement for trace element analysis. However, there are corrections for trace elements, due to interelement effects. A modification of the Leake et al. (1968) briquetting method was chosen to present the samples for trace element analysis to the spectrometer.

The 20- to 25-gram aliquots for trace element analysis were first ground for 5 minutes in a large tungsten carbide ball mill with two tungsten carbide balls. The samples were then ground for 5 additional minutes in the same tungsten ball mill with 2.5 ml of Chemplex polymeric binder and grinding agent. The additional grinding reduced more than 95 percent of the particles to 10 - 20 micrometers. The ground samples were split into 7-gram aliquots, using a small riffle splitter, and each was taken through the remaining sample preparation separately. The duplicate splits were again ground in an agate mortar and pestle to further reduce the particle size of the material. The specimens were placed in a 1.25-inch die and pressed to 20 tons/square inch for 4 minutes while under a vacuum. The resulting briquets were 4 mm in height and met all the requirements for an infinitely thick sample (Appendix B). To insure consistency, the standard rock materials were prepared in the same way, although they were not ground in the tungsten carbide ball mill.

Quality Assessment

The samples were all analyzed on a Rigaku S/MAX fluorescence spectrometer with a rhodium end window tube. A dedicated PDP 11/03 Digital computer was employed to reduce both the major element (Fundamental Parameter method) and the trace element data (linear and quadratic regression, and scattered ratio method). The spectrometer control conditions are explained in Appendix C.

The reliability of the concentration values determined for the unknown samples is assessed using the mean, standard deviation and variance of values determined from standard reference materials used for major elemental analysis. A measurement process is said to be in a state of statistical control when replicate measurements on duplicate samples can be shown to have the same mean and standard deviation (Taylor, 1985). Once a measurement process is in a state of statistical control the precision and accuracy of that process can be used to characterize all the data produced by it. The reliability of a measurement or a spectrochemical analysis is also expressed as the degree to which it possesses precision and accuracy (Bertin, 1975, p. 460). Duplicate samples were made and analyzed for the major elements.

The student "T" test and the "F" test were used to assess the equality of the sample and duplicate mean and variance, respectively. However, there was not enough standard reference material to make duplicate samples for trace element analysis, because the method chosen utilized 7 grams of material. Therefore, the reliability of the trace elemental analysis was based solely on the precision and accuracy of the results.

The counting times for the peaks and the background(s) were calculated so that the total accumulated counts at these positions achieved a specified relative standard deviation in a minimal counting time. The optimal fixed-time method of Mack and Speilberg (1958, p. 171) was chosen for the analysis of the Sentinel Butte ash/bentonite, and has the advantage that counting errors are minimized compared to the fixed-time and fixed-count methods (Bertin, 1975, p. 485).

Error and Contamination

Undoubtedly the most likely place to introduce an error in the data is in the process of sample preparation. Care was taken not to contaminate the standards or the unknowns during the preparation of the fused disks, although contamination of the standard reference materials could have occurred before this study was undertaken. The unknown samples were prepared in such a way that between-sample contamination was minimized (see page 24). The magnitude of the standard deviation of the results of ten replicate determinations on a given analyte did not differ significantly from the magnitude of the standard counting error. Therefore, the analysis is free of significant error and the precision is limited by the counting statistics (Bertin, 1975, p. 494).

Near the end of collecting data on the unknown samples a heat sensitive regulator chip was found to be malfunctioning. This chip was located on the pulse height analyzer (PHA) logic board, which controls the flow of counts to the scaler and computer. The temperature in the laboratory was not controlled and would vary from day to day, and during

a given day. When the temperature of the room, and hence the S/MAX, was high (75° to 90° F) the count rate would be reduced and occasionally drop to zero. The heat sensitivity of this chip would have created a larger variation in the count rate than normally would have been expected. Hence, the data reduction program (FP) attempted to correct for the variation in counting rates. This temperature variation undoubtedly had an effect on the counting rates and the calculated oxide weight percents, although it is not known to what extent.

The large temperature variations may have also affected the pentaerythritol terakis (PET) analyzing crystal. This crystal is situated in the analyzing chamber, which is under vacuum, and is not exposed to the direct temperature fluctuations as are the rest of the components in the system. However, slight temperature variations can cause drastic changes in the number of counts detected from this crystal (Rigaku S/MAX operating manual).

A systematic error was found in the results of the standard materials used for the major element analysis. This error was introduced during the weighing of the flux and sample, prior to the fusion process. The resulting totals for each standard material were higher than expected, and each of the ten major analyte concentrations was multiplied by a correction factor of 0.988.

Major Elemental Chemistry

The major element concentrations of the five analyzed standard reference materials, MA-N, GS-N, GA, GH, G-2, were obtained by the

method of fundamental parameters (FP) (Criss and Birks, 1968). This mathematical method is applicable to samples for which complete analyses are made. Such is the case when determining major element concentrations of geologic materials where the major elements constitute 95 to 99.5 percent of the sample weight.

The analyzed standard reference materials and duplicates were tested for equal means and standard deviations. Reference standards GH, GA, MA-N, and SDC-1 all had at least one element which did not pass the equivalence test. Standard G-2 passed the test with all element means and standard deviations equal. Those values that did not meet the equivalence tests had standard deviation and counting error magnitudes that were not significantly different. The tests revealed that it was not a single element or a given concentration range which was consistently unequal.

Major Element Precision and Accuracy

The precision of the fusion technique, utilizing fundamental parameters, is shown by the chemical results obtained on five standard rock samples. These standards are acidic by definition, i.e., greater than 66 percent SiO_2 (Williams et al., 1982, p.159) and closely approximate the composition of the unknowns. Ten replicate readings were made for each analyte determination. Both the absolute (standard deviation) and relative (coefficient of variation) errors were calculated, although only the former is used in this discussion. The relative error for samples containing an oxide in very low

concentrations becomes so large that it dominates the statistical evaluation of the results. The use of absolute errors gives results that are controlled by the errors associated with the high concentrations, and will overestimate the values for the low concentrations. Table 4 summarizes the results of the precision tests on the five rock standards. The precision and accuracy tests calculated for ten replicate runs on both sample and duplicate standard reference materials show that the resulting data are of high quality.

Trace Element Chemistry

Trace Element Precision and Accuracy

To facilitate data analyses the trace elements were divided into two groups; TR1, which consisted of V, Cr, Co, Ni, Cu, Zn, Ga, and S, and TR2, which consisted of Rb, Sr, Y, Zr, Nb, and Pb. The elemental concentrations of the trace elements were determined by several methods: linear regression, quadratic regression, and the scattered radiation method of Andermann and Kemp (1958). Quadratic and linear regression techniques were applied to the lower atomic number trace elements S, Cr, Co and Ni. The scattered radiation method was employed for the trace elements Cu, Zn, Ga, Rb, Sr, Y, Zr, Nb, Ba and Pb. A total of fifteen standard reference materials were used to calculate the trace element concentrations in parts per million (PPM). These standard reference materials included FK-N, BHVO-1, STM-1, SY-3, PCC-1, W-1, MAG-1, GS-N, DNC-1, AGV-1, MA-N, DTS-1, SCO-1, DR-N, and MRG-1.

Table 2. Precision tests of the five standard reference samples

	G-2	GH	GA	MA-N	SDC-1
Na_2O	a 4.03	3.83	3.51	5.91	2.04
	b(0.10)	(0.11)	(0.15)	(0.10)	(0.12)
MgO	0.71	0.04	0.95	0.04	1.69
	(0.03)	(0.05)	(0.06)	(0.03)	(0.05)
Al_2O_3	15.14	12.47	14.61	17.73	15.67
	(0.11)	(0.08)	(0.07)	(0.09)	(0.10)
SiO_2	69.02	75.45	69.77	66.88	66.00
	(0.28)	(0.18)	(0.24)	(0.23)	(0.21)
P_2O_5	0.14	0.01	0.12	1.40	0.18
	(<0.01)	(0.01)	(<0.01)	(0.01)	(0.01)
K_2O	4.47	4.77	4.06	3.19	3.26
	(0.01)	(0.01)	(0.01)	(0.01)	(0.01)
CaO	1.87	0.70	2.38	0.59	1.40
	(0.01)	(0.01)	(0.02)	(0.01)	(0.01)
TiO_2	0.50	0.08	0.38	0.003	1.01
	(0.01)	(<0.01)	(0.01)	(0.01)	(0.01)
MnO	0.03	0.05	0.09	0.04	0.12
	(<0.01)	(<0.01)	(<0.01)	(<0.01)	(<0.01)
Fe_2O_3	2.70	1.34	2.79	0.48	6.89
	(0.01)	(0.01)	(0.01)	(<0.01)	(0.01)
LOI	0.49	0.40	0.72	1.14	0.98
Total	98.10	99.14	99.38	97.36	99.24

a = oxide weight percent
b = standard deviation (n = 10)
LOI = Loss on ignition

The advantages of the scattered radiation method over the internal standard method are: 1) no additional standard material(s) needs to be added to the sample, 2) it is applicable to samples in any form, and 3) it is applicable to many analyte lines in the same specimen (Bertin, 1975, p.608). This method is especially useful in the analysis of minor and trace analytes in low atomic number matrices. However, no absorption edge should lie between the analyte line and the scattered x-rays from the target (Bertin, 1975, p.609). This condition is met in geologic samples, where iron commonly has the highest atomic number among the major elements. Andermann and Kemp (1958) found that the intensities of the analyte and the scattered radiation were affected by the absorption of the specimen, so that ideally the ratio of analyte intensity to the scattered radiation intensity should be independent of the matrix. This ratio was also found to be insensitive to excitation conditions, drift, and variations in particle size and compactness of powdered samples. Therefore, the absorption of the specimen at shorter wavelengths than the iron absorption edge is a smooth curve (Tertian and Claisse, 1982, p. 258).

The 360 Dataflex software package has the capabilities to calculate calibration curves by utilizing the initial analysis of the standard materials. This allows the user to input those standards which best approximate the composition of the analyte in question. The concentration ranges of the standard materials were also chosen to closely approximate the concentration of the unknowns. The resulting analyte concentrations were adjusted for interelement effects by utilizing algorithms based on intensity (Lucas-Tooth and Pyne model),

and concentration corrections (Lachance-Traill, and Rasberry-Heinrich models).

Spectral contamination from the internal parts of the fluorescence unit was corrected for by utilizing the slope of a contaminant analyte line as a calibration factor. The effect of this contamination is to move the calibration curve upwards so it no longer passes through the origin. This was the case with the calibration curves of Cu, Ni, and Zn. Some contamination was also observed for Fe and Ti; however, background values were measured for these elements, and net intensities plotted, so no correction was needed. The method chosen to correct these trace elements was simply to fix the intercept at zero (Bertin, 1975, p. 584).

Vanadium is very difficult to determine precisely with x-ray fluorescence, due primarily to line overlap. The vanadium K-alpha line can not be separated from the titanium K-beta line, and the vanadium K-beta lines lie underneath the chromium K-alpha line. Therefore, the vanadium determinations were used to correct for interelement effects and are not reported in the results.

The concentrations of Cr and Co were greatly overestimated by the 360 Dataflex software. For both of these elements, a high and low background and a peak position were analyzed. The position of Co with respect to Fe and the Fe absorption edge makes its determination difficult, due to enhancement effects from iron (Leake et al., 1968). The concentration values calculated for Cr may have also been influenced by another analyte line, although it is relatively free of enhancement effects. The results of the precision and accuracy tests for Cr and Co

reveal that the standard deviations of these two elements are excessively large. Because of this large standard deviation the concentration values of these elements were not satisfactory for use in this study.

The precision of the trace element analysis, utilizing linear and quadratic regression, and the scattered ratio method, is shown by the results obtained using the selected standard materials (Tables 5 and 6). As with the major elements, the absolute error (standard deviation) was used to denote the precision of the resulting data.

Statistical Procedures

The data were analyzed by three statistical techniques: cluster analysis, discriminant analysis, and factor analysis. Cluster analysis classifies the measured variables into groups based on the similarity of the measured variables. Discriminant analysis was used to determine which chemical variables produced the largest differences between the defined units of the Sentinel Butte ash/bentonite. R-mode factor analysis was employed to determine if a useful chemical fingerprint existed for of the Sentinel Butte ash/bentonite.

The first step in clustering a group of objects by cluster analysis is to calculate a matrix of all combinations of similarities between objects. Two primary types of similarity measures have been employed, the Euclidean distance and the correlation coefficient; the latter was used for this study. The first step in clustering is the construction of a matrix of similarity values of each object (sample) with all the

Table 3. Precision tests of the fifteen standard reference materials (for measured trace element group TR1)

	Cr	Co	Ni	Cu	Zn	Ga
MA-N	a4		4			80
	b		(3)			(1)
BHVO-1		44		139		20
				(2)		(0.2)
PCC-1				8	35	1
				(0.2)	(1)	(0.1)
SCO-1	77	15		38	122	
				(0.5)	(3)	
DNC-1	57				36	11
					(1)	(0.2)
MAG-1	100	23	50			24
			(1)			(0.4)
STM-1	7	3			269	37
					(5)	(0.4)
DTS-1			2337	8		1
			(10)	(0.1)		(0.1)
FK-N		17				19
						(0.1)
GS-N		64			55	20
					(1)	(0.5)
DR-N	38		16	52	136	20
			(1)	(1)	(3)	(0.4)
SY-3	11	9	7	12		24
			(2)	(0.2)		(0.3)
W-1		48	75		61	14
			(1)		(2)	(0.2)
AGV-1	8	10		56	87	21
				(1)	(2)	(0.2)
MRG-1	450					20
						(0.3)

a = concentration in PPM
b = standard deviation in PPM
Blank spaces indicate the standard was not used in calibration

Table 4. Precision tests of the fifteen standard reference materials (for measured trace element group TR2)

	Rb	Sr	Y	Zr	Nb	Ba	Pb
MA-N	a3615	83	1	25		50	26
	b(16)	(2)	(1)	(2)		(9)	(3)
BHVO-1		414	31	172	16		
		(3)	(1)	(2)	(1)		
PCC-1		3		3	1		14
		(4)		(2)	(1)		(1)
SCO-1	116	237	24		9	643	34
	(1)	(2)	(1)		(1)	(17)	(1)
DNC-1	6		20	40	5		5
	(0.2)		(1)	(1)	(0.4)		(0.2)
MAG-1	149		25		12	548	20
	(1)		(1)		(0.5)	(38)	(1)
STM-1	120	636	45	1307		579	18
	(1)	(22)	(2)	(4)		(23)	(1)
DTS-1	0	5		0.2	2		10
		(6)		(0.5)	(1)		(0.5)
FK-N	864	41	0.2	13			242
	(5)	(2)	(0.5)	(1)			(3)
GS-N	186		18	234	22	1448	57
	(2)		(2)	(5)	(1)	(63)	(1)
DR-N		421		134	2	361	
		(2)		(2)	(1)	(30)	
SY-3	208	307	742	198	131		133
	(2)	(5)	(6)	(4)	(1)		(1)
W-1	19		22		10		6
	(1)		(1)		(0.5)		(0.4)
AGV-1	65		20	228	17		34
	(2)		(2)	(4)	(1)		(1)
MRG-1	8	266	14	110			10
	(1)	(5)	(1)	(2)			(1)

a = concentration in PPM
b = standard deviation in PPM
Blank spaces indicate the standard was not used in calibration

other objects. Upon forming the similarity matrix a search is made of all the elements, excluding the diagonals, to locate the two objects with the greatest similarity. Because the matrix is symmetrical only half of it is used in these calculations. The two most similar objects are then combined into one group and the similarity of this group, with the other objects is calculated as the average between each member of the group and each object. This procedure is repeated until all of the objects have been joined together. This clustering technique, unweighted pair group averaging, weights each cluster proportionally to the number of objects in a group or cluster.

Averaging individual objects and treating them as a single new object produces some distortion in the clustering process. This inherent distortion becomes more pronounced with large numbers of objects and at lower levels of similarity. Evaluating the level of distortion in the clustering process is accomplished by the cophenetic correlation coefficient. The cophenetic correlation coefficient is the correlation coefficient of the original similarities between objects, and the clustering levels of those objects. Cophenetic correlation coefficients less than 0.80 are considered to represent unacceptable distortion levels in the results of cluster analysis. A dendrogram is commonly used to illustrate the results of cluster analysis. One axis represents the similarity values, and the other represents the objects. The lines joining the individual objects or groups are the similarity level at which they cluster.

Discriminant analysis is a statistical technique for distinguishing between two or more groups on the basis of measured variables. Two

populations are differentiated by calculating a discriminant function from a population of objects in which k variables have been measured. These variables form a cluster of points in k-dimensional space. The second population is also described in terms of the same k variables in k-dimensional space. The discriminant function is the k-1 dimensional plane upon which the k-variables are projected. The projection of the variables onto the k-1 dimensional plane shows the greatest separation of the population means compared to the variation within each population. The statistical procedure required to evaluate two populations by discriminant analysis can be summarized as follows. The covariance matrix $\underline{B}$, which is the matrix of the sums of squares and cross-products of the variables from the two populations, is calculated. The differences between the means of the variables in each population are calculated and form a matrix $\underline{d}$. The coefficients of the discriminant function are contained in yet another matrix $\underline{a}$. These three matrices are then related by the equation $\underline{B}\underline{a} = \underline{d}$. Matrix $\underline{B}$ is inverted ($\underline{B}^{-1}$) and is multiplied by matrix $\underline{d}$ to obtain the coefficient matrix $\underline{a}$, which can be written as: $\underline{B}^{-1}\underline{d} = \underline{a}$. In two dimensional space the discriminant function is described by:

$$D = a_1X_1 + a_2X_2 + \ldots a_nX_n$$

The discriminant index (D_o) is the value of D that is midway between the multivariate means, and is calculated by:

$$D_o = a_1X_1 + a_2X_2 + \ldots a_nX_n$$

The measure of the separation between the group of multivariate means is described by Mahalanobis' distance function D^2. The significance of the separation of the means is tested by:

$$q = \frac{n_1 n_2 (n_1 + n_2 - k - 1)\, D^2}{k(n_1 n_2)(n_1 + n_2 - 2)}$$

Where k is the number of variables, and n_1 and n_2 are the number of objects in each population. The value of q is then compared to the tabled F-distribution value for $F(k_1 n_1 + n_2 - k - 1)$ degrees of freedom. If q exceeds the tabled value of F, then the two populations are considered to be statistically different.

All of the variables are not equally useful in separating two populations. Therefore, testing the contribution that each variable possesses is accomplished by comparing the differences for each variable with the total separation.

$$C_j = \frac{a_j (X_{aj} - X_{bj})}{D^2}$$

Where C_j is the contribution of the j_{th} variable, a_j is the coefficient of the j_{th} term in the discriminant function, X_{aj} and X_{bj} are the means of variable j for population A and B respectively, and D^2 is Mahalanobis' distance function. The total of the contribution is 100 percent although, a negative contribution to the separation may occur, and indicates a decrease to the total separation by that particular variable. Contributions of greater than 100 percent are then feasible. The discriminant function can then be used to assign unknown samples to one population or the other.

R-mode factor analysis, which was employed for this study determines the inter-relationships among variables measured on a group of objects. The objects in this case are the physical samples, and the variables are the chemical constituents of those samples. These

are arranged into a data matrix consisting of rows of objects and columns of variables. This data matrix can be expressed as $X_{N,n}$, and the basic problem is to determine m linear combinations of the original n variables that describe the physical samples without any loss of information. The m linear combinations are termed factors, and the method is performed on the matrix of correlation coefficients of variables with one another.

The data matrix can be considered to define the locations of points in n dimensional space; the values for the n variables define the coordinates along each of the m axes. The correlation coefficient matrix is used to derive the characteristics of an n-dimensional ellipsoid which encloses the data points. The ellipsoid is defined so that the direction of the greatest data variability is the largest axis of the ellipsoid, the direction of the greatest variability normal to the first direction is the next largest axis, and so on. By definition, the axes are all mutually perpendicular.

The eigenvalues of the data set are the relative lengths of the axes of the ellipsoid; the first eigenvalue is the largest and represents the largest axis of the ellipsoid. Associated with each eigenvalue are n eigenvectors, which are the direction cosines of the ellipsoid axis with the n coordinate axes. The factor loadings referred to in the literature and below are the direction cosines of the ellipsoid axes.

Factor analysis, as commonly performed, is a two step process. The first step is the calculation of the eigenvalues and eigenvectors. The second step is the rotation of the factor axes (ellipsoid axes) in

order to simplify the relation between the factor axes and the variability of the data set. Rotation of the factor axes in space is performed to maximize the variance of the loadings on the factors. Each of the factor axes is rotated so that projections from each variable are either near the extremities or near the origin of the vector. Maximizing the variance will maximize the range of the factor loadings, which produces either extreme (positive or negative) or near zero loadings.

The factor scores are the projection onto each axis of the data points. The interpretation of factor analytic results is often done by plotting the factor scores on the first two factor axes, before or after rotation (as in Fig. 18). For a complete description of cluster analysis, discriminant analysis, and factor analysis the reader is referred to Davis, (1973) and Krumbein and Graybill, (1965).

RESULTS

Geochemical Characteristics of the Sentinel Butte Ash/Bentonite

The Sentinel Butte ash/bentonite is a unique deposit, in that a well preserved ash is sandwiched between two bentonite layers. Because the parent ash is sandwiched between the upper and lower bentonites the geochemistry of the bentonites can be directly compared to that of the ash. Geochemical variability over the lateral extent of the Sentinel Butte ash/bentonite must be documented before an accurate assessment of the geochemical characteristics can be made. The use of whole rocks for geochemical analysis can also add to this variability. Erosion and sedimentation processes can play a major role in concentrating some mineral phases and trace elements (Lindsey, 1975). Therefore, detrital or induced contamination can make characterization of a given geologic unit very difficult.

Surficial mapping of the Sentinel Butte ash/bentonite was undertaken primarily to determine the distribution of the deposit. Mapping of the ash/bentonite enlarged its previously known extent, established by Forsman (1985) (Fig. 5), and also provided a more complete "picture" of its diagenetic and depositional history.

The Sentinel Butte ash/bentonite has been classified as rhyolitic in composition based on its major element concentrations (Forsman, 1984,1985). The major element concentrations determined for this study also indicate a rhyolitic source magma for the Sentinel Butte ash. As a check of the rhyolitic classification, the Nb/Y versus Zr/TiO_2 ratios were plotted on a volcanic rock distribution diagram

Figure 5. Plot of the expanded range of the Sentinel Butte ash/bentonite. The shaded area represents the previously known extent determined by Forsman (1985). The dots represent both the random and grab sample locations.

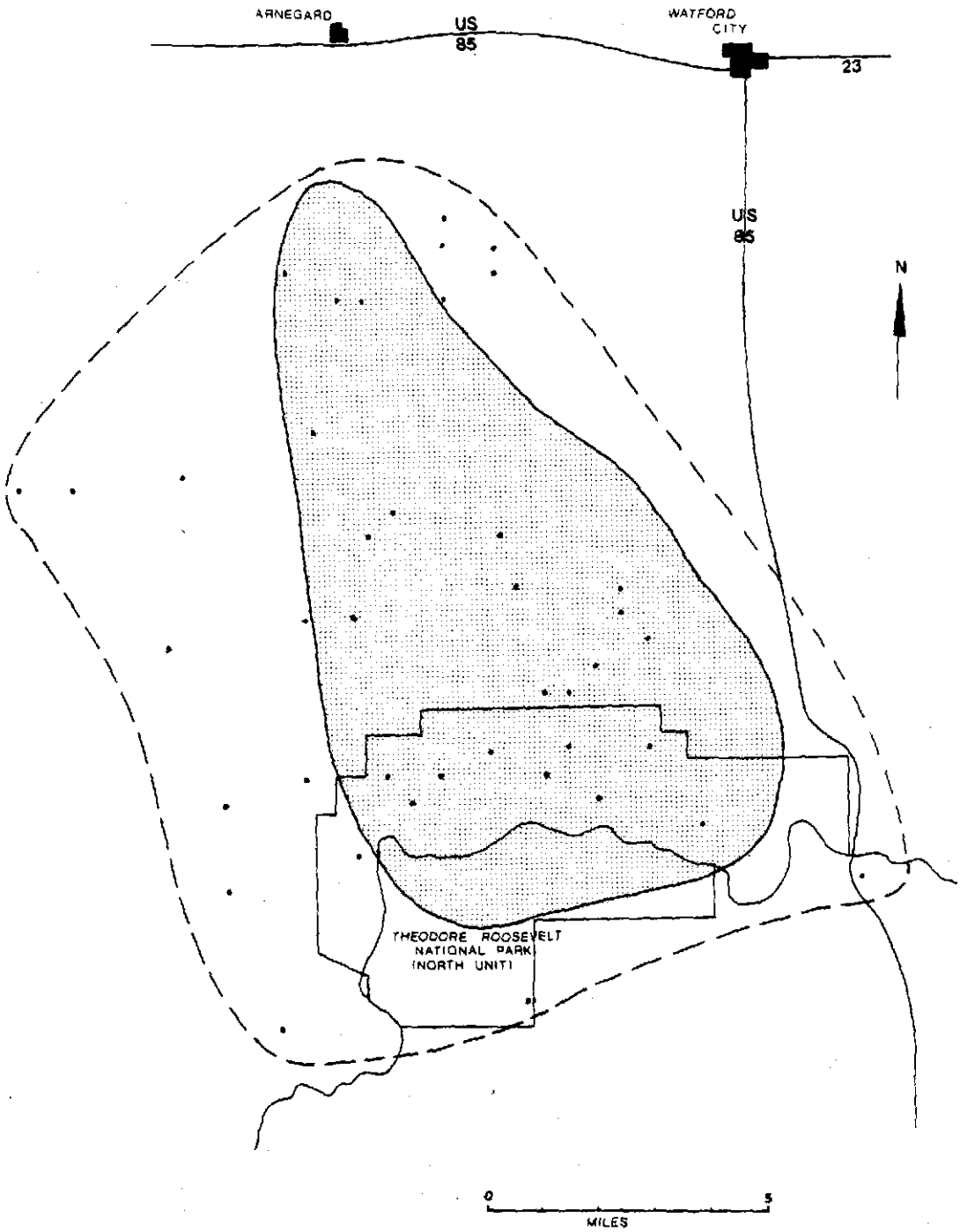
ARNEGARD
US
85
WATFORD
CITY
23
US
85
N
THEODORE ROOSEVELT
NATIONAL PARK
(NORTH UNIT)
0
5
MILES

(Floyd and Winchester, 1978), and this data also supports the rhyolitic classification (Fig. 6).

Geochemical Variability of the Sentinel Butte Ash/bentonite

The major element oxides and the trace element concentrations for each individual sample are listed in Appendix D. The geochemical characteristics of the Sentinel Butte ash/bentonite were summarized by averaging each major element oxide, and trace element PPM value for each unit, i.e., upper and lower bentonite, and ash (Appendix D). The geochemical ranges and mean values of the major element oxides are illustrated in Table 2. Those of the trace elements are depicted in Table 3. Sulfur was not included with trace element variability because of its erratic mean concentration values.

Major Element Variability

The major element oxides that have a higher mean concentration in the ash than in the bentonites include Na_2O, SiO_2, and K_2O. The major element oxide differences between the upper and the lower bentonites are typified by higher concentrations of Na_2O, Al_2O_3, SiO_2, K_2O, and Fe_2O_3 in the lower bentonite. Only MgO and CaO occur in higher concentrations in the upper bentonite.

The ash is characterized by lower elemental ranges for all major element oxides, with the exception of MgO and Fe_2O_3. The concentration of iron tends to increase from the upper to the lower bentonite. The

Figure 6. A plot of Nb/Y and Zr/TiO_2 ratios from the Sentinel Butte ash on a volcanic rock distribution diagram (modified after Floyd and Winchester, 1978).

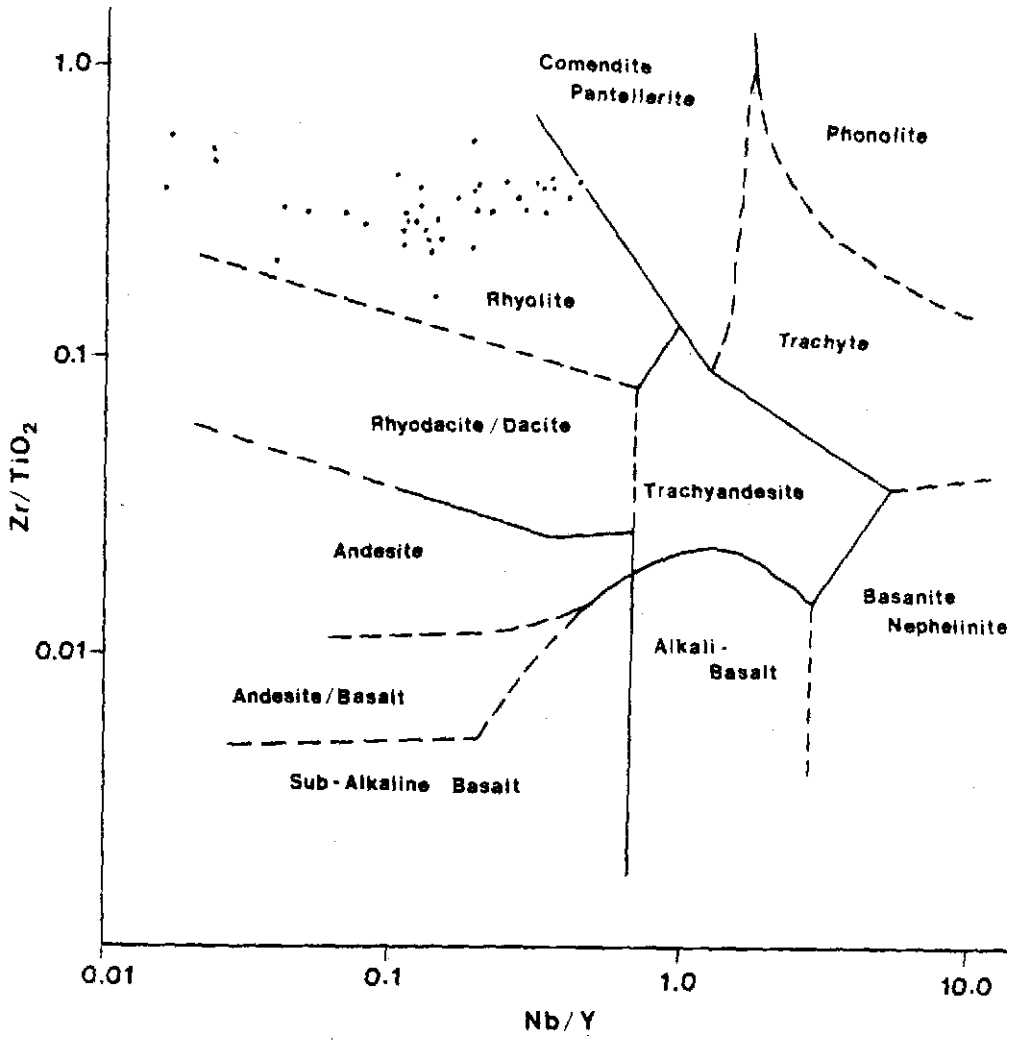
1.0
0.1
0.01
Zr/TiO2
Comendite
Pantellerite
Phonolite
Rhyolite
Trachyte
Rhyodacite / Dacite
Trachyandesite
Andesite
Basanite
Nephelinite
Alkali-
Basalt
Andesite / Basalt
Sub-Alkaline Basalt
0.01
0.1
1.0
10.0
Nb/Y

Table 5. Summary of the major element oxide mean values and concentration ranges for the Sentinel Butte ash/bentonite

Upper Bentonite

	Mean (%)	Range (%)
Na_2O	2.06	1.25 - 2.62
MgO	3.07	2.65 - 3.63
Al_2O_3	16.08	14.46 - 18.43
SiO_2	66.91	63.98 - 69.32
P_2O_5	0.10	0.07 - 0.15
K_2O	1.03	0.63 - 1.60
CaO	2.82	1.52 - 4.13
TiO_2	0.39	0.31 - 0.54
MnO	0.04	0.02 - 0.08
Fe_2O_3	4.20	3.95 - 4.83

Middle Ash

	Mean (%)	Range (%)
Na_2O	2.97	2.64 - 3.47
MgO	1.93	1.28 - 2.61
Al_2O_3	15.31	14.49 - 16.87
SiO_2	68.42	66.76 - 69.91
P_2O_5	0.09	0.06 - 0.13
K_2O	1.82	1.48 - 2.10
CaO	2.65	1.66 - 3.28
TiO_2	0.31	0.24 - 0.36
MnO	0.05	0.04 - 0.07
Fe_2O_3	3.09	2.57 - 3.85

Lower Bentonite

	Mean (%)	Range (%)
Na_2O	2.18	1.94 - 2.43
MgO	2.76	2.48 - 3.33
Al_2O_3	16.77	15.75 - 17.73
SiO_2	67.76	65.50 - 70.73
P_2O_5	0.08	0.05 - 0.11
K_2O	1.10	0.61 - 1.43
CaO	2.38	1.44 - 3.32
TiO_2	0.38	0.24 - 0.47
MnO	0.03	0.02 - 0.04
Fe_2O_3	4.39	4.04 - 5.35

Table 6. Summary of the trace element mean PPM values and concentration ranges for the Sentinel Butte ash/bentonite

Upper Bentonite		
	Mean (PPM)	Range (PPM)
Cr	29	16 - 50
Co	33	26 - 54
Ni	51	40 - 63
Cu	25	22 - 32
Zn	94	85 - 109
Ga	23	22 - 25
Rb	56	41 - 76
Sr	315	216 - 426
Y	27	24 - 32
Zr	167	141 - 191
Nb	3	0 - 7
Ba	338	225 - 471
Pb	43	37 - 50

Middle Ash		
	Mean (PPM)	Range (PPM)
Cr	19	6 - 32
Co	30	20 - 41
Ni	54	47 - 68
Cu	22	18 - 26
Zn	84	68 - 101
Ga	23	22 - 25
Rb	155	97 - 139
Sr	429	353 - 496
Y	25	21 - 29
Zr	150	137 - 166
Nb	9	7 - 11
Ba	697	571 - 851
Pb	56	51 - 64

Lower Bentonite		
	Mean (PPM)	Range (PPM)
Cr	28	7 - 41
Co	34	27 - 43
Ni	49	40 - 57
Cu	26	18 - 30
Zn	101	75 - 119
Ga	24	21 - 27
Rb	59	38 - 71
Sr	304	257 - 346
Y	26	20 - 31
Zr	152	133 - 182
Nb	3	0 - 5
Ba	364	156 - 495
Pb	43	36 - 49

major oxide ranges of Na_2O, Al_2O_3, SiO_2, K_2O, and CaO are greater in the upper than in the lower bentonite. The larger concentration ranges for the upper bentonite suggest that post-depositional processes, i.e.,sheet wash, have contaminated this unit. A plot of the major element oxide ranges, for each unit of the Sentinel Butte ash/bentonite, is illustrated in Figure 7.

Trace Element Variability

The trace elements that have higher PPM concentrations in the ash than in the bentonites include Ni, Rb, Sr, Nb, Ba, and Pb. The trace element differences between the upper and the lower bentonites are negligible. Barium is found in higher PPM concentration in the lower bentonite, and the other trace element concentrations are essentially equal for both the upper and the lower bentonites. All of the trace elements show a smaller concentration range in the ash, except for Rb.

The compositional ranges of the trace elements vary greatly. Those trace elements with larger ranges in the upper bentonite include Rb, Co, Ni, Zr, Nb, and Sr. The lower bentonite exhibits higher compositional ranges for Cu, Zn, Ga, Y, and Ba. The trace elements Cr and Pb show essentially equal ranges for both the upper and the lower bentonites. A plot of the trace element concentration ranges, for each unit of the Sentinel Butte ash/bentonite is illustrated in Figure 8.

Figure 7. A plot of the major oxide concentration ranges in weight percent. The upper, middle and lower horizontal lines correspond to the upper bentonite, ash and the lower bentonite, respectively. Both P_2O_5 and MnO were left out of this illustration because of the very small ranges associated with these oxides.

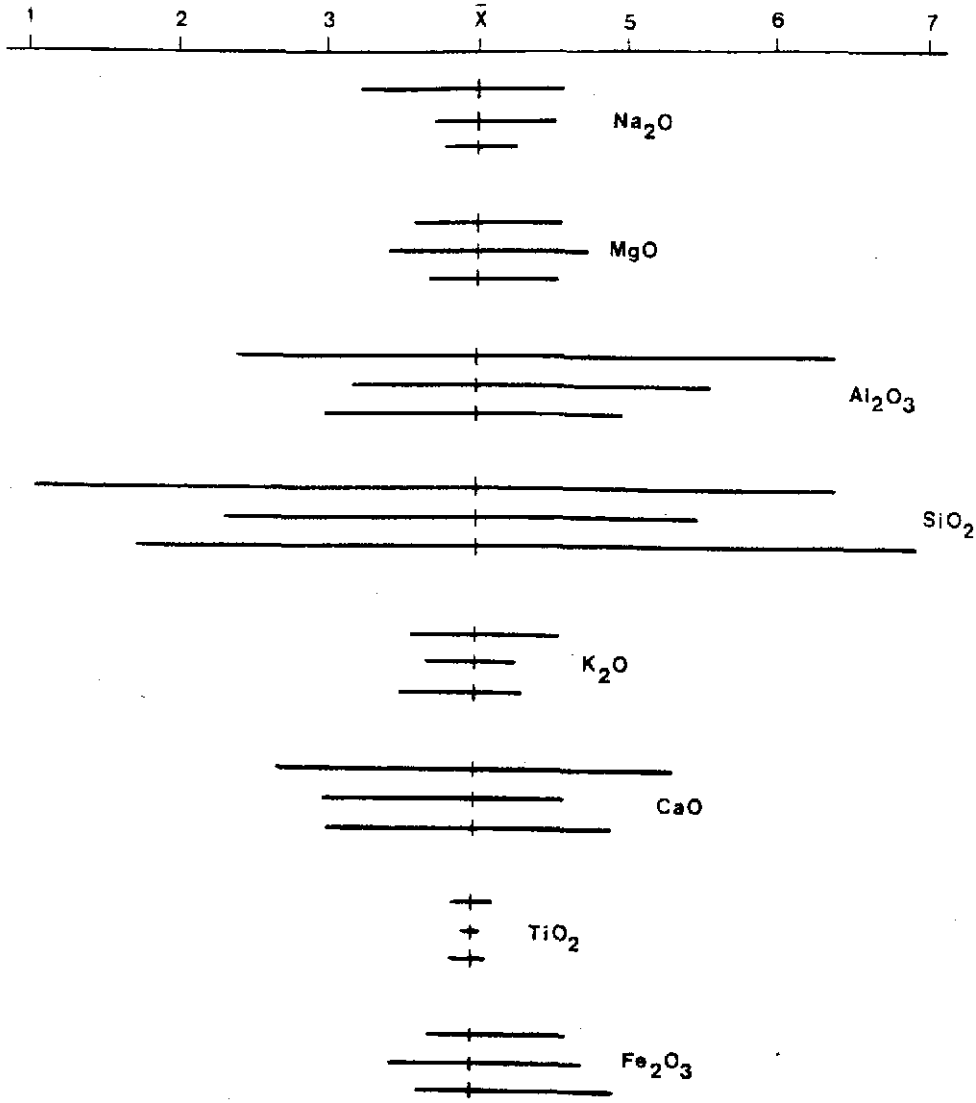
1
2
3
X̄
5
6
7
Na2O
MgO
Al2O3
SiO2
K2O
CaO
TiO2
Fe2O3

Figure 8. A plot of the trace element concentration ranges in PPM. The upper, middle and lower horizontal lines correspond to the upper bentonite, ash and the lower bentonite respectively. Sr and Ba have been plotted on a different scale to accommodate their large concentration ranges.

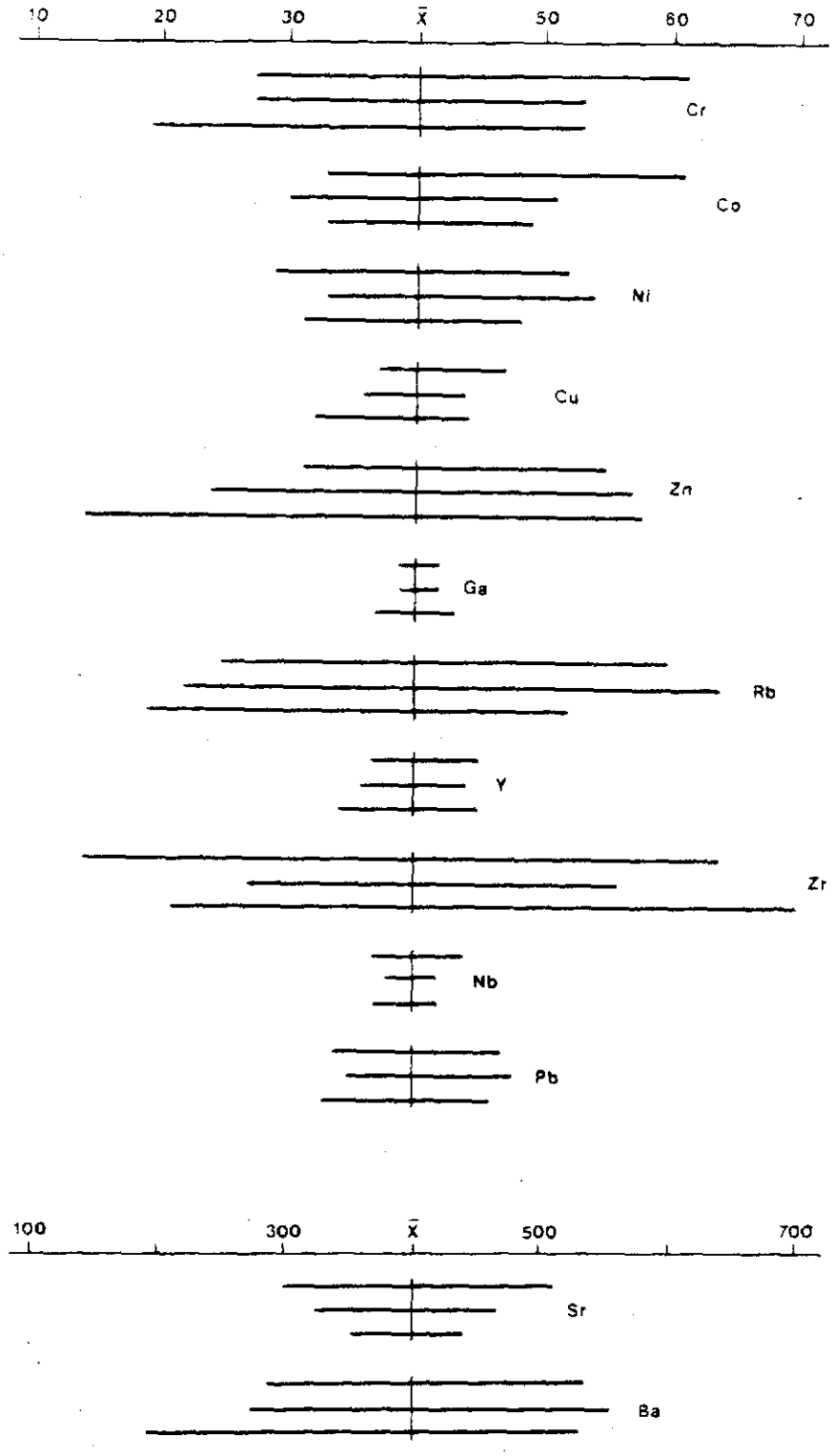
10
20
30
X̄
50
60
70
Cr
Co
Ni
Cu
Zn
Ga
Rb
Y
Zr
Nb
Pb
100
300
X̄
500
700
Sr
Ba

Geochemical Variation with Unit Thickness

The evaluation of the geochemical variation associated with the thickness of each unit of the Sentinel Butte ash/bentonite was accomplished by grouping the data into 1-meter-thick classes. The mean weight percent, the PPM value of each oxide, and trace element determinations were calculated from those samples that fell into a given class.

The upper bentonite was divided into 3 classes, 0 to 1, 1 to 2, and greater than 2 meters thick. The 1- to 2-meter class was the most heavily weighted group, with ten samples. The 0- to 1-meter class contained one sample, and the greater than 2-meter class contained four samples. The mean weight percent of Na_2O does not vary greatly. However, the 1- to 2-meter class has a lower mean, and represents a better estimate of the mean. The weight percentages of MgO, Al_2O_3, CaO, and Fe_2O_3 all show a decrease in concentration with an increase in thickness. The concentrations of SiO_2 and K_2O tend to increase with an increase in thickness in the upper bentonite. The oxide weight percentages of P_2O_5, TiO_2, and MnO were not included in the assessment of geochemical variation with thickness, due to their low concentration values. The lower bentonite was divided into four classes, 1 to 2, 2 to 3, 3 to 4, and greater than 4 meters thick. Four samples comprised the 1- to 2-meter class, three samples comprised both the 2 to 3, and greater than 4-meter classes, and the class of 3 to 4 meters contained five samples. The overall weight percentages of Na_2O, MgO, and Al_2O_3 tend, although not uniformly, to increase with an increase in thickness in the lower bentonite. The concentrations of SiO_2, K_2O, and CaO also

vary between classes, and tend to be slightly higher in the 2- to 3-, and 3- to 4-meter classes. The weight percent of Fe_2O_3 tends to decrease with an increase in thickness.

The ash was divided into three classes, 0 to 1, 1 to 2, and greater than 2 meters. The thickness classes of 0 to 1, and 1 to 2 meters had seven samples representing the mean. The greater than 2-meter class had one sample that represented the mean. In the ash the concentrations of Na_2O, SiO_2, and K_2O all show an increase with an increase in thickness. The oxides of MgO, Al_2O_3, and Fe_2O_3 show a decrease in concentration with an increase in thickness. The concentration of CaO is essentially equal for each thickness class of the ash. The mean concentration value of each major element oxide for each thickness class, for the upper and lower bentonites, and the ash are illustrated in Figure 9.

The thickness classes used to assess the geochemical variability of the trace elements are the same as those used for the major element oxides. The concentration of sulfur was not included in the assessment of the thickness variation, because of the erratic mean value for this element. The mean PPM values of Cu, Ga, Y, Nb, and Pb are essentially equal for each thickness class of the upper bentonite. The trace elements Co, Sr, and Ba decrease with an increase in thickness, and Cr, Ni, Zn, Rb, and Zr tend to increase with an increase in thickness.

The lower bentonite also exhibits essentially equal mean values for Cu, Ga, Y, Nb, and Pb, although Pb tends to increase slightly with an increase in thickness. The trace elements Ni and Rb also show equal mean values for each thickness class in the lower bentonite. The trace

Figure 9. A plot of thickness versus the major element oxide concentration range for the upper and lower bentonites and the ash.

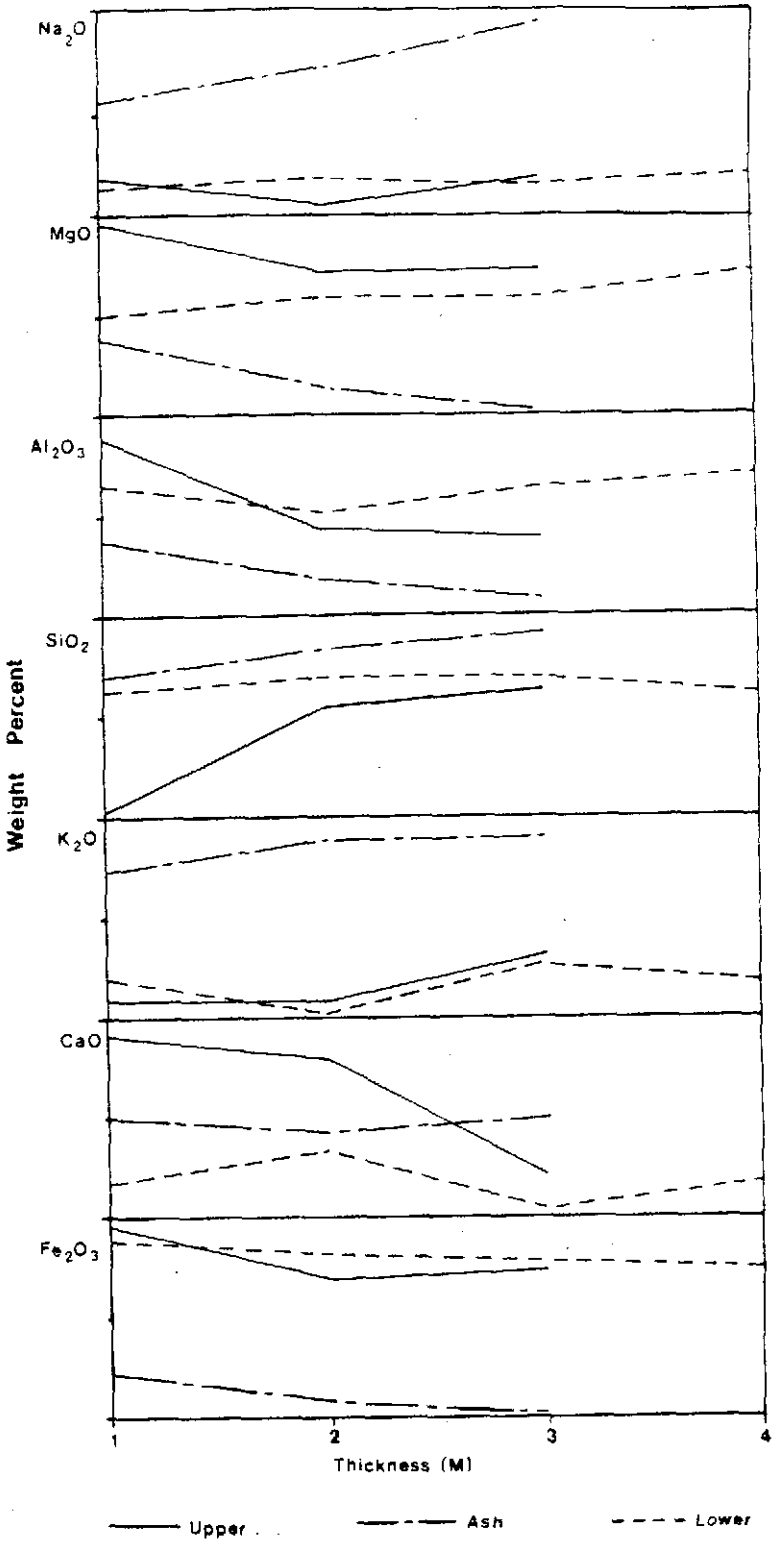
Na_2O
MgO
Al_2O_3
SiO_2
K_2O
CaO
Fe_2O_3
Weight Percent
1
2
3
4
Thickness (M)
Upper
Ash
Lower

elements Cr and Co tend to decrease in concentration with an increase in thickness, and Zn, Sr, Zr, and Ba tend to increase in concentration with an increase in thickness.

As in the upper and lower bentonites the ash exhibits equal mean concentration values for Cr, Ni, Cu, Ga, Y, Nb, and Pb in each thickness class. However, minor variations between classes are present, and Nb shows a slight increase in concentration with an increase in thickness. The trace elements Co, Zn, and Zr tend to decrease in concentration with an increase in thickness. The trace elements that show a tendency to increase in concentration with an increase in thickness are Rb and Ba. The variation in thickness associated with the trace elements is illustrated in Figure 10.

Geographic and Geologic Variation

The major and trace element geographic variation was assessed by establishing two groups of samples, a northern group that consists of samples 1, 2, 3, 5, 6, and 8, and a southern group that consists of samples 12, 17, 18, 20, 21, 24, 25, 26, and 27. It was necessary to treat the geographic variation in this fashion because of the random sampling scheme chosen, and the paucity of ash/bentonite deposits in the central portion of the study area. The geochemical means and variances of each sample in each group were tested for equality at the 97.5 percent confidence level using the student T test, and the F test, respectively (Davis, 1973, p.93-105).

Figure 10. A plot of thickness versus the trace element concentration range for the upper and lower bentonites and the ash.

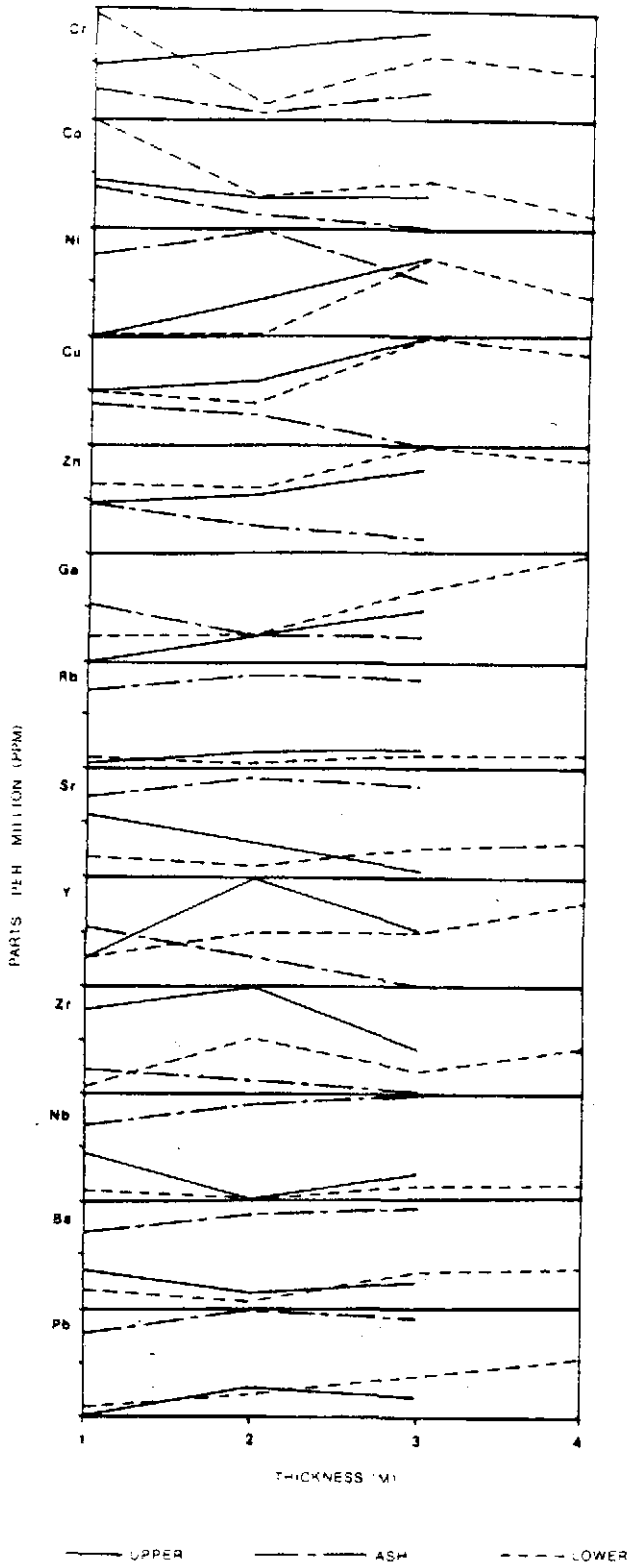
Cr
Co
Ni
Cu
Zn
Ga
Rb
Sr
Y
Zr
Nb
Ba
Pb
PARTS PER MILLION (PPM)
1
2
3
4
THICKNESS (M)
UPPER
ASH
LOWER

The oxide weight percentages of P_2O_5, MnO, and TiO_2 were not used in these tests due to their low concentration levels. In the upper bentonite, the concentrations of Na_2O, CaO, and SiO_2 were significantly different in the northern and southern groups. Those oxide mean values that were not equal in the lower bentonite included Na_2O, MgO, and K_2O, and the exchangeable cations Na_2O, K_2O, and CaO were not equal in the ash. The mean concentration values of elements in each unit of the Sentinel Butte ash/bentonite are illustrated in Figure 11.

The trace element concentrations were all found to be not significantly different in the northern and the southern groups, although the geochemical variability of the bentonites was greater than the variability of the ash.

Figure 11. A bar diagram of the mean concentrations of the major elements for the northern and southern groups. The weight percent scale on the right relates to Al_2O_3 and SiO_2.

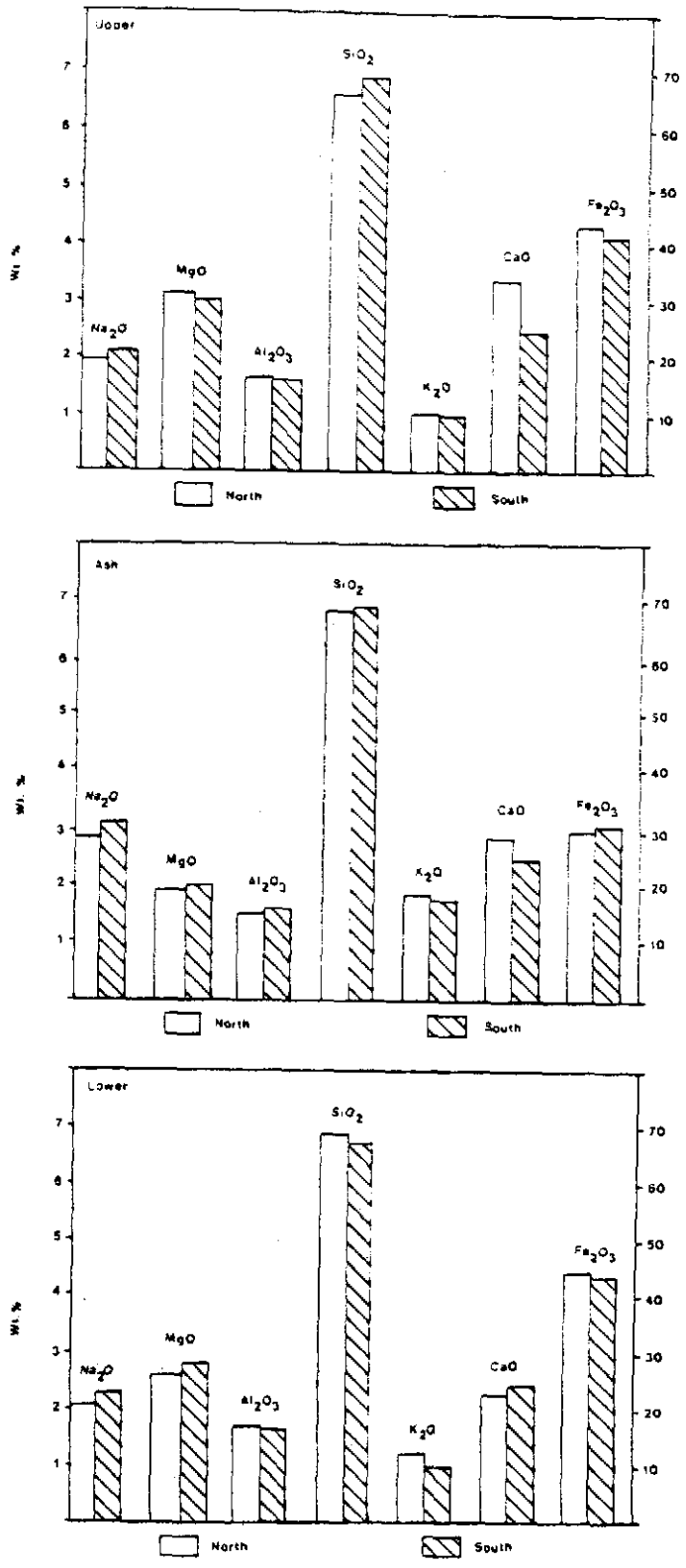
Upper
Ash
Lower
Wt. %
Na_2O
MgO
Al_2O_3
SiO_2
K_2O
CaO
Fe_2O_3
North
South

DISCUSSION

Statistical Analysis

Cluster Analysis

Cluster analysis was used primarily to determine if the upper and lower bentonites and the ash could be classified as separate units on the basis of the measured chemical variables. The three chemical groups, which cluster analysis was applied to, revealed that the major element group is characterized by three predominant clusters (Fig. 12) and the trace element group TR1 (Fig. 13) can be classified into three clusters. Trace element group TR2 can be classified into 2 clusters (Fig. 14). The major element clustering had a cophenetic correlation coefficient of 0.80, and the trace element groups, TR1 and TR2 had coefficients of 0.66 and 0.86, respectively. The ash in all three dendrograms is a chemically distinct group, undoubtedly reflecting its preservation history. The upper and lower bentonites, having undergone chemical alteration, reflect the diagenetic history of the original ash. The occurrence of some bentonite samples within the ash clusters, and some ash samples in the bentonite clusters, suggests either that micro-environments may have played a crucial role in controlling the dispersion of the chemical elements (Lowe, 1986, p. 283), or that the alteration process has not gone to completion. One ash sample was not classified as an ash when clustering the major element data, and instead was classified as a bentonite. Within the TR1 chemical group three ash samples were classified as bentonites. The TR1 chemical cluster also had five bentonite samples which were grouped with the ash.

Figure 12. Cluster dendrogram of the major oxide geochemical analysis of the Sentinel Butte ash/bentonite. The upper and lower bentonites and the ash are represented by A, C, and B, respectively.

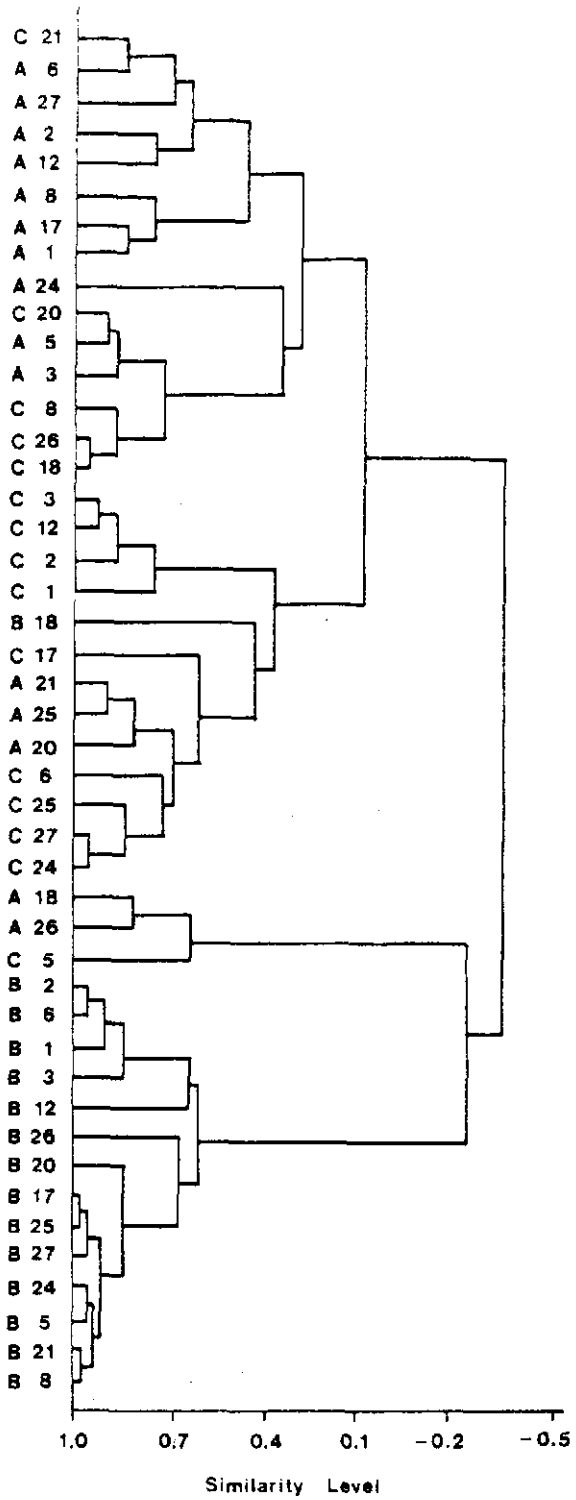
C 21
A 6
A 27
A 2
A 12
A 8
A 17
A 1
A 24
C 20
A 5
A 3
C 8
C 26
C 18
C 3
C 12
C 2
C 1
B 18
C 17
A 21
A 25
A 20
C 6
C 25
C 27
C 24
A 18
A 26
C 5
B 2
B 6
B 1
B 3
B 12
B 26
B 20
B 17
B 25
B 27
B 24
B 5
B 21
B 8
1.0
0.7
0.4
0.1
-0.2
-0.5
Similarity Level

Figure 13. Cluster dendrogram of the trace element group TR1 of the Sentinel Butte ash/bentonite. The upper and lower bentonites and the ash are represented by A, C, and B, respectively.

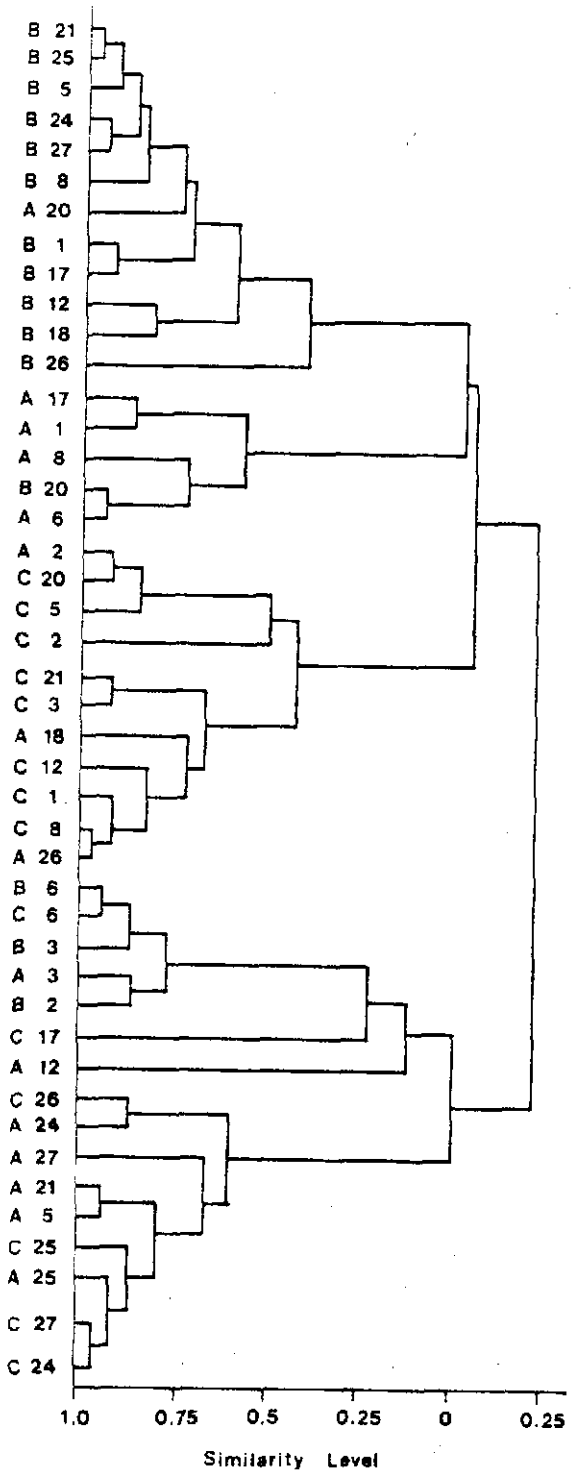
B 21
B 25
B 5
B 24
B 27
B 8
A 20
B 1
B 17
B 12
B 18
B 26
A 17
A 1
A 8
B 20
A 6
A 2
C 20
C 5
C 2
C 21
C 3
A 18
C 12
C 1
C 8
A 26
B 6
C 6
B 3
A 3
B 2
C 17
A 12
C 26
A 24
A 27
A 21
A 5
C 25
A 25
C 27
C 24
1.0
0.75
0.5
0.25
0
0.25
Similarity Level

Figure 14. Cluster dendrogram of the trace element group TR2 of the Sentinel Butte ash/bentonite. The upper and lower bentonites and the ash are represented by A, C, and B, respectively.

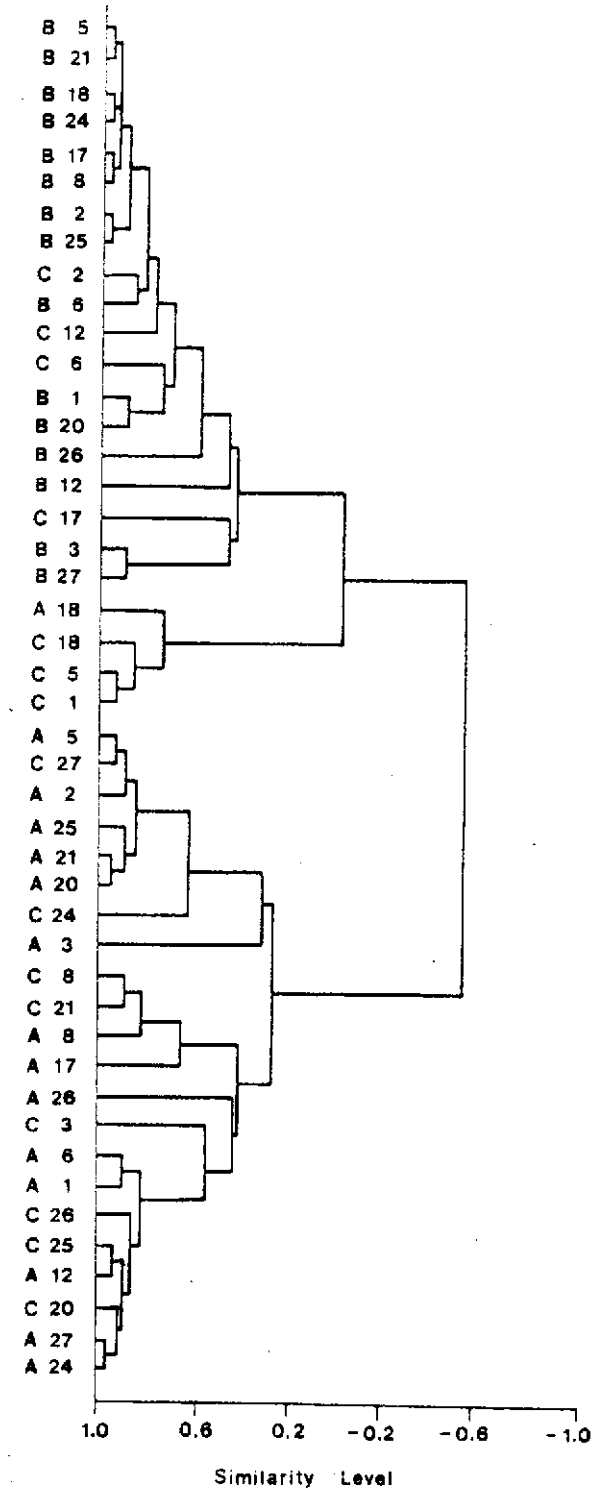
B 5
B 21
B 18
B 24
B 17
B 8
B 2
B 25
C 2
B 6
C 12
C 6
B 1
B 20
B 26
B 12
C 17
B 3
B 27
A 18
C 18
C 5
C 1
A 5
C 27
A 2
A 25
A 21
A 20
C 24
A 3
C 8
C 21
A 8
A 17
A 26
C 3
A 6
A 1
C 26
C 25
A 12
C 20
A 27
A 24
1.0
0.6
0.2
-0.2
-0.6
-1.0
Similarity Level

In the chemical group TR2, eight bentonite samples were included within the ash cluster. The upper and lower bentonites did not cluster into distinct groups. The clusters that were present, and included only bentonite samples, contained both upper and lower bentonites. This probably reflects a common chemical signature and parent material.

Discriminant Analysis

Discriminant analysis was used to establish the ability of all measured variables to distinguish between groups. A discriminant function was applied to each unit of the Sentinel Butte ash/bentonite. The percent contribution of each element to the separation is listed in Appendix E.

A significant discriminant function distance at the 99 percent confidence level was obtained between the upper, lower and ash units of the Sentinel Butte ash/bentonite. The results of the calculation of the percent contribution from each oxide variable shows that K_2O, Fe_2O_3, and TiO_2 contribute the most to the separation of the upper bentonite and the ash. The most significant contributions to the separation of the lower bentonite and the ash were from K_2O, TiO_2, and Na_2O. The discriminant results for the upper and lower bentonites show that P_2O_5, MgO, and Al_2O_3 are the primary contributors to the separation of these two units. The results of the major element discriminant analysis for the upper and lower bentonites and the ash are summarized in Figure 15.

The major element discriminators are probably not as useful as the trace element results for correlation purposes. However, several

Figure 15. Projection of the major element samples from Appendix E onto discriminant function lines. D^2 = Mahalonobis' distance. CL = confidence level.

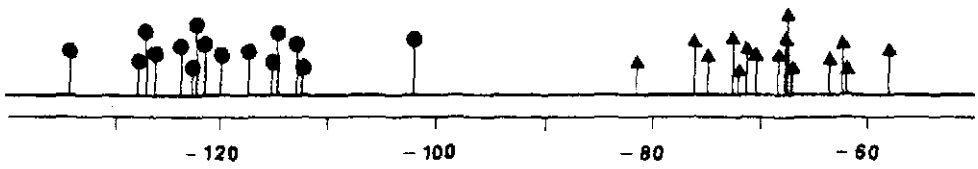

● = Upper Bentonite ▲ = Ash

$D^2 = 50.24$
CL = 99%

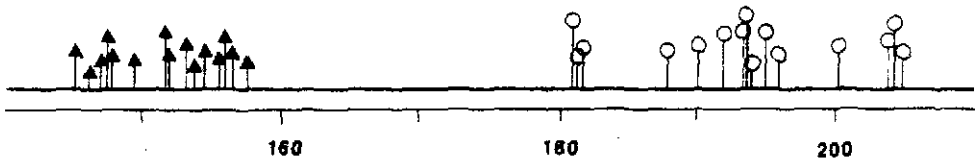

▲ = Ash ○ = Lower Bentonite

$D^2 = 40.21$
CL = 99%

● = Upper Bentonite ○ = Lower Bentonite

$D^2 = 35.55$
CL = 99%

generalizations can be made about the major element discriminators. The high percent contribution of K_2O and Na_2O in the discrimination of the upper and lower bentonites reflects the high alkali cation-exchange capacity of the montmorillonite clay structure. Cation exchange commonly occurs in an aqueous environment and therefore, much of the absorbtion of elements was probably syndepositional. Sodium becomes easier to release from the clay structure as the degree of saturation with Na^{++} becomes less (Grim, 1953, p. 146). It should also be noted that the dominant clay phase of the Sentinel Butte Formation is Na-montmorillonite. Caution should, therefore, be exercised when using these elements for discriminating clay units of the Sentinel Butte Formation.

Discriminant analysis of the TR1 trace element group shows that no significant differences exist between the upper and lower bentonites at the 99 percent confidence level. The null hypothesis was not rejected, and the variable means are equal. There are, however, significant differences between the upper and lower bentonites and the ash, as one would expect. Calculation of the percent contribution from the trace element variables of the upper bentonite and the ash showed that Zn, Cu, Ni, Cr, and Ga could be used to distinguish between these two units, although the elements Zn, Cu, and Ni contribute 81 percent of the total to the separation of the upper bentonite and the ash. The most significant discriminators at the 99 percent confidence level, when distinguishing the ash and the lower bentonite, are Zn, Ni, Cr, and Co. The discriminant analysis for the TR1 trace element group is summarized in Figure 16.

Figure 16. Projection of the trace element samples, TR1 from Appendix E onto discriminant function lines. D^2 = Mahalonobis' distance. CL = confidence level.

□ = Upper Bentonite ◆ = Ash

D^2 = 15.49

CL = 99%

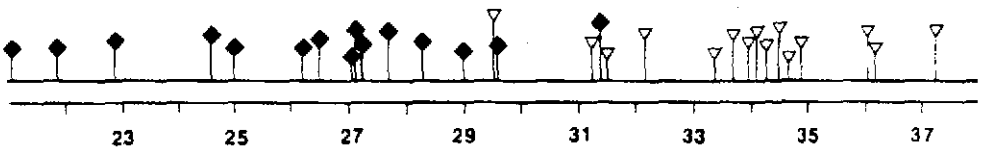

◆ = Ash ▽ = Lower Bentonite

D^2 = 7.18

CL = 99%

The TR2 chemical group responded to the discriminant analysis in much the same way as the TR1 chemical group. At the 99 percent confidence level the discriminant analysis showed that the upper and lower bentonites were very similar. The variable means were not equal; however, there is very little difference between the calculated F ratio and the tabled F value. This would suggest that the trace element chemistry of the upper and lower bentonites is similar. A comparison of the bentonite trace element chemistry to that of the parent ash reveals that Ba, Pb, Rb, Sr, and Nb have been leached from the ash. The leaching of these trace elements has been relatively uniform during the glass to bentonite alteration process and reflects the mobility of these elements. Yttrium concentration values for the ash/bentonite show that this element has remained essentially immobile during the alteration process. Zirconium concentration values tend to be higher in the upper and lower bentonites than in the ash. The higher Zr values in the bentonites supports the hypothesis that both syndepositional and post-depositional processes have controlled the distribution of this element. Calculation of the percent contribution of the TR2 variables reveals that the elements Zr, Y, Rb, Pb, and Nb all contribute to the separation of the upper and lower bentonites, although Zr alone contributes 97 percent to the separation.

Discriminant analysis of the upper bentonite and the ash shows that there is a large difference in elemental concentration of the TR2 group at the 99 percent confidence level. The percent contribution of the variables shows that Rb, Ba, Y, and Sr are significant contributors to the separation. The lower bentonite and the ash can be discriminated

by the elements Rb, Sr, Nb, and Y, although the most significant contributors to the separation are Rb and Sr. The discriminant analysis for the TR2 trace element group is summarized in Figure 17.

Three samples were collected from the ash at each randomly chosen sample site. Discriminant analysis was applied to each of these samples (see page 24). This was done to ascertain if the ash was geochemically uniform. The results of all three discriminant function tests showed that the means, of each chemical group, i.e., TR1, TR2, and the major elements, were equal and, therefore, the elemental compositions of the ash samples were uniform.

Factor Analysis

Factor analysis was employed to determine which measured variables, or combination of variables, account for the greatest variability between the units of the Sentinel Butte ash/bentonite. To evaluate the variability those elements that had the smallest variability between the units and geographically were used to establish a geochemical fingerprint. R - mode factor analysis, using a correlation coefficient matrix and retaining two factors on rotation, was used to perform the analyses. The rotated factor loadings are summarized in Appendix F.

Factor analysis of the major elements revealed that MgO and Fe_2O_3 account for the least amount of the variability in factor 1. The oxides of Ti and Al also exhibit a low variability in factor 1. The least amount of variability in factor 2 is accounted for by Na_2O, Al_2O_3 and SiO_2 (Table 16). A plot of the varimax factor scores (Fig. 18) shows that the ash forms a distinctive group, and the upper and lower

Figure 17. Projection of the trace element samples, TR2 from Appendix E onto discriminant function lines. D^2 = Mahalonobis' distance. CL = confidence level.

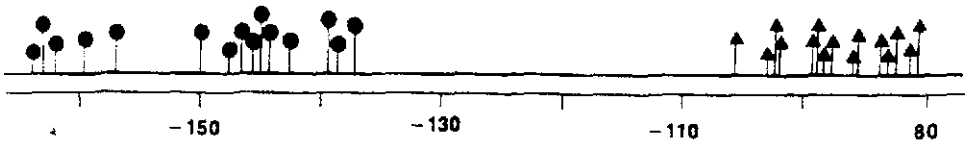

● = Upper Bentonite ▲ = Ash

$D^2 = 52.17$

CL = 99%

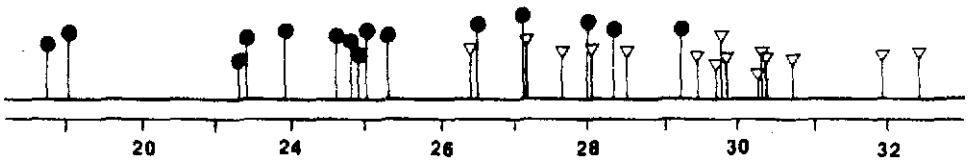

● = Upper Bentonite ▽ = Lower Bentonite

$D^2 = 4.41$

CL = 99%

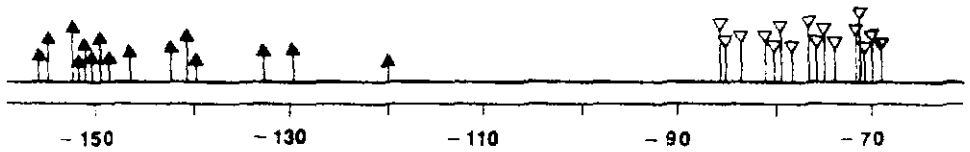

▲ = Ash ▽ = Lower Bentonite

$D^2 = 67.76$

CL = 99%

Figure 18. A plot of the major element group varimax scores from Appendix F. Open circles = upper bentonite, closed squares = lower bentonite, open squares = ash.

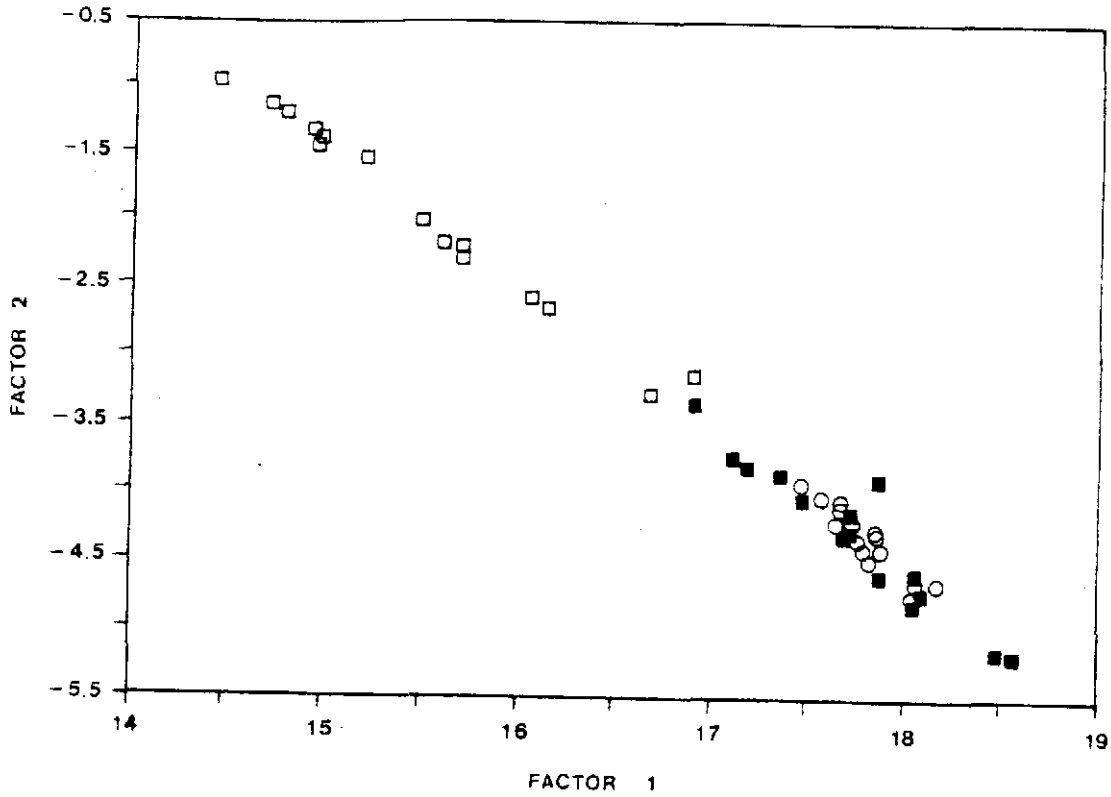
-0.5
-1.5
-2.5
-3.5
-4.5
-5.5
FACTOR 2
14
15
16
17
18
19
FACTOR 1

bentonites do not differ significantly from one another. The variability within the ash appears to be much greater than the variability between the bentonites. This probably reflects the varying degree of alteration of the metastable volcanic glass within the ash as compared to more complete alteration in the bentonites.

Factor analysis of the two trace element groups TR1 and TR2 was accomplished by combining the two groups to form one group (Table 16). Sulfur was not included in the trace element factor analysis, because of its erratic variability throughout the Sentinel Butte ash/bentonite. As stated above, the concentration values of Cr and Co were included in the statistical evaluation, but were not considered in the final results.

The measured variables that exhibit the least amount of variability, and hence are useful as geochemical fingerprints, are Cu, Zn, Ga, Y, and Zr. This fingerprint can be used to assess whether other bentonites and/or ashes are correlative with the Sentinel Butte ash/bentonite. A plot of the first two factor scores shows that the data plot as two well-defined groups (Fig. 19). The ash plots as a distinct group, and the upper and lower bentonites plot as another group. Factors 1 and 2 appear to represent the degree of alteration within each unit of the Sentinel Butte ash/bentonite. Discriminant analysis shows that the units can be chemically distinguished from one another (excluding the upper and lower bentonites, using chemical group TR1). Factor analysis results suggest that the degree of alteration within the upper and lower bentonites is very similar, and that the ash is a distinct group. The upper and lower bentonites plot as one

Figure 19. Plot of the combined trace element varimax factor scores from groups TR1 and TR2. Open circles = upper bentonite, closed circles = lower bentonite, and the open squares = ash.

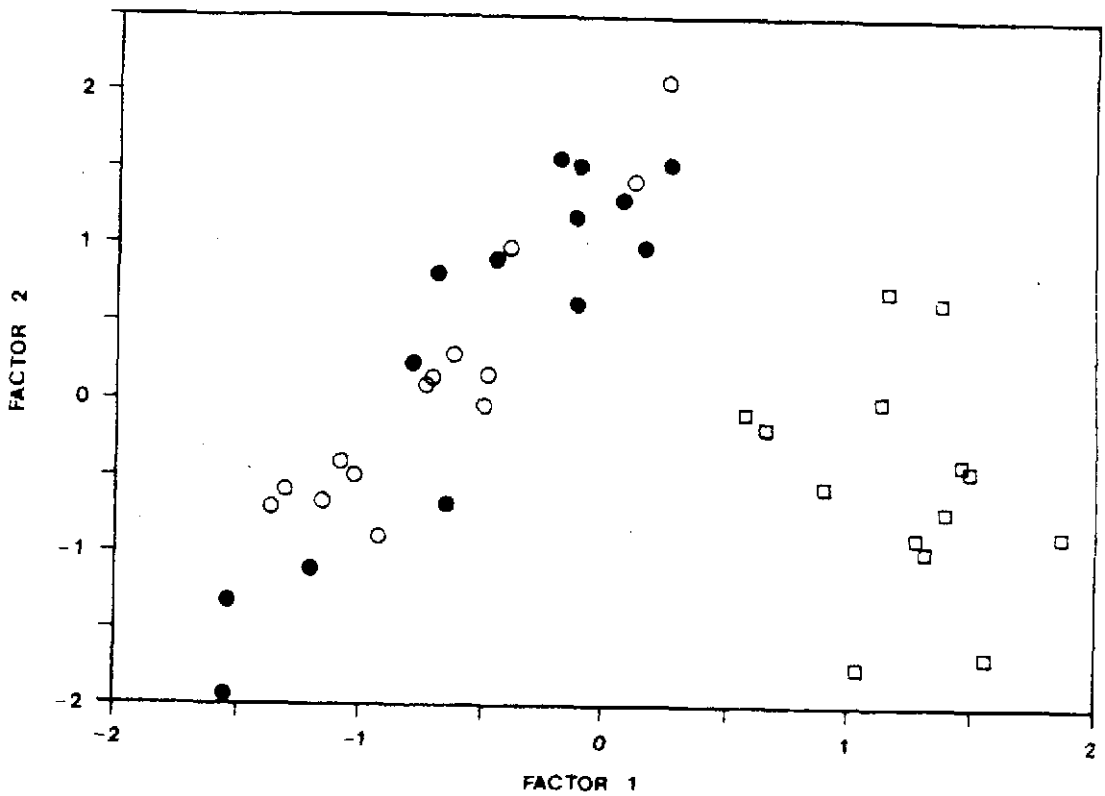
FACTOR 2
FACTOR 1
2
1
0
-1
-2
-2
-1
0
1
2

group within the major element group, and the ash plots as a separate group. However, two ash samples plot with the bentonite group (see Fig. 18), suggesting that these samples are altered more than the other ash samples. The failure of factor analysis to differentiate between the bentonite units suggests that the alteration process has been relatively uniform through the deposit.

Comparison of this Study to Previous Works

Geochemical fingerprinting of tephra units has focused primarily on deposits that are no older than Tertiary, although an Ordovician K-bentonite has been successfully fingerprinted and correlated over 300 kilometers (Huff, 1983). Volcanic glasses are thermodynamically unstable in most geologic environments, and typically alter and become less recognizable as a volcanic deposit. The metastability of volcanic glass provides a unique opportunity to study the alteration process of an ash to a bentonite or tonstein (Zielinski, 1985). These alteration products also retain a significant geochemical signature, and can be used for correlation purposes. A comparison of the present study to previous works will provide a basis for the techniques used, and a broader understanding of geochemically fingerprinting volcanic tephras and their alteration products.

The use of glass and clay separates for geochemically fingerprinting a geologic unit has been the sample preparation technique used by many geochemists to reduce the effects of detrital contamination (Howorth and Rankin, 1975; Martz and Brown, 1981; Randle et al., 1971; Sarna-Wojcicki et al., 1979; Smith and Nash, 1976). Many techniques have been established for the separation of specific phases, although the Sentinel Butte ash/bentonite did not lend itself to those techniques. The use of whole rock analysis to characterize the geochemistry of a unit has also been used successfully. Borchardt et al. (1971) determined that the concentration of major and trace elements in the clay fraction of Mazama soils were independent of distance from the source. Lindsey (1975), in assessing the affects of sedimentation

and diagenesis on trace element composition of tuffs, found that sedimentation and erosion effectively concentrated some minerals and trace elements. He also found that diagenesis did not alter the trace element composition of the tuffs. Bowles et al. (1973) found that the chemical signature of an ash, collected from extensive areas of the Pacific seafloor, was not destroyed by devitrification, chemical alteration by seawater, or masking by contamination and mechanical mixing. Whole rock analysis can be useful for geochemically fingerprinting a stratigraphic unit, but it is necessary to carefully document the existing compositional variation present in the samples.

X-ray fluorescence techniques were used for the present study primarily because of available instrumentation. This analytical technique has proven to be an effective method for the analysis of major elements and a wide range of trace elements. Sarna-Wojcicki et al. (1979) found that trace element results obtained by x-ray fluorescence were comparable to those obtained by neutron activation analysis. X-ray fluorescence data were also found to compare well with Sr and O isotope ratios (Jack et al., 1968).

Statistical analysis provides a basis by which separated geologic units can be compared and contrasted. Cluster and discriminant analysis have been employed to group and categorize different tephra units based on their geochemistry. Smith (1975) used a similarity matrix established by Borchardt et al. (1971, equation 1) to initially distinguish between differing ash units. Cluster analysis based on weighted-pair group means was then applied to normalized geochemical

data. Smith found that a significant refinement of the chemical groups was possible using cluster analysis over the similarity matrix.

Discriminant analysis has been employed to establish the ability of all variables to discriminate between groups. This statistical technique has been used with excellent success (Huff, 1983, Smith-Pope, 1975, Borchardt et al., 1971). Smith-Pope (1975) was able to differentiate seven different tephra units in the Bonneville Basin, Utah by utilizing discriminant analysis on trace element data. Huff (1983) successfully differentiated six different Ordovician potassium rich bentonites over 300 kilometers using discriminant analysis. Forsman (1985) used discriminant analysis to assess whether significant major element differences exist between clays of detrital, glass-derived, precipitated, and of unknown origins. He found that glass-derived clays are distinct from Sentinel Butte clays of other origins. The silicon values accounted for most of the major element differences between these clay types.

Various trace and major elements have been useful for fingerprinting specific tephra units. A comparison of those elements useful for fingerprinting, in previous works to those found useful in this study, reveals that several elements recur in geochemical signatures. Table 7 summarizes the useful elements for the above mentioned studies. Izett et al. (1970) found Fe, Zn, Ca, Rb, and Sr useful for distinguishing rhyolitic ashes. To chemically fingerprint acidic volcanic rocks, Jack and Carmichael (1968) found Ti, Mn, Co, Ni, Cu, Zn, Ga, Rb, Sr, Y, Nb, and Ba to be useful geochemical fingerprints; and that Ba, Sr, and Zr varied according to source area.

Richardson and Ninkovich (1976) utilized Zr and Y to correlate and trace ashes, whereas Smith and Nash (1976) used Ba, Fe, and Rb. Huff (1983) correlated Ordovician K-Bentonites using Rb, Cr, Fe, Ga, and K as geochemical fingerprints.

Table 7. A summary of the elements used as geochemical fingerprints in previous studies and the present study

Present Study 1988	Izett et al. 1970	Jack and Carmichael 1968	Richardson and Ninkovich 1976	Smith and Nash 1976	Huff 1983
(Cr)	Fe	Ti	Zr	Ba	Rb
(Co)	Zn	Mn	Y	Fe	Cr
Cu	Ca	Co		Rb	Fe
Zn	Rb	Ni			Ga
Ga	Sr	Cu			K
Y		Zn			
Zr		Ga			
Fe		Rb			
Ti		Sr			
		Y			
		Nb			
		Ba			

Huff also found that, using three elements, he could assign an unknown sample to a specific K-bentonite with 70 percent confidence. The elements useful for this study, and common to the above mentioned previous studies, are Cr, Co, Cu, Zn, Ga, Y, Zr, Fe, and Ti. These elements are those that had the least amount of variability associated with the ash/bentonite as a whole, and are considered to be useful geochemical fingerprints.

Utility of the Major Elements for Correlation

The geochemical characteristics and variability of the Sentinel Butte bentonites are largely controlled by the composition of the parent ash, the high cation exchange capacity of the montmorillonite clay, and detrital contamination. The geochemistry of the ash is also affected by these three factors, although not to the same degree. The sandwiched nature of the ash has preserved it from alteration, and hence it exhibits a much more uniform geochemical variability. Detrital contamination, (syndepositional, and a minor amount of post-depositional contamination) and local hydrolysis of the vesicle walls control what geochemical variability is present in the ash.

Concentration variations with thickness are not unexpected, assuming that the thinner bentonite and ash deposits are altered to a greater degree than the thicker deposits. The silica concentration in each of the units of the Sentinel Butte ash/bentonite increases with an increase in thickness. This would suggest that the thicker deposits are less altered, or that the silica released during alteration was not flushed from that given unit. The concentrations of the exchangeable cations, i.e., Na_2O, K_2O, CaO, and MgO would be expected to be variable between thickness classes due to the high cation exchange capacity of the montmorillonite clay.

The major element geographic variability of the Sentinel Butte ash/bentonite is dominated by the exchangeable cations of, Na, K, Ca, Mg and SiO_2. In the upper bentonite the greater variability of SiO_2 reflects the effects of detrital contamination from the overlying geologic units. Between the northern and southern groups the ash and

lower bentonite exhibit significant major element variability at the 95 percent confidence level. The elements that contribute the most to this variability are the exchangeable cations (Na, Mg, K, and Ca).

Discriminant analysis of the major oxides shows that each unit of the ash/bentonite is geochemically distinct. These differences can be accounted for by leaching of elements through devitrification of the glass, and subsequent cation exchange of the alkali cations Na, Mg, K, and Ca. Detrital contamination can also account for some of the major oxide variability. Forsman (1985) determined that the compositional range of the plagioclase grains was larger than would be expected for phenocrysts from a single volcanic event. However, mineralogical zoning in the magma chamber may have produced a larger compositional range for the phenocrysts.

The presence of a silica-enriched zone at the top of the underlying unit, and the presence of cristobalite primarily in the lower bentonite, indicates that silica was leached from the ash during alteration. The depletion of Na_2O and K_2O in the bentonites relative to the ash is expected given the relative solubility of the alkali cations. A large variation in concentration from sample to sample is also expected of these cations, due to the variable alkali exchange accompanying hydration of the volcanic glass. The variable concentration of CaO in the Sentinel Butte ash/bentonite can be attributed to detrital contamination of Ca-rich phases and/or the addition of Ca^{++} through ion-rich groundwater. The latter is a more favorable hypothesis due to the presence of calcite in the clay separate fraction (see p. 25), which is present in the 0.3- to 0.6-micrometer size range, and is

undoubtedly authigenic in origin. However, the upper bentonite shows a higher compositional range for CaO, than the ash or lower bentonite suggesting that post-depositional processes have contaminated the upper bentonite with Ca-rich phases.

The major oxides that occur in higher concentrations in the bentonites are, TiO_2, MgO, and Fe_2O_3. The enrichment of TiO_2 in both the upper and lower bentonites compared with the ash is presumably the result of detrital contamination. Syndepositional mixing of the underlying unit and the original tephra may explain the higher concentrations in the lower bentonite. Higher TiO_2 values in the upper bentonite can also be explained by both syndepositional and post-depositional contamination.

Aluminum is assumed to be relatively immobile under low-temperature alteration, and, therefore, is presumably present in higher concentrations in the bentonites because of detrital contamination by aluminum silicate phases. The compositional range of Al_2O_3 is larger in the upper bentonite than the lower bentonite or the ash, supporting the hypothesis of post-depositional sheet wash contamination from the overlying units.

The oxides Fe_2O_3 and MgO are required for the formation of montmorillonite (Blatt et al., 1980, p. 388), and both are found in higher concentrations in the bentonites than in the ash. The enrichment of MgO in the bentonites has presumably occurred through cation exchange of Mg^{++}, which was introduced by groundwater during the alteration of the ash. The enrichment of Fe_2O_3 is also presumed to have resulted from the introduction by groundwater. This hypothesis is partially

supported by the larger compositional range for MgO in the ash. The compositional range of MgO would be expected to be more variable in the ash, because of the varying degree of glass alteration, and hence available cation exchange sites. The well-crystallized bentonites have the required Mg^{++} and Fe^{++} to fill the montmorillonite clay structure, and hence only minor cation exchange can occur with these elements in the bentonites. Some of the available Mg^{++} and Fe^{++} was probably initially introduced into the bentonites by leaching mechanisms, from the ash. Grim (1953) stated " ... the ash must have a moderate content of MgO, since ash devoid of magnesia does not seem to alter to montmorillonite."

Factor analysis of the major elements showed that Fe_2O_3, MgO, Al_2O_3, and TiO_2 had the least amount of variability in the Sentinel Butte ash/bentonite. These oxides can, therefore, be useful as geochemical fingerprints, although MgO is an exchangeable cation, and the concentration of Al_2O_3 is not sufficiently unique to be useful as a geochemical fingerprint. Both Fe_2O_3 and TiO_2 have been useful as fingerprint elements in previous studies (see Table 7). Because of the large variability associated with many of the other major oxides, excluding Fe_2O_3 and TiO_2, they are not considered to be useful for correlation purposes.

Utility of the Trace Elements for Correlation

Trace element geochemistry is by far the most useful correlation tool available to the geologist, provided the geochemical variation can be documented. The trace elements found useful for this study are primarily transition metals that are essentially immobile under low temperature and pressure conditions. The remaining trace elements are exchangeable cations, and their variability is larger than was acceptable for fingerprinting and geochemical correlation.

The geochemical fingerprint of the Sentinel Butte ash/bentonite was based on the results of factor analysis. Those trace elements that exhibited the least amount of variability, and hence are useful as fingerprints, included Cr, Co, Cu, Ni, Zn, Zr, Y, and Ga. However, the within-sample variation for Cr and Co (standard deviation) on the standard reference materials varied greatly, and, therefore, these elements were not considered in the final results.

The concentration of gallium shows very little variation, which is expected due to its geochemical affinity with aluminum. Yttrium is also considered to be relatively immobile during low-temperature alteration processes (Wedephol, 1969). The Zr concentration is, at least in part, the result of the presence of this element in a resistant accessory mineral, zircon.

The trace element fingerprint of the Sentinel Butte ash/bentonite has been used in comparisons with other bentonitic units in the Sentinel Butte Formation. Fifteen grab samples possibly correlative with the Sentinel Butte ash/bentonite were collected from locations outside the random sampling area. Both discriminant and factor analysis were

employed to determine if the unknown grab samples were, in fact, geochemically distinct from the ash/bentonite.

Discrimination of the upper and lower bentonites with the grab samples revealed that the means were not equal at the 99 percent confidence level for both trace element groups TR1 and TR2. Calculation of the percent contribution of the variables for trace element group TR1 reveals that the significant contributors to the separation of the grab samples and the lower bentonite are Cu and Co. The significant contributors to the separation of the grab samples and the upper bentonite for trace element group TR1 are Cu, Zn, and Co.

Calculation of the percent contribution of the variables for trace element group TR2 reveals that the significant contributors to the separation of the grab samples and the lower bentonite are Ba, Rb, and Zr. The significant contributors to the separation of the grab samples and the upper bentonite for trace element group TR2 are Ba and Rb. However, Ba alone contributes 543 percent to the total separation of the grab samples and the lower bentonite. The total of all the variables must be 100 percent, although a negative variable, which decreases the total separation is possible. As with the discriminant analysis of the lower bentonite and the grab samples, Ba contributes 579 percent to the separation of the upper bentonite and the grab samples. The discriminant scores of the upper and lower bentonites and the grab samples are illustrated in Figure 20.

The large percent contribution to the separation of the upper and lower bentonites, and the grab samples may be due, in part, to the presence of Ba in more than one chemical form, i.e., $BaSO_4$, and BaO.

Figure 20. Projection of the trace element group TR2, with the upper and lower bentonites, and the grab samples from Appendix E onto discriminant function lines. A = trace element group TR1, and B = trace element group TR2. D^2 = Mahalonobis' distance. CL = confidence level.

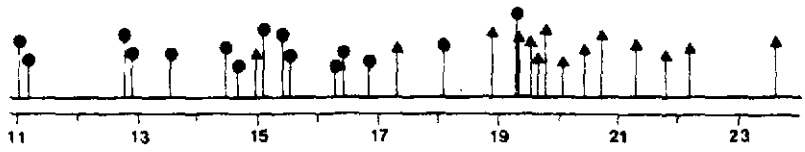

● = Grab Samples ▲ = Upper Bentonite

$D^2 = 5.06$

CL = 99%

A

● = Grab Samples ▲ = Lower Bentonite

$D^2 = 7.59$

CL = 99%

▲ = Upper Bentonite ● = Grab Samples

$D^2 = 11.81$

CL = 99%

B

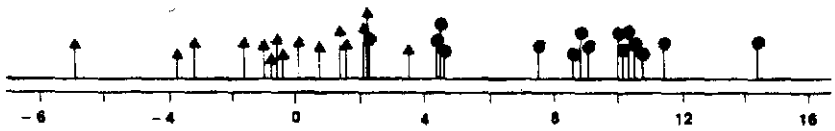

▲ = Lower Bentonite ● = Grab Sample

$D^2 = 8.93$

CL = 99%

The Dataflex software was programmed to quantify Ba, although backscatter scanning electron microprobe techniques reveal the presence of BaO in the ash (Fig. 21). In the field, barite nodules occur at various locations, indicating that Ba is also in the form $BaSO_4$.

Careful field mapping and lateral tracing of the ash/bentonite indicated that many of the grab samples are at the same stratigraphic position with the Sentinel Butte ash/bentonite. However, discriminant analysis suggests that the grab samples are geochemically distinct from the ash/bentonite. Sedimentation mechanisms and variable diagenesis along the lateral extent of the ash/bentonite may account for this. The presence of aqueous ripple marks directly below the lower bentonite, and the fact that the ash is everywhere laminated, supports the hypothesis that the Sentinel Butte ash/bentonite was deposited in a lacustrine environment. If this hypothesis is true, then the grab samples were collected near the shoreline of the lake. The lacustrine environment would act as a sink for the airfall debris, and deposition of the ash (10 to 60 micron grain size) would take place slowly. The shoreline would tend to be a zone where volcanic debris and the surrounding sediments mixed. Whole rock chemical analysis of samples that were collected from this environment would tend to have a wider range of composition, compared to the samples collected from the "lake." The physical boundaries of the bentonite would also be obscured, making it more difficult to sample that unit specifically. Considering sedimentation effects, and a poorly defined unit, the discriminant function for the grab samples and for the upper and lower bentonites would show that the two groups are not chemically equivalent. Variable

Figure 21. Backscatter and secondary electron photomicrograph of BaO in an ash sample. Left view is the backscattered image, the light region in the center is BaO. Right view is the secondary image.

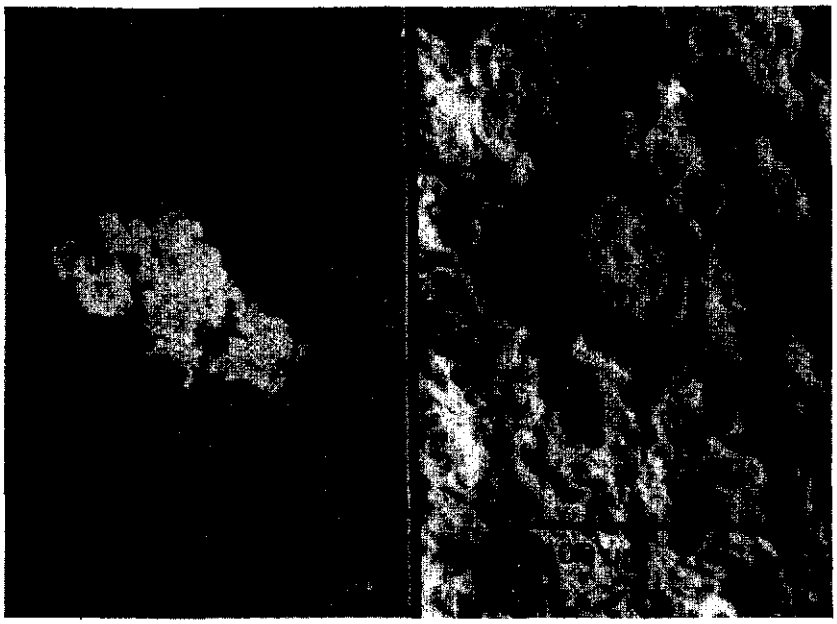

diagenesis along the lateral extent of the Sentinel Butte ash/bentonite may have also played a role in chemically differentiating this unit and the grab samples. Micro-environments that can concentrate some trace elements may have also played a role geochemically differentiating the grab samples and the upper and lower bentonites. However, Lindsey (1975) and Bowles et al. (1973) concluded that diagenetic effects do not alter the geochemical signature of a tephra unit. Factor analysis supports this result, and shows that the trace element variability in all but three grab samples is the same as that of the upper and lower bentonites (Fig. 22). Those samples, LX-6, SM-6, and LB-6, correspond to sample locations that have been considered to be correlative bentonitic deposits. These three outlier grab samples have greater geochemical variability and, are, therefore, not correlative with, the Sentinel Butte bentonites.

Grab sample BR was collected from a bentonitic unit in the Sentinel Butte Formation approximately 30 to 40 feet above the contact with the Bullion Creek Formation. This bentonite caps prominent buttes and can be traced for several miles in the tributary drainages on the east side of the Little Missouri River. This is in contrast to the Sentinel Butte ash/bentonite which is approximately 300 feet above the contact in the Theodore Roosevelt National Park. To date, no volcanic glass has been identified in the grab sample BR (personal communication, Dr. Forsman, 1987). However, the results of factor analysis show that its geochemical variability and chemical signature are similar to that of the known Sentinel Butte deposit, and suggest that it is correlative with the Sentinel Butte bentonites. The questions that this observation

Figure 22. Plot of the trace element and the grab sample varimax factor scores. Open circles = upper and lower bentonites, open squares = ash, and the closed triangles = grab samples.

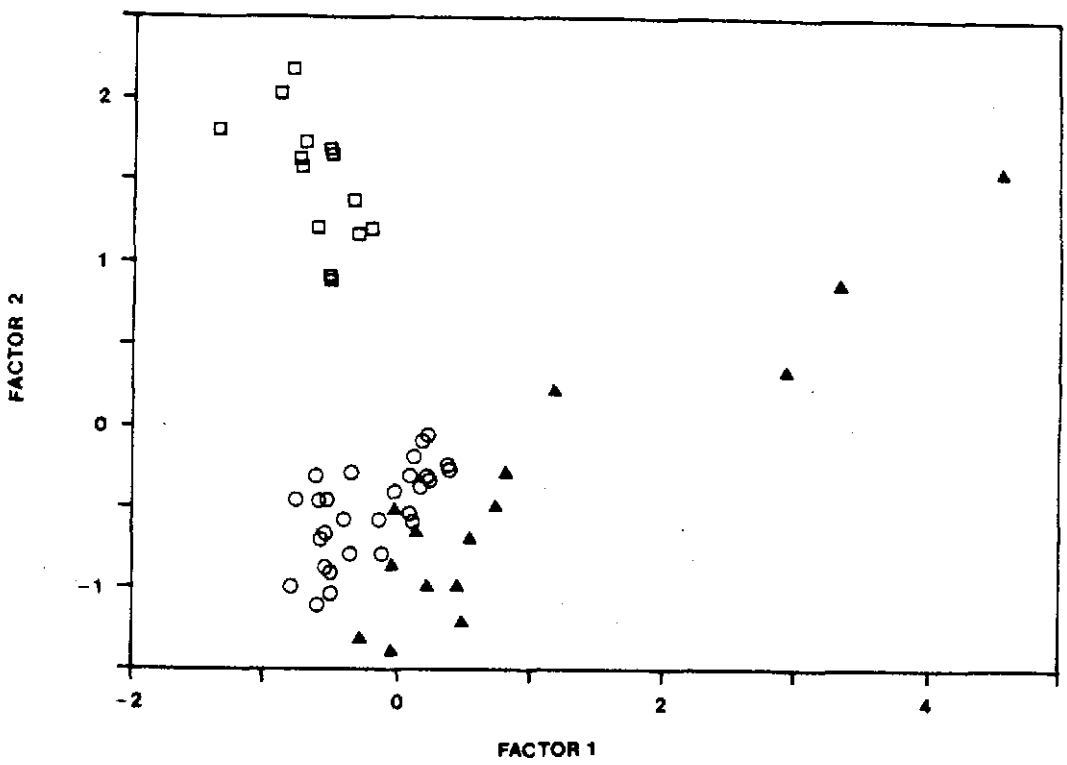
FACTOR 2
2
1
0
-1
-2
0
2
4
FACTOR 1

creates deserve further scrutiny, although they are beyond the scope of this study.

The utility of the trace elements for correlation of the Sentinel Butte ash/bentonite based on discriminant analysis is plagued with the problem of sedimentation effects. This effect has been to dilute the Sentinel Butte bentonite where it is thin, i.e., less than 50 to 70 centimeters, and hence the grab samples geochemically appear different than the known bentonite samples. The use of clay separates would undoubtedly reduce the effects of sedimentation, although sampling these thin bentonites would still pose a problem.

The geochemical signature of the Sentinel Butte bentonites has not been lost through sedimentation effects. Factor analysis effectively identified three grab samples that were not correlative with the Sentinel Butte bentonites, based on their geochemical signature and variability. The same separation of sample groups was also found using just trace element group TR2. The use of clay separates would refine the comparisons of the grab samples and the upper and lower bentonite groups even further. This statistical technique would provide a powerful tool for unravelling the stratigraphic and sedimentologic history of the Paleocene section in western North Dakota and surrounding areas.

CONCLUSIONS

1. Mapping of the Sentinel Butte ash/bentonite has extended the previously known range, primarily to the west and southwest. Although not the primary purpose of this study, mapping provided insight into the depositional history and a better understanding of the processes that effect the chemical variability.

2. The major and the trace element variability can be classified into four groups; those elements that occur in higher concentrations in the ash, those that are higher in the bentonites, those that are essentially equal throughout the unit, and those that are higher in the upper bentonite. Leaching of the soluble cations, introduction of elements through ion-rich groundwater, and syn-depositional and post-depositional contamination are the primary processes that control the geochemical variability of the Sentinel Butte ash/bentonite. The geochemical variation of the trace elements shows that compositional differences between the upper and lower bentonites are negligible.

3. Classification of the Sentinel Butte ash/bentonite by cluster analysis shows that the ash is chemically a distinct unit. The upper and lower bentonites can not be classified into separate units utilizing cluster analysis. Discriminant analysis reveals that significant differences are present in the major element concentrations of the upper and lower bentonites and the ash.

Discrimination of the trace element group TR1 shows that no significant chemical differences exist between the upper and lower bentonites, whereas calculation of the discriminant function for the trace element group TR2 indicates a significant difference between the upper and lower bentonites. Factor analysis of the major element oxides shows that the ash is geochemically distinct from the upper and lower bentonites. The trace elements also show the same differentiation between the ash and the bentonites.

4. Factor analysis of the major element oxides indicates that Fe_2O_3 and TiO_2 show the least amount of variability. The trace elements that show the least amount of variability within the Sentinel Butte ash/bentonite are Cu, Zn, Ga, Y, and Zr. These trace elements, and major element oxides define a preliminary geochemical signature for the ash/bentonite (Fe_2O_3, TiO_2, Cu, Zn, Ga, Y, and Zr).

5. The utility of the Sentinel Butte bentonite for correlation purposes is demonstrated by the results of factor analysis comparisons on the ash/bentonite and grab samples. Factor analysis successfully identified three of the grab samples as not correlative to the Sentinel Butte ash/bentonite.

APPENDICES

APPENDIX A

Sample Descriptions

Sample: 1 Location:149-99-7ba

Upper Bentonite: A 1.1, 1.0, 1.2
Middle Ash: B 1.1, 1.0, 1.2
Lower Bentonite: C 1.1, 1.0, 1.2

Description of Sentinel Butte ash/bentonite:

Thickness of each layer: U. Ben. = 1.70
Ash = 1.01
L. Ben. = 1.83
Total thickness in meters = 4.54

Contacts with surrounding strata:
The lower contact is sharp, and is partially covered due to the draping of the lower bentonite.
The upper contact is gradational.

Ash/bentonite contact:
Horizontal, and transitional; upper: 5-10cm., lower: 10-15cm.

Sedimentary Structures:
Ash: laminated, with plant fragments between some of the laminations.
Grain size of ash: .01-.02 mm.
Bentonite: massive
Oval to circular iron-stained blotches occur on each layer.

Concretions: Barite occurs on the lower bentonite.

Evidence of detrital admixture: none

Sample: 2 Location:149-99-5cc

Upper Bentonite: A 2.1, 2.0, 2.2
Middle Ash: B 2.1, 2.0, 2.2
Lower Bentonite: C 2.1, 2.0, 2.2

Description of Sentinel Butte ash/bentonite:

Thickness of each layer: U. Ben. = 1.73
Ash = 0.30
L. Ben. = 3.25
Total thickness in meters = 5.28

Contacts with surrounding strata:
The lower contact is sharp, and is partially covered due to the draping of the lower bentonite.
The upper contact is gradational.

Ash/bentonite contact:
Horizontal, and transitional; upper: 5-10cm., lower: 10-15cm.

Sedimentary Structures:
Ash: laminated
Grain size of ash: .01-.02 mm.
Bentonite: massive
Oval to circular iron-stained blotches occur on each layer.

Concretions: Barite occurs on the lower bentonite.

Evidence of detrital admixture: none

Sample: 3 Location:149-99-5bc
Upper Bentonite: A 3.1, 3.0, 3.2
Middle Ash: B 3.1, 3.0, 3.2
Lower Bentonite: C 3.1, 3.0, 3.2

Description of Sentinel Butte ash/bentonite:
Thickness of each layer: U. Ben. = 0.43
Ash = 0.74
L. Ben. = 3.05
Total thickness in meters = 4.22
Contacts with surrounding strata:
The lower contact is sharp.
The upper contact is gradational.
Ash/bentonite contact: ash/bentonite contact:
Horizontal, and transitional; upper: 5-10cm.
lower: 10-15cm.
Sedimentary Structures:
Ash: laminated.
Grain size of ash: .01-.02 mm.
Bentonite: massive
Oval to circular iron-stained blotches occur on the ash and upper bentonite.
Concretions: Barite occurs on the lower bentonite.
Evidence of detrital admixture: none

Sample: 4 Location:150-99-31cc
Upper Bentonite: A 4.1, 4.0, 4.2
Middle Ash: B 4.1, 4.0, 4.2
Lower Bentonite: C 4.1, 4.0, 4.2

Description of Sentinel Butte ash/bentonite:
Thickness of each layer: U. Ben. = 1.83
Ash = 1.12
L. Ben. = 2.57
Total thickness in meters = 5.52
Contacts with surrounding strata:
The lower contact is not exposed at this location.
The upper contact is gradational.
Character of the ash/bentonite contact:
Horizontal, and transitional; upper: 5-10cm.,
lower: 10-15cm.
Sedimentary Structures:
Ash: laminated
Grain size of ash: .01-.02 mm.
Bentonite: massive
Oval to circular iron-stained blotches occur at the top of the ash and on the upper bentonite.
Concretions: none
Evidence of detrital admixture: none

Sample: 5 Location:149-99-1aa

Upper Bentonite: A 5.1, 5.0, 5.2
Middle Ash: B 5.1, 5.0, 5.2
Lower Bentonite: C 5.1, 5.0, 5.2

Description of Sentinel Butte ash/bentonite:

Thickness of each layer: U. Ben. = 2.34
Ash = 1.68
L. Ben. = 3.35
Total thickness in meters = 7.37

Contacts with surrounding strata:
The lower contact is sharp.
The upper contact is gradational.

Ash/bentonite contact:
Horizontal, and transitional; upper: 3-8cm., lower: 8-14cm.

Sedimentary Structures:
Ash: laminated.
Grain size of ash: .01-.02 mm.
Bentonite: massive
Oval to circular iron-stained blotches occur on each layer.

Concretions: none

Evidence of detrital admixture: none

Sample: 6 Location:149-100-3cd

Upper Bentonite: A 6.1, 6.0, 6.2
Middle Ash: B 6.1, 6.0, 6.2
Lower Bentonite: C 6.1, 6.0, 6.2

Description of Sentinel Butte ash/bentonite:

Thickness of each layer: U. Ben. = 1.73
Ash = 0.61
L. Ben. = 1.27
Total thickness in meters = 3.61

Contacts with surrounding strata:
The lower contact is sharp and marked by a silicified zone.
The upper contact is gradational.

Ash/bentonite contact:
Horizontal, and transitional; upper: 5-10cm., lower: 10-15cm.

Sedimentary Structures:
Ash: laminated
Grain size of ash: .01-.02 mm.
Bentonite: massive
Oval to circular iron-stained blotches occur on the upper bentonite.

Concretions: Barite occurs on the lower bentonite.

Evidence of detrital admixture: none

Sample: 7 Location:149-100-11ba

Upper Bentonite: A 7.1, 7.0, 7.2
Middle Ash: B 7.1, 7.0, 7.2
Lower Bentonite: C 7.1, 7.0, 7.2

Description of Sentinel Butte ash/bentonite:

Thickness of each layer: U. Ben. = 1.47
Ash = 1.57
L. Ben. = 1.61
Total thickness in meters = 4.65

Contacts with surrounding strata:
The lower contact is sharp, and is marked by a silicified zone.
The upper contact is gradational.

Ash/bentonite contact:
Horizontal, and transitional; upper: 5-9cm.,
lower: 15-20cm.

Sedimentary Structures:
Ash: laminated
Grain size of ash: .01-.02 mm.
Bentonite: massive
Oval to circular iron-stained blotches occur on the ash and upper bentonite.

Concretions: Barite occurs on the lower bentonite.

Evidence of detrital admixture: none

Sample: 8 Location:149-100-11ad

Upper Bentonite: A 8.1, 8.0, 8.2
Middle Ash: B 8.1, 8.0, 8.2
Lower Bentonite: C 8.1, 8.0, 8.2

Description of Sentinel Butte ash/bentonite:

Thickness of each layer: U. Ben. = 1.12
Ash = 1.27
L. Ben. = 1.12
Total thickness in meters = 3.51

Contacts with surrounding strata:
The lower contact is not exposed.
The upper contact is gradational.

Ash/bentonite contact:
Horizontal, and transitional; upper: 5-10cm., lower: 10-15cm.

Sedimentary Structures:
Ash: laminated
Grain size of ash: .01-.02 mm.
Bentonite: massive
Oval to circular iron-stained blotches occur on each layer.

Concretions: none

Evidence of detrital admixture: none

Sample: 9 Location:149-100-36cd

Upper Bentonite: A 9.1, 9.0, 9.2
Middle Ash: B 9.1, 9.0, 9.2
Lower Bentonite: C 9.1, 9.0, 9.2

Description of Sentinel Butte ash/bentonite:

Thickness of each layer: U. Ben. = 2.03
Ash = 1.80
L. Ben. = 1.93
Total thickness in meters = 5.76

Contacts with surrounding strata:
The lower contact is sharp, and is marked by a silicified zone.
The upper contact is gradational.

Ash/bentonite contact:
Horizontal, and transitional; upper: 5-10cm., lower: 10-15cm.

Sedimentary Structures:
Ash: laminated, with plant fragments between some of the laminations.
Grain size of ash: .01-.02 mm.
Bentonite: massive
Oval to circular iron-stained blotches occur on each layer.

Concretions: Barite occurs on the lower bentonite.

Evidence of detrital admixture: none

Sample: 10 Location:149-100-35dd

Upper Bentonite: A 10.1, 10.0, 10.2
Middle Ash: B 10.1, 10.0, 10.2
Lower Bentonite: C 10.1, 10.0, 10.2

Description of Sentinel Butte ash/bentonite:

Thickness of each layer: U. Ben. = NA
Ash = 0.81
L. Ben. = 2.34
Total thickness in meters = 3.15

Contacts with surrounding strata:
The lower contact is sharp, and is marked by a silicified-rippled zone.
The upper contact is gradational.

Ash/bentonite contact:
Horizontal, and transitional; upper: 5-10cm., lower: 10-15cm.

Sedimentary Structures:
Ash: massive to cross-bedded
Grain size of ash: .5-1 mm.
Bentonite: massive
Oval to circular iron-stained blotches occur on ash and the lower bentonite.

Concretions: Barite occurs on the lower bentonite.

Evidence of detrital admixture: none

Sample: 11 Location:149-99-32cc

Upper Bentonite: A 11.1, 11.0, 11.2
Middle Ash: B 11.1, 11.0, 11.2
Lower Bentonite: C 11.1, 11.0, 11.2

Description of Sentinel Butte ash/bentonite:

Thickness of each layer: U. Ben. = 2.18
Ash = 0.76
L. Ben. = 3.45
Total thickness in meters = 6.39

Contacts with surrounding strata:
The lower contact is sharp, and is marked by a thin silicified zone.
The upper contact is gradational.

Ash/bentonite contact:
Horizontal, and transitional; upper: 3-5cm., lower: 5-10cm.

Sedimentary Structures:
Ash: laminated
Grain size of ash: .01-.02 mm.
Bentonite: massive

Concretions: silicified (?) nodules occur on the lower bentonite.

Evidence of detrital admixture: none

Sample: 12 Location:149-99-6db

Upper Bentonite: A 12.1, 12.0, 12.2
Middle Ash: B 12.1, 12.0, 12.2
Lower Bentonite: C 12.1, 12.0, 12.2

Description of Sentinel Butte ash/bentonite:

Thickness of each layer: U. Ben. = 1.73
Ash = 0.69
L. Ben. = 4.11
Total thickness in meters = 6.53

Contacts with surrounding strata:
The lower contact is sharp, and is partially covered due to the draping of the lower bentonite.
The upper contact is gradational.

Ash/bentonite contact:
Horizontal, and transitional; upper: 5-10cm., lower: 10-15cm.

Sedimentary Structures:
Ash: laminated
Grain size of ash: .01-.02 mm.
Bentonite: massive
Oval to circular iron-stained blotches occur on the upper bentonite and the ash.

Concretions: none

Evidence of detrital admixture: none

Sample: 13 Location:148-99-7ab

Upper Bentonite: A 13.1, 13.0, 13.2
Middle Ash: B 13.1, 13.0, 13.2
Lower Bentonite: C 13.1, 13.0, 13.2

Description of Sentinel Butte ash/bentonite:

Thickness of each layer: U. Ben. = ?
Ash = NA
L. Ben. = ?
Total thickness in meters = 5.18

Contacts with surrounding strata:
The lower contact is sharp.
The upper contact is gradational.

Ash/bentonite contact:
The ash is not present at this sample site.

Sedimentary Structures:
Ash: NA
Grain size of ash: NA
Bentonite: massive
Oval to circular iron-stained blotches occur on the lower bentonite.

Concretions: none

Evidence of detrital admixture: none

Sample: 14 Location:148-99-8bc

Upper Bentonite: A 14.1, 14.0, 14.2
Middle Ash: B 14.1, 14.0, 14.2
Lower Bentonite: C 14.1, 14.0, 14.2

Description of Sentinel Butte ash/bentonite:

Thickness of each layer: U. Ben. = 1.73
Ash = 0.35
L. Ben. = 4.88
Total thickness in meters = 6.96

Contacts with surrounding strata:
The lower contact is sharp, and is partially covered due to the draping of the lower bentonite.
The upper contact is gradational.

Ash/bentonite contact:
Horizontal, and transitional; both contacts: 15-30cm.

Sedimentary Structures:
Ash: laminated (?)
Grain size of ash: .01-.02 mm.
Bentonite: massive
Oval to circular iron-stained blotches occur on ash and the upper bentonite.

Concretions: petrified wood occurs on the lower bentonite.

Evidence of detrital admixture: none

Sample: 15 Location:149-100-22db

Upper Bentonite: A NA NA NA
Middle Ash: B NA NA NA
Lower Bentonite: C 15.1, 15.0, 15.2

Description of Sentinel Butte ash/bentonite:

Thickness of each layer: U. Ben. = NA
Ash = NA
L. Ben. = 1.73
Total thickness in meters = 1.73

Contacts with surrounding strata:
The lower contact is sharp, and marked by a silicified rippled zone.
The upper contact is not present.

Ash/bentonite contact: NA

Sedimentary Structures:
Ash: NA
Grain size of ash: NA
Bentonite: massive

Concretions: Barite occurs near the base of the lower bentonite.

Evidence of detrital admixture: none

Sample: 16 Location:148-100-18ab

Upper Bentonite: A 16.1, 16.0, 16.2
Middle Ash: B 16.1, 16.0, 16.2
Lower Bentonite: C 16.1, 16.0, 16.2

Description of Sentinel Butte ash/bentonite:

Thickness of each layer: U. Ben. = 1.63
Ash = 0.58
L. Ben. = 1.12
Total thickness in meters = 3.33

Contacts with surrounding strata:
The lower contact is sharp, and is marked by silicified, rippled surface.
The upper contact is gradational.

Ash/bentonite contact:
Horizontal, and transitional; upper: 5-10cm., lower: 5-10cm.

Sedimentary Structures:
Ash: laminated
Grain size of ash: .01-.02 mm.
Bentonite: massive
Oval to circular iron-stained blotches occur on the lower and upper bentonites.

Concretions: Barite occurs on the lower bentonite, with petrified wood fragments.

Evidence of detrital admixture: a coarse cross-bedded sand is present.

Sample: 17 Location:148-100-13ca

Upper Bentonite: A 17.1, 17.0, 17.2
Middle Ash: B 17.1, 17.0, 17.2
Lower Bentonite: C 17.1, 17.0, 17.2

Description of Sentinel Butte ash/bentonite:

Thickness of each layer: U. Ben. = 2.84
Ash = 2.03
L. Ben. = 3.45
Total thickness in meters = 8.32

Contacts with surrounding strata:
The lower contact is sharp, and is marked by a silicified zone which is rippled.
The upper contact is gradational.

Ash/bentonite contact:
Horizontal, and transitional; upper: 5-10cm., lower: 10-15cm.

Sedimentary Structures:
Ash: laminated
Grain size of ash: .01-.02 mm.
Bentonite: massive
Oval to circular iron-stained blotches occur on each layer.

Concretions: none

Evidence of detrital admixture: none

Sample: 18 Location:148-100-13dd

Upper Bentonite: A 18.1, 18.0, 18.2
Middle Ash: B 18.1, 18.0, 18.2
Lower Bentonite: C 18.1, 18.0, 18.2

Description of Sentinel Butte ash/bentonite:

Thickness of each layer: U. Ben. = 2.67
Ash = 0.97
L. Ben. = 4.42
Total thickness in meters = 8.06

Contacts with surrounding strata:
The lower contact is sharp, and is partially covered due to the draping of the lower bentonite.
The upper contact is gradational.

Ash/bentonite contact:
Horizontal, and transitional; upper: 5-10cm., lower: 5-10cm.

Sedimentary Structures:
Ash: laminated
Grain size of ash: .01-.02 mm.
Bentonite: massive
Oval to circular iron-stained blotches occur on the ash and upper bentonite.

Concretions: none

Evidence of detrital admixture: none

Sample: 19 Location:148-100-24dd

Upper Bentonite: A NA NA NA
Middle Ash: B NA NA NA
Lower Bentonite: C 19.1, 19.0, 19.2

Description of Sentinel Butte ash/bentonite:

Thickness of each layer: U. Ben. = NA
Ash = NA
L. Ben. = 1.88
Total thickness in meters = 1.88

Contacts with surrounding strata:
The lower contact is sharp, and is partially covered due to the draping of the lower bentonite.
The upper contact is gradational.

Ash/bentonite contact: NA

Sedimentary Structures:
Ash: NA
Grain size of ash: NA
Bentonite: massive
Oval to circular iron-stained blotches occur on the lower bentonite.

Concretions: Barite occurs on the lower bentonite.

Evidence of detrital admixture: none

Sample: 20 Location:148-100-25b

Upper Bentonite: A 20.1, 20.0, 20.2
Middle Ash: B 20.1, 20.0, 20.2
Lower Bentonite: C 20.1, 20.0, 20.2

Description of Sentinel Butte ash/bentonite:

Thickness of each layer: U. Ben. = 1.57
Ash = 1.47
L. Ben. = 4.93 *
Total thickness in meters = 7.97

Contacts with surrounding strata:
The lower contact is not exposed at this site.
The upper contact is gradational.

Ash/bentonite contact:
Horizontal, and transitional; upper: 2-5cm., lower: 15-20cm.

Sedimentary Structures:
Ash: laminated
Grain size of ash: .01-.02 mm.
Bentonite: massive
Oval to circular iron-stained blotches occur on the ash and the upper bentonite.

Concretions: none

Evidence of detrital admixture: none

* The lower bentonite has flowed at this location and hence appears thicker than normal.

Sample: 21 Location:148-99-18ba

Upper Bentonite: A 21.1, 21.0, 21.2
Middle Ash: B 21.1, 21.0, 21.2
Lower Bentonite: C 21.1, 21.0, 21.2

Description of Sentinel Butte ash/bentonite:

Thickness of each layer: U. Ben. = 1.78
Ash = 1.37
L. Ben. = 2.84
Total thickness in meters = 5.99

Contacts with surrounding strata:
The lower contact is sharp.
The upper contact is gradational.

Ash/bentonite contact:
Horizontal, and transitional; upper: 2-5cm., lower: 5-10cm.

Sedimentary Structures:
Ash: laminated
Grain size of ash: .01-.02 mm.
Bentonite: massive
Oval to circular iron-stained blotches occur on each layer.

Concretions: Barite occurs on the lower bentonite.

Evidence of detrital admixture: none

Sample: 22 Location:148-99-33bb

Upper Bentonite: A NA NA NA
Middle Ash: B NA NA NA
Lower Bentonite: C 22.1, 22.0, 22.2

Description of Sentinel Butte ash/bentonite:

Thickness of each layer: U. Ben. = NA
Ash = NA
L. Ben. = 0.61
Total thickness in meters = 0.61

Contacts with surrounding strata:
The lower contact is sharp, and is partially covered due to the draping of the lower bentonite.
The upper contact is not exposed.

Ash/bentonite contact: NA

Sedimentary Structures:
Ash: NA
Grain size of ash: NA
Bentonite: massive
Oval to circular iron-stained blotches occur on the lower bentonite.

Concretions: Barite occurs on the lower bentonite.

Evidence of detrital admixture: none

Sample: 23 Location:148-99-31ba

Upper Bentonite: A NA NA NA
Middle Ash: B NA NA NA
Lower Bentonite: C 23.1, 23.0, 23.2

Description of Sentinel Butte ash/bentonite:

Thickness of each layer: U. Ben. = NA
Ash = NA
L. Ben. = 4.57
Total thickness in meters = 4.57

Contacts with surrounding strata:
The lower contact is sharp, and is partially covered due to the draping of the lower bentonite.
The upper contact is not exposed.

Ash/bentonite contact: NA

Sedimentary Structures:
Ash: NA
Grain size of ash: NA
Bentonite: massive

Concretions: none

Evidence of detrital admixture: none

Sample: 24 Location:148-100-28bd

Upper Bentonite: A 24.1, 24.0, 24.2
Middle Ash: B 24.1, 24.0, 24.2
Lower Bentonite: C 24.1, 24.0, 24.2

Description of Sentinel Butte ash/bentonite:

Thickness of each layer: U. Ben. = 1.52
Ash = 0.92
L. Ben. = 1.07
Total thickness in meters = 3.51

Contacts with surrounding strata:
The lower contact is sharp, and is marked by a silicified rippled zone.
The upper contact is gradational.

Ash/bentonite contact:
Horizontal, and transitional; upper: 2-5cm., lower: 2-5cm.

Sedimentary Structures:
Ash: laminated
Grain size of ash: .01-.02 mm.
Bentonite: massive
Oval to circular iron-stained blotches occur on the ash and the upper bentonite.

Concretions: none

Evidence of detrital admixture: none

Sample: 25 Location:148-100-27ba

Upper Bentonite: A 25.1, 25.0, 25.2
Middle Ash: B 25.1, 25.0, 25.2
Lower Bentonite: C 25.1, 25.0, 25.2

Description of Sentinel Butte ash/bentonite:

Thickness of each layer: U. Ben. = 1.96
Ash = 1.38
L. Ben. = 2.03
Total thickness in meters = 5.37

Contacts with surrounding strata:
The lower contact is sharp, and is marked by a silicified zone.
The upper contact is gradational.

Ash/bentonite contact:
Horizontal, and transitional; upper: 2-5cm., lower: 15-20cm.

Sedimentary Structures:
Ash: laminated
Grain size of ash: .01-.02 mm.
Bentonite: massive
Oval to circular iron-stained blotches occur on the upper bentonite and the ash.

Concretions: Barite occurs on the lower bentonite.

Evidence of detrital admixture: none

Sample: 26 Location:148-100-23cb

Upper Bentonite: A 26.1, 26.0, 26.2
Middle Ash: B 26.1, 26.0, 26.2
Lower Bentonite: C 26.1, 26.0, 26.2

Description of Sentinel Butte ash/bentonite:

Thickness of each layer: U. Ben. = 2.84
Ash = 0.76
L. Ben. = 3.66
Total thickness in meters = 7.26

Contacts with surrounding strata:
The lower contact is sharp, and is marked by a silicified zone.
The upper contact is gradational.

Ash/bentonite contact:
Horizontal, and transitional; upper: 2-5cm., lower: 5-10cm.

Sedimentary Structures:
Ash: laminated
Grain size of ash: .01-.02 mm.
Bentonite: massive
Oval to circular iron-stained blotches occur on the lower and the upper bentonite.

Concretions: Barite occurs on the lower bentonite.

Evidence of detrital admixture: none

Sample: 27 Location:148-100-28da

Upper Bentonite: A 27.1, 27.0, 27.2
Middle Ash: B 27.1, 27.0, 27.2
Lower Bentonite: C 27.1, 27.0, 27.2

Description of Sentinel Butte ash/bentonite:

Thickness of each layer: U. Ben. = 1.30
Ash = 1.37
L. Ben. = 2.03
Total thickness in meters = 4.70

Contacts with surrounding strata:
The lower contact is sharp, and is marked by a silicified rippled zone.
The upper contact is gradational.

Ash/bentonite contact:
Horizontal, and transitional; upper: 5-10cm., lower: 5-10cm.

Sedimentary Structures:
Ash: laminated
Grain size of ash: .01-.02 mm.
Bentonite: massive
Oval to circular iron-stained blotches occur on the ash and the upper bentonite.

Concretions: none

Evidence of detrital admixture: none

Sample: 28 Location:148-100-32dc

Upper Bentonite: A NA NA NA
Middle Ash: B NA NA NA
Lower Bentonite: C 28.1, 28.0, 28.2

Description of Sentinel Butte ash/bentonite:

Thickness of each layer: U. Ben. = NA
Ash = NA
L. Ben. = 2.08
Total thickness in meters = 2.08

Contacts with surrounding strata:
The lower contact is sharp, and is marked by a silicified zone.
The upper contact is gradational.

Ash/bentonite contact: NA

Sedimentary Structures:
Ash: NA
Grain size of ash: NA
Bentonite: massive
Oval to circular iron-stained blotches occur on the lower bentonite.

Concretions: none

Evidence of detrital admixture: none

Sample: 29 Location:148-99-20cd

Upper Bentonite: A NA NA NA
Middle Ash: B NA NA NA
Lower Bentonite: C 29.1, 29.0, 29.2

Description of Sentinel Butte ash/bentonite:

Thickness of each layer: U. Ben. = NA
Ash = NA
L. Ben. = 2.13
Total thickness in meters = 2.13

Contacts with surrounding strata:
The lower contact is sharp.
The upper contact is gradational.

Ash/bentonite contact: NA

Sedimentary Structures:
Ash: NA
Grain size of ash: NA
Bentonite: massive
Oval to circular iron-stained blotches occur on the lower bentonite.

Concretions: none

Evidence of detrital admixture: none

Sample: 30 Location:148-100-2dd

Upper Bentonite: A NA NA NA
Middle Ash: B NA NA NA
Lower Bentonite: C 30.1, 30.0, 30.2

Description of Sentinel Butte ash/bentonite:

Thickness of each layer: U. Ben. = NA
Ash = NA
L. Ben. = 1.88
Total thickness in meters = 1.88

Contacts with surrounding strata:
The lower contact is sharp.
The upper contact is gradational.

Ash/bentonite contact: NA

Sedimentary Structures:
Ash: NA
Grain size of ash: NA
Bentonite: massive

Concretions: none

Evidence of detrital admixture: none

Additional Sample Sites, Not Randomized
"Grab Samples"

Sample: OP-1 Location: 147-99-1bc

Thickness:

Bentonite: 1.37 meters

Contacts:

The lower contact is sharp, and partially covered due to draping of the lower bentonite.

The upper contact is gradational.

Structures:

Oval to circular iron-stained blotches occur on the bentonite.

Approximately 1.5 to 2.0 feet below this bentonite a partially silicified coal is present.

Sample: BR-1 Location: 146-101-34ba

Thickness:

Bentonite: 2.08 meters (slumped, difficult to tell)

Contacts:

The lower contact is not visable due to draping of the bentonite over the underlying sediments.

The upper contact was not exposed.

This sample location occurs approximately 50 feet above the base of the Sentinel Butte Formation.

Sample: WG-1 Location: 148-101-29bd

Thickness:

Bentonite: 2.90 meters

Contacts:

The lower contact is sharp. The upper contact is gradational.

Structures:

Oval to circular iron-stained blotches occur on the bentonite.

The bentonite is bi-colored at this location, darker grey on the bottom and lighter grey on the top half.

Sample: RD-1 and RD-2 Location: RD-1 148-100-24cd
RD-2 148-100-25ba

Thickness:

Bentonite: RD-1 = 1.02 meters
RD-2 = 0.69 meters

Contacts:

RD-1: The lower contact is sharp, and the upper contact is gradational.

RD-2: The lower contact is sharp, but not as distinct as the lower contact of RD-1. The upper contact is gradational.

The bentonite is present as two separate tongues at this location. Gastropod shell fragments were found in the light tan to brown silty mudstone between the two tongues.

Sample: A-1 Location: 148-100-11cc

Thickness:

Bentonite: 1.98 meters

Contacts:

The lower contact is sharp and is marked by a silica-enriched zone which has preserved ripples in the underlying strata.

The upper contact is gradational.

Sample: DC-1 and DC-2 Location:149-100-33cc

Thickness:

Bentonite: DC-1 = 1.12, and DC-2 = 0.76 meters

Contacts:

DC-1: The lower contact is sharp, and the upper contact is gradational.

DC-2: The lower contact is sharp, but not as distinct as the lower contact of DC-1. The upper contact is gradational.

Concretions: Barite occurs near the base of the lower bentonites.

Two distinct bentonite units are present at this location separated by a silty mudstone.

Sample: WM-1 Location: 149-101-26cd

Thickness:

Bentonite: 0.41 meters

Contacts:

The lower contact is sharp, and the upper contact is gradational.

Two distinct bentonite units are present at this sample location, and are separated by a silty mudstone.

This is the western most exposure of the Sentinel Butte bentonite which was found.

Sample: LB-6 Location: 148-95-27cb

Thickness:

Bentonite: 0.81 meters

Contacts:

The lower contact is sharp, and the upper contact is gradational.

This sample location, north of Lost Bridge, forms a small bench and is positioned approximately 20 feet below what appears to be the yellow bed. Directly below the sampled unit a carbonaceous zone is present.

Sample: C-6 Location: 147-101-11bd

Thickness:

Bentonite: 0.61 meters

Contacts:

Both the upper and lower contacts are sharp.

This bentonite lies directly on a coal bed and occurs about 20 to 30 feet below known Sentinel Butte bentonite.

Sample: R-6 Location: 147-101-1bd

Thickness:

Bentonite: 1.07 meters

Contacts:

The lower contact is sharp and marked by a silica-enriched zone which has preserved ripples in the underlying strata. The upper contact appears to be gradtional, where exposures exist.

Structures:

A petrified log, approximately 4 feet long lies on the surface of the bentonite. Oval to circular iron-stained blotches occur near the base of this unit.

Sample: SM-6 Location: 147-100-18cc

Thickness:

Bentonite: 0.46 meters

Contacts:

The lower contact is distinctive, but not sharp and well defined. The upper contact is gradational.

The Sentinel Butte bentonite is very difficult to place at this location. The bentonite which lies directly on the coal bed (e.g.,Coal 6-11) is present, as is the lower yellow bed. However, no distinct bentonite similar to the Sentinel Butte bentonite is present. The unit sampled was a clay unit directly below a coal bed and between the yellow bed and the correlative bentonite unit of Coal 6-11.

Sample: LX-1 Location:148-99-36aa

Thickness:

Bentonite: 0.71 meters

Contacts:

The lower contact is relatively sharp, and the upper contact is gradational.

It is not clear if this is the correlative to the Sentinel Butte bentonite. However it does occur approximately at the same stratigraphic level as OL-1.

Sample: SR-6 Location: 148-100-36cc

Thickness:

Bentonite: 1.22 meters

Contacts:

The lower contact is not exposed, and the upper contact is gradational.

This sample location is an isolated site which appears to be part of a larger slump block.

Sample: PL-1 and PL-2 Location: 149-100-29bc

Thickness:

Bentonite: PL-1 = 1.93 meters
PL-2 = 2.39 meters

Contacts:

PL-1; The lower contact is sharp. The upper contact is also sharp but not as distinct. The contact is placed where "popcorny" clay is replaced by silty clay ("non-popcorn").

PL-2; The lower contact is sharp, but not as distinct as the lower contact of Pl 6-13. The upper contact is gradational.

Structures:

The lower unit has oval to circular iron-stained blotches near the base of the unit. The upper unit also has the same blotches, although they are found throughout the unit.

Concretions: Barite is present in minor amounts at the base of the lower unit.

The bentonite at this location is separated by a shaley mudstone, which is approximately 3.5 feet thick. Gastropod fragments are found in this middle mudstone. Horizontal laminations also occur thoroughout this sandstone.

APPENDIX B

Calculation of Infinite Thickness

Calculation of Infinite Thickness

The calculation of infinite thickness, used in this study is described in full in Bertin (1963, p. 624). An integral part of this calculation relies on knowing the specific gravity of the material being analyzed. An estimate of the specific gravity of both the glass and clay separates was established by utilizing a Hubbard specific gravity bottle (pycnometer). Before applying the pycnometer to the unknowns it was first calibrated with minerals of known specific gravities. During the calibration and determination of the unknown specific gravities the temperature was held constant to avoid temperature effects on volume.

The pycnometer was weighed dry, filled with distilled water, and reweighed to determine the weight of a specific volume of water. It was emptied and dried with laboratory air. The fused glass beads, and the briquetted pellets were broken into particles, placed in the pycnometer and weighed. Distilled water was then added until the pycnometer was filled, and any trapped air was liberated by stirring the material in the bottle. The pycnometer was again weighed and the specific gravity, of the material was calculated using the formula below.

$$S.G. = A/(B-C-D+E)$$

where:

A = sample weight
B = weight of pycnometer filled with distilled water
C = weight of pycnometer
D = weight of pycnometer, distilled water and sample
E = weight of pycnometer and dry sample

The specific gravities of the upper and the lower bentonties, and the middle ash were calculated from the best fit line (R - value equal to 0.9995), established from materials with known specfic gravities. The calculated specific gravity of the briquetted specimens fell within the range for bentonites, (1.7 to 2.7gm/cm^3) and averaged 2.28gm/cm^3. The average specific gravity of the fused glass beads was 2.45gm/cm^3.

The infinite thickness calculation also relies on knowing the mass absorption coefficient of an element in a given matrix. Therefore, to determine the mass absorption coefficient of the element in question the weighted averages of the matrix elements were calculated. This average was, in turn, used to calculate a net matrix absorption coefficient which was utilized in the initial calculation of infinite thickness (Bertin, 1975, p.623, 624). The infinite thicknesses for the analyzed elements are listed in Table 8.

Table 8.

Infinite thickness (in micrometers)

Major Elements Glass Beads		Trace Elements Briquets			
Na	11	S	23	Y	3143
Mg	11	V	148	Zr	3143
Al	20	Cr	234	Nb	4095
Si	29	Co	275	Ba	89
P	44	Ni	606	Pb	1681
K	138	Cu	606		
Ca	307	Zn	606		
Ti	509	Ga	1789		
Mn	936	Rb	1916		
Fe	936	Sr	2357		

APPENDIX C

Spectrometer Analyzing Conditions

Spectrometer Conditions

A Rigaku (S/MAX) fully automated wavelength dispersive x-ray fluorescent spectrometer was employed to obtain the chemical analysis of the Sentinel Butte ash/bentonite samples. A scintillation counter was used to analyze the elements greater than atomic number 21 (V), and to estimate the intensities of the Compton scattering peak. This counter utilizes a LiF-1 (200) diffracting crystal. A gas flow proportional counter was used for the detection of the lighter elements. The gas flow counter relies on a mixture of argon (90 percent) and methane (10 percent) for its operation. This counter was used in conjunction with PET (002), ADP (200), LiF-6 (220), TAP (100), and GE (111) analyzing crystals. All analyte lines satisfied Braggs equation and were first order (n = 1). The samples were analyzed in a vacuum utilizing a rhodium end-window x-ray tube, under the following conditions:

Anode voltage:	50kV
Anode current:	40mA
Filter(s):	None
Sample spin:	On
Repeat count:	1
Silt:	Fine for Co and Sr Coarse for all other elements
Absorber:	1
Pulse height analyzer:	10-30 10-35 (for Ti, Mn and Fe)
Quantitative analysis:	Criss Fundamental parameters (for major elemental analysis) Linear or Quadratic Regression and Scattered Target-Line Ratio Method (for trace elements).

The analyte locations were chosen by manually optimizing the intensities for each element utilizing the pulse height analyzer (PHA), slit, crystals, and absorber. The counting times for the peak and the background(s), were calculated so that the total accumulated counts, at the peak and at the background, achieved a specified relative standard deviation in a minimal counting time (Mack and Speilberg, 1958, p. 171). The trace elements, above the Fe absorption edge (atomic number 27 and up) were ratioed to the Compton scattered line, and hence only the peak location was used to determine the concentration. One background value was used to determine the concentration of SiO_2. These optimum settings were then input into the group setup program of Rigaku's Dataflex 360 software package. The locations for the wavelengths of interest are given in Table 9.

Table 9. Spectrometer conditions for the analyte lines of interest

Element	Analyzing Crystal	Lower BKG	Peak Location	Upper BKG	X-Ray Line
Na	TAP	52.90(20)	55.12(40)	56.25(20)	Ka
Mg	ADP	134.00(20)	136.53(40)	139.00(20)	Ka
Al	PET	140.90(4)	145.01(20)	148.00(4)	Ka
Si	PET		109.11(4)	111.00(1)	Ka
P	GE	139.20(20)	140.91(40)	143.70(20)	Ka 1
S	GE	105.00(10)	110.55(20)	117.00(10)	Ka 1
K	LiF-1*	133.50(1)	136.68(10)	140.00(1)	Ka
Ca	LiF-1*	111.00(4)	113.07(10)	115.00(4)	Ka
Ti	LiF-1	84.90(20)	86.18(40)	87.75(20)	Ka 1
V	LiF-1	76.60(40)	76.98(40)	77.05(40)	Ka 1
Cr	LiF-1	68.60(40)	69.39(40)	70.50(40)	Ka 1
Mn	LiF-1	62.10(20)	63.01(20)	63.70(20)	Ka
Fe	LiF-1	55.50(1)	57.54(10)	58.90(1)	Ka
Co	LiF-1	50.50(40)	52.81(40)	54.00(40)	Ka 1
Ni	LiF-1		48.64(100)		Ka 1
Cu	LiF-1		45.04(20)		Ka 1
Zn	LiF-1		41.82(20)		Ka 1
Ga	LiF-1		38.93(100)		Ka 1
Rb	LiF-1		26.62(40)		Ka 1
Sr	LiF-1		25.16(40)		Ka 1
Y	LiF-1		23.82(100)		Ka 1
Zr	LiF-1		20.11(40)		Ka 1
Ba	LiF-1		87.20(100)		Lb 1
Pb	LiF-1		28.27(40)		Lb 1
Nb	LiF-1		21.45(100)		Ka 1
CM2	LiF-1		18.42(1)		

Abbreviations: (*) indicates the LiF-1 (220) crystal was used for the analysis. Analyzing times are depicted in parenthesis.

APPENDIX D

X-Ray Fluorescence Chemical Analysis

Table 10. Major Chemical Oxide Weight Percent of whole rock samples. Sample description: A = Upper Bentonite, B = Middle Ash, C = Lower Bentonite. a = weight percent (average of 4 analyses) b = standard deviation. Total iron calculated as Fe_2O_3. Calculated H_2O-free

Sample		Na	Mg	Al	Si	P	K	Ca	Ti	Mn	Fe	Total
A1	(a)	1.80	2.65	14.46	67.76	0.13	1.13	4.13	0.42	0.03	3.92	95.27
	(b)	0.12	0.08	0.31	0.53	<0.01	0.01	0.02	0.01	<0.01	<0.01	
A2		2.18	3.08	16.27	66.90	0.10	0.92	2.91	0.37	0.02	3.95	95.55
		0.14	0.10	0.37	0.55	<0.01	0.01	0.01	0.01	<0.01	0.01	
A3		2.22	3.53	18.01	64.10	0.11	0.98	3.05	0.40	0.03	4.83	96.10
		0.15	0.09	0.38	0.64	<0.01	0.01	0.01	0.01	<0.01	0.01	
A5		2.52	3.63	18.43	63.98	0.08	0.80	2.43	0.33	0.03	4.49	95.56
		0.14	0.13	0.43	0.58	<0.01	<0.01	0.01	0.01	<0.01	0.01	
A6		1.25	3.20	16.00	65.87	0.11	1.01	4.12	0.41	0.03	4.23	95.07
		0.13	0.06	0.28	0.70	<0.01	<0.01	0.01	0.01	<0.01	0.01	
A8		1.92	2.78	15.39	65.80	0.15	1.60	3.67	0.54	0.06	4.54	95.30
		0.12	0.13	0.27	0.60	<0.01	<0.01	0.02	<0.01	<0.01	0.01	
A12		2.27	2.97	15.43	68.12	0.10	0.98	2.82	0.37	0.03	3.97	95.89
		0.20	0.10	0.28	0.42	<0.01	0.01	0.01	0.01	<0.01	0.01	
A17		2.62	2.82	14.77	67.45	0.14	1.39	3.92	0.50	0.05	4.00	96.50
		0.14	0.06	0.22	0.44	<0.01	0.01	0.02	<0.01	<0.01	0.01	
A18		1.76	2.84	15.09	69.32	0.10	1.51	1.97	0.46	0.05	4.29	96.23
		0.16	0.12	0.28	0.58	<0.01	0.01	0.01	0.01	<0.01	0.01	
A20		2.08	3.02	16.02	68.42	0.07	0.74	1.83	0.31	0.02	4.02	95.38
		0.14	0.08	0.27	0.37	<0.01	0.01	0.01	0.01	<0.01	0.01	
A21		2.34	3.20	17.17	66.63	0.07	0.63	1.76	0.30	0.02	4.08	95.06
		0.14	0.06	0.03	0.13	<0.01	0.01	0.01	0.01	<0.01	0.01	
A24		2.01	3.24	16.63	66.55	0.09	0.88	2.80	0.36	0.08	4.35	95.81
		0.10	0.08	0.05	0.17	<0.01	0.01	0.01	0.01	0.11	0.01	
A25		2.10	3.09	16.50	66.93	0.08	0.78	2.22	0.33	0.02	4.13	95.04
		0.15	0.12	0.04	0.49	<0.01	0.01	<0.01	0.01	<0.01	0.01	
A26		1.92	2.88	15.21	69.03	0.08	1.26	1.52	0.42	0.03	3.98	95.18
		0.07	0.11	0.07	0.14	<0.01	0.01	0.01	0.01	<0.01	0.01	
A27		1.98	3.15	15.80	66.76	0.08	0.87	3.13	0.33	0.03	4.27	95.24
		0.12	0.09	0.08	0.30	<0.01	0.01	0.01	0.01	<0.01	0.01	

Table 10 -- continued

	Na	Mg	Al	Si	P	K	Ca	Ti	Mn	Fe	Total
B1.0	2.61	2.01	15.13	67.44	0.10	1.86	3.27	0.35	0.05	3.25	94.92
	0.17	0.08	0.18	0.41	<0.01	0.01	0.01	0.01	<0.01	0.01	
B2.0	2.61	2.17	15.16	67.47	0.11	1.72	3.17	0.34	0.05	3.06	94.72
	0.18	0.11	0.16	0.55	<0.01	0.01	0.02	<0.01	<0.01	0.01	
B3.0	2.86	2.35	15.96	66.76	0.12	1.65	3.28	0.33	0.05	3.44	95.64
	0.23	0.16	0.19	0.28	0.02	<0.01	0.02	<0.01	<0.01	0.01	
B5.0	3.05	1.28	14.68	69.81	0.07	2.10	1.89	0.26	0.06	2.57	94.62
	0.12	0.05	0.16	0.38	<0.01	0.01	0.01	0.01	<0.01	0.01	
B6.0	2.76	2.04	14.86	67.87	0.13	1.87	3.27	0.31	0.05	3.13	95.14
	0.27	<0.01	0.02	0.08	0.01	<0.01	<0.01	0.01	<0.01	0.01	
B8.0	3.12	1.63	15.07	68.81	0.08	1.97	2.46	0.31	0.06	2.84	95.21
	0.16	0.07	0.31	0.36	<0.01	0.01	0.01	0.01	<0.01	0.01	
B12.0	2.64	2.61	16.78	68.45	0.09	1.53	2.92	0.34	0.05	3.45	97.67
	0.20	0.11	0.34	0.58	<0.01	0.01	0.01	<0.01	<0.01	0.01	
B17.0	3.36	1.52	14.49	69.62	0.09	1.93	2.66	0.29	0.06	2.80	95.65
	0.23	0.10	0.25	0.54	<0.01	0.01	0.02	<0.01	<0.01	0.01	
B18.0	2.80	2.47	16.87	66.88	0.08	1.48	1.66	0.36	0.04	3.85	95.34
	0.18	0.08	0.17	0.29	<0.01	0.01	0.01	0.01	<0.01	0.01	
B20.0	2.90	2.24	14.98	68.08	0.10	1.79	2.73	0.36	0.05	3.20	95.28
	0.18	0.07	0.16	0.23	<0.01	0.02	0.02	0.01	<0.01	0.01	
B21.0	3.23	1.62	14.97	69.45	0.08	1.90	2.20	0.29	0.07	2.81	95.47
	0.11	0.06	0.16	0.11	<0.01	0.01	0.01	0.01	<0.01	0.01	
B24.0	2.98	1.48	15.01	69.91	0.06	1.96	2.50	0.25	0.06	2.69	95.74
	0.15	0.03	0.22	0.34	<0.01	0.01	0.02	0.01	<0.01	0.01	
B25.0	3.11	1.77	14.91	69.48	0.09	1.94	2.89	0.30	0.06	2.88	96.26
	0.20	0.06	0.27	0.12	<0.01	0.01	0.01	0.01	<0.01	0.01	
B26.0	3.02	2.27	16.18	67.22	0.09	1.76	2.01	0.36	0.05	3.59	95.40
	0.16	0.07	0.32	0.26	<0.01	0.01	0.02	0.01	<0.01	0.02	
B27.0	3.47	1.55	14.64	69.02	0.10	1.91	2.86	0.24	0.06	2.72	95.41
	0.06	0.01	0.12	0.19	0.02	0.01	<0.01	<0.01	<0.01	0.01	

Table 10 -- continued

	Na	Mg	Al	Si	P	K	Ca	Ti	Mn	Fe	Total
B1.1	2.95	2.22	15.63	66.45	0.13	1.87	3.25	0.36	0.05	3.38	95.13
	0.03	0.04	0.14	0.02	0.02	0.01	0.01	<0.01	<0.01	<0.01	
B2.1	2.67	2.25	15.65	67.84	0.10	1.64	2.97	0.34	0.04	3.26	95.59
	0.23	0.04	0.25	0.58	<0.01	0.02	<0.01	0.01	<0.01	0.01	
B3.1	2.63	1.96	16.27	66.51	0.09	1.53	2.59	0.33	0.04	3.64	94.44
	0.08	0.28	0.24	0.46	<0.01	0.01	0.01	0.01	<0.01	0.02	
B5.1	2.89	1.45	14.47	69.55	0.08	2.08	2.27	0.30	0.06	2.63	94.63
	0.21	0.08	0.20	0.50	<0.01	0.01	0.02	0.01	<0.01	0.01	
B6.1	2.18	2.36	14.73	67.16	0.12	1.72	4.22	0.38	0.04	3.15	94.92
	0.08	0.10	0.16	0.21	<0.01	0.01	<0.01	0.01	<0.01	0.02	
B8.1	3.24	1.32	14.85	69.84	0.07	2.09	2.02	0.26	0.06	2.67	95.27
	0.06	0.08	0.14	0.46	<0.01	0.01	0.01	0.01	<0.01	0.02	
B12.1	2.75	2.42	16.05	67.40	0.09	1.60	2.74	0.33	0.05	3.35	95.62
	0.11	0.12	0.15	0.48	<0.01	0.01	0.01	0.01	<0.01	0.01	
B17.1	3.36	1.37	14.80	69.70	0.07	1.94	2.16	0.27	0.06	2.71	95.30
	0.19	0.03	0.08	0.21	<0.01	0.01	0.02	0.02	<0.01	0.01	
B18.1	2.73	2.38	16.54	67.42	0.08	1.48	1.95	0.31	0.04	3.63	95.40
	0.17	0.07	0.16	0.03	<0.01	0.01	0.02	0.01	<0.01	0.01	
B20.1	3.13	1.99	14.63	69.63	0.09	1.93	2.58	0.35	0.06	2.97	96.19
	0.06	0.04	0.10	0.53	<0.01	0.01	0.01	0.01	<0.01	0.01	
B21.1	3.01	1.90	14.48	68.88	0.10	1.91	2.99	0.35	0.06	3.14	95.68
	0.19	0.05	0.03	0.33	0.01	0.01	0.01	<0.01	<0.01	0.01	
B24.1	3.12	1.53	14.79	69.96	0.07	1.96	2.52	0.26	0.06	2.67	95.78
	0.10	0.05	0.04	0.21	0.01	0.02	0.01	<0.01	<0.01	0.02	
B25.1	3.06	1.56	14.76	69.62	0.08	1.96	2.61	0.28	0.06	2.74	95.56
	0.06	0.05	0.07	1.15	<0.01	0.01	<0.01	0.01	<0.01	<0.01	
B26.1	2.96	2.15	15.57	68.46	0.08	1.72	2.12	0.33	0.05	3.27	95.57
	0.03	0.03	0.01	0.16	<0.01	0.02	0.02	0.01	<0.01	<0.01	
B27.1	3.33	1.67	14.83	68.70	0.07	1.84	2.99	0.24	0.05	2.81	95.37
	0.04	0.09	0.16	0.34	<0.01	0.02	0.01	0.01	<0.01	0.02	

Table 10 -- continued

	Na	Mg	Al	Si	P	K	Ca	Ti	Mn	Fe	Total
B1.2	2.51	2.04	15.61	68.15	0.09	1.91	3.05	0.34	0.05	3.30	95.90
	0.21	0.09	0.32	0.45	<0.01	0.01	0.02	0.01	<0.01	0.01	
B2.2	2.62	2.15	15.64	68.06	0.10	1.69	2.92	0.34	0.05	3.02	95.42
	0.17	0.11	0.31	0.71	<0.01	0.01	0.01	0.01	<0.01	0.01	
B3.2	2.62	2.15	15.93	67.95	0.09	1.69	2.57	0.32	0.05	3.24	95.46
	0.19	0.05	0.34	0.73	<0.01	0.01	0.01	<0.01	<0.01	<0.01	
B5.2	2.89	1.21	14.98	70.57	0.07	2.06	1.71	0.24	0.06	2.53	95.18
	0.25	0.07	0.23	0.70	<0.01	0.01	0.02	0.01	<0.01	0.01	
B6.2	1.84	2.40	16.14	64.90	0.12	1.86	3.69	0.43	0.05	3.78	94.07
	0.16	0.08	0.18	0.49	<0.01	0.01	0.02	<0.01	<0.01	0.01	
B8.2	3.10	1.36	14.93	69.71	0.07	2.06	1.99	0.28	0.06	2.67	95.09
	0.16	0.08	0.22	0.42	<0.01	0.01	0.01	0.01	<0.01	0.01	
B12.2	2.65	2.62	16.43	66.65	0.09	1.49	2.90	0.34	0.04	3.33	95.40
	0.20	0.09	0.22	0.30	<0.01	0.01	0.01	<0.01	<0.01	0.01	
B17.2	3.13	1.44	14.56	69.77	0.09	1.93	2.65	0.30	0.06	2.71	95.49
	0.12	0.07	0.18	0.55	<0.01	0.01	0.01	0.01	<0.01	0.01	
B18.2	2.79	2.05	15.76	68.44	0.07	1.63	1.86	0.28	0.05	3.43	95.21
	0.19	0.06	0.15	0.47	<0.01	0.01	0.01	0.01	<0.01	0.01	
B20.2	3.11	1.93	14.64	69.15	0.09	1.93	2.49	0.35	0.06	2.91	95.51
	0.19	0.03	0.17	0.26	<0.01	0.01	0.01	<0.01	<0.01	0.01	
B21.2	3.00	1.64	14.63	69.19	0.08	1.92	2.37	0.29	0.06	3.21	95.24
	0.15	0.05	0.03	0.20	<0.01	0.02	0.02	0.01	<0.01	0.01	
B24.2	3.01	1.54	14.88	69.68	0.06	1.90	2.61	0.25	0.05	2.77	95.60
	0.05	0.10	0.06	0.21	<0.01	0.02	0.02	<0.01	<0.01	0.01	
B25.2	2.93	1.66	14.68	69.47	0.08	1.94	2.55	0.29	0.06	3.02	95.51
	0.08	0.10	0.04	0.13	<0.01	0.01	0.04	<0.01	<0.01	0.01	
B26.2	2.91	2.10	15.55	68.51	0.09	1.76	2.03	0.34	0.05	3.30	95.48
	0.08	0.09	0.04	0.27	0.01	<0.01	0.01	0.01	<0.01	0.01	
B27.2	2.76	1.78	14.45	68.90	0.09	1.84	3.77	0.28	0.06	2.75	95.52
	0.21	0.04	0.02	0.32	0.01	0.02	0.01	<0.01	<0.01	0.01	

Table 10 -- continued

	Na	Mg	Al	Si	P	K	Ca	Ti	Mn	Fe	Total
C1	2.06	2.55	17.30	67.53	0.09	1.38	2.15	0.42	0.04	4.34	96.70
	0.18	0.04	0.42	0.67	<0.01	0.01	0.01	0.01	<0.01	0.02	
C2	2.13	2.59	17.73	68.02	0.08	1.17	1.63	0.40	0.03	4.35	96.96
	0.12	0.08	0.41	0.71	<0.01	0.01	0.02	<0.01	<0.01	0.01	
C3	2.23	2.62	16.84	68.72	0.08	1.07	1.44	0.42	0.03	4.31	96.59
	0.06	0.10	0.37	0.63	<0.01	0.01	0.01	0.01	<0.01	0.01	
C5	1.94	2.68	16.45	70.73	0.10	1.34	2.85	0.45	0.04	4.04	99.42
	0.14	0.12	0.42	0.53	<0.01	<0.01	0.02	0.01	<0.01	0.01	
C6	1.95	2.48	16.16	68.15	0.07	0.98	2.53	0.33	0.03	5.35	96.85
	0.16	0.07	0.32	0.84	0.01	0.01	0.02	0.01	<0.01	0.02	
C8	2.04	3.03	17.11	65.50	0.11	1.43	3.22	0.47	0.04	4.38	96.16
	0.06	0.04	0.28	0.71	<0.01	0.01	0.02	<0.01	<0.01	0.01	
C12	2.14	2.53	16.97	69.36	0.08	1.07	1.48	0.37	0.03	4.09	96.94
	0.16	0.05	0.24	0.44	<0.01	0.01	<0.01	0.06	<0.01	0.01	
C17	2.28	2.61	16.22	67.97	0.09	1.17	2.82	0.37	0.03	4.26	96.65
	0.15	0.04	0.26	0.64	<0.01	0.01	0.01	0.01	<0.01	0.01	
C18	2.27	2.98	16.95	66.12	0.10	1.33	2.57	0.47	0.04	4.38	96.06
	0.13	0.04	0.22	0.42	0.01	0.01	0.01	0.01	<0.01	0.01	
C20	2.34	3.33	17.28	66.00	0.09	0.98	3.15	0.37	0.03	4.13	96.54
	0.18	0.08	0.23	0.78	<0.01	0.01	0.01	0.01	<0.01	0.01	
C21	2.02	2.91	15.75	68.13	0.10	1.21	3.32	0.42	0.04	4.34	97.06
	0.15	0.12	0.20	0.63	<0.01	0.01	0.01	<0.01	<0.01	0.02	
C24	2.43	2.49	17.08	68.09	0.05	0.61	1.57	0.24	0.02	4.76	96.19
	0.20	0.08	0.20	0.60	0.01	<0.01	0.01	0.01	<0.01	0.01	
C25	2.36	2.94	16.42	67.99	0.06	0.77	2.48	0.29	0.02	4.17	96.34
	0.11	0.09	0.16	0.35	<0.01	0.01	0.02	<0.01	<0.01	0.01	
C26	2.18	3.06	17.00	66.08	0.09	1.25	2.55	0.44	0.04	4.37	95.91
	0.16	0.08	0.20	0.52	<0.01	0.01	0.01	0.01	<0.01	0.01	
C27	2.34	2.55	16.41	67.94	0.06	0.79	1.88	0.29	0.03	4.65	95.78
	0.09	0.12	0.23	0.28	0.01	0.01	0.01	0.01	<0.01	0.01	

Table 11. Trace Element Analysis, in parts per million, of the Sentinel Butte ash/bentonite. Sample description: A = Upper Bentonite, B = Middle Ash, C = Lower Bentonite.
a = PPM (average of 3 analysis)
b = standard deviation (PPM)

Sample		Cr	Co	Ni	Cu	Zn	Ga	Rb	Sr	Y	Zr	Nb	Ba	Pb
A1T	(a)	33	28	52	26	86	22	58	328	29	168	4	310	37
	(b)	3	3	1	0	1	0	0	4	1	1	1	16	1
A2T		29	30	53	24	96	24	50	341	26	176	3	392	46
		2	4	1	0	0	1	1	4	0	0	0	16	1
A3T		26	54	47	24	89	22	52	379	25	167	6	471	40
		2	6	1	1	1	0	0	4	1	2	1	33	0
A5T		21	32	48	23	90	23	47	283	24	169	2	288	43
		2	4	1	1	1	1	0	4	0	3	1	33	1
A6T		29	36	57	25	86	22	56	426	32	191	4	305	38
		4	3	1	1	2	0	1	6	0	1	1	35	1
A8T		50	43	63	32	99	23	76	338	30	154	7	439	34
		2	5	1	1	1	0	1	4	1	1	0	19	1
A12T		26	26	50	25	99	23	57	328	30	169	2	315	44
		2	2	1	1	4	1	1	1	1	1	0	27	1
A17T		46	34	62	30	96	23	65	341	27	163	6	451	38
		3	6	1	1	0	0	1	4	1	4	0	66	2
A18T		42	34	54	29	109	24	74	216	27	141	5	387	41
		5	5	2	1	3	0	1	3	1	2	1	25	2
A20T		17	26	47	22	85	23	46	324	26	169	0	317	50
		2	2	1	1	3	0	1	4	1	2	---	22	1
A21T		16	30	44	22	96	24	41	307	26	175	0	259	50
		1	5	0	0	1	0	1	1	1	1	---	9	0
A24T		21	31	40	23	92	23	49	294	28	169	1	257	43
		3	4	0	1	2	0	1	3	1	1	1	1	1
A25T		21	33	48	24	90	23	46	316	27	183	1	287	47
		1	5	1	1	2	0	0	1	0	0	0	1	1
A26T		35	31	49	28	105	25	66	234	27	156	3	363	47
		2	4	2	1	3	1	1	1	1	0	1	13	2
A27T		21	34	44	22	88	22	50	277	27	161	0	225	41
		3	4	2	1	2	1	1	1	1	1	---	17	0

Table 11 -- continued

Sample	Cr	Co	Ni	Cu	Zn	Ga	Rb	Sr	Y	Zr	Nb	Ba	Pb
B1.0T	24	25	56	23	81	23	97	461	22	157	12	836	56
	3	1	1	0	1	0	0	2	0	0	1	4	0
B2.0T	23	39	50	23	89	24	113	413	25	143	10	710	52
	3	2	1	0	2	1	0	6	1	1	1	41	0
B3.0T	18	41	54	23	84	23	101	434	28	157	7	590	51
	1	4	1	0	2	0	1	2	1	3	0	16	1
B5.0T	12	20	53	21	80	24	139	427	24	135	11	793	64
	1	3	1	1	1	1	1	1	1	1	1	25	1
B6.0T	22	40	54	21	78	22	107	455	26	155	8	668	53
	4	1	1	0	1	0	0	5	1	1	0	23	0
B8.0T	15	29	54	22	88	24	124	423	24	142	10	742	57
	1	2	0	0	1	1	2	3	1	2	0	25	1
B12.0T	22	29	51	23	96	24	98	419	27	164	7	572	52
	0	0	1	1	2	0	1	1	0	1	1	4	1
B17.0T	20	22	51	20	74	23	117	426	24	146	11	741	56
	5	1	0	1	1	1	0	2	0	1	0	11	1
B18.0T	25	34	55	26	100	25	102	353	25	148	7	597	53
	1	1	1	1	1	0	0	2	1	0	0	21	1
B20.0T	32	40	68	24	87	23	109	440	27	166	10	672	53
	1	1	1	0	1	0	1	1	1	2	1	32	1
B21.0T	17	26	54	22	77	23	131	413	25	149	10	731	59
	0	0	1	1	1	0	1	0	1	1	1	6	1
B24.0T	6	20	47	19	75	23	125	432	21	137	11	851	63
	1	1	3	0	5	1	1	2	1	0	1	1	1
B25.0T	15	24	52	21	75	23	118	438	25	145	11	719	53
	1	2	1	0	2	1	0	2	0	2	1	16	0
B26.0T	23	37	62	25	101	24	120	401	28	150	8	571	53
	4	1	0	0	2	0	1	2	1	1	1	66	2
B27.0T	7	22	47	18	68	22	128	496	29	151	8	667	59
	1	0	1	0	1	0	1	1	0	0	1	11	1

Table 11 -- continued

Sample	Cr	Co	Ni	Cu	Zn	Ga	Rb	Sr	Y	Zr	Nb	Ba	Pb
B1.1T	26 1	28 1	48 1	25 1	104 1	24 0	110 1	386 5	28 1	149 2	8 1	580 32	48 0
B2.1T	20 0	28 1	45 0	22 0	88 2	23 0	102 0	420 2	26 0	162 1	8 0	633 13	51 0
B3.1T	20 2	34 1	41 1	23 1	98 1	24 0	96 1	396 3	28 2	162 2	7 0	545 26	50 1
B5.1T	17 2	34 4	53 1	21 0	86 0	24 1	131 2	425 1	25 0	141 0	10 0	741 7	59 1
B6.1T	29 1	31 4	50 0	23 1	78 1	22 0	98 1	466 1	30 1	204 1	9 1	562 18	45 1
B8.1T	12 0	30 1	50 1	20 0	79 0	23 0	135 1	411 4	24 1	130 2	11 0	757 5	59 1
B12.1T	21 1	30 1	51 2	22 0	91 1	24 1	103 1	432 1	28 1	162 2	8 1	608 15	54 1
B17.1T	14 0	27 3	54 1	20 1	78 2	23 0	129 0	441 1	25 1	141 2	10 0	753 21	60 1
B18.1T	16 4	38 2	54 1	22 0	105 0	25 0	104 1	411 1	28 1	157 2	4 1	532 33	55 1
B20.1T	29 2	32 1	59 1	24 0	88 4	24 1	117 0	419 4	26 1	156 1	12 1	739 30	54 0
B21.1T	26 3	32 1	55 4	23 0	85 4	23 1	116 1	402 4	27 1	160 3	11 1	662 29	49 0
B24.1T	9 4	24 4	46 0	19 1	77 1	23 1	130 1	429 0	27 2	151 1	9 0	673 21	59 1
B25.1T	12 3	28 2	47 2	21 1	79 0	23 0	124 0	420 1	24 0	142 3	10 1	710 8	57 1
B26.1T	21 2	43 0	61 2	23 1	111 1	25 0	119 1	393 5	27 0	152 1	7 0	608 13	55 1
B27.1T	8 1	22 1	44 1	18 1	75 1	22 0	121 1	420 2	26 1	145 1	7 0	664 100	57 1

Table 11 -- continued

Sample	Cr	Co	Ni	Cu	Zn	Ga	Rb	Sr	Y	Zr	Nb	Ba	Pb
B1.2T	23	27	53	24	86	23	118	409	28	144	10	648	50
	3	1	0	1	0	0	1	5	1	4	1	52	1
B2.2T	22	30	46	23	93	24	106	420	26	163	8	634	54
	3	1	2	0	4	0	0	2	1	3	1	45	0
B3.2T	20	31	52	22	85	23	108	416	27	153	9	647	54
	1	1	1	0	1	0	1	2	0	5	1	49	1
B5.2T	11	26	48	19	87	24	143	421	23	128	11	808	63
	2	1	1	0	0	0	0	2	1	4	1	40	1
B6.2T	44	41	59	28	103	24	95	422	22	138	13	863	48
	0	3	1	1	1	0	1	1	2	6	0	40	1
B8.2T	12	57	50	21	90	24	133	397	24	130	11	753	59
	1	4	1	1	2	0	1	1	1	4	1	30	0
B12.2T	20	36	48	23	95	24	97	412	29	164	7	528	51
	1	2	1	1	1	0	1	2	2	4	1	51	0
B17.2T	20	25	47	20	78	23	123	436	25	153	11	725	56
	5	2	1	0	1	0	1	1	1	2	1	20	1
B18.2T	13	31	52	21	95	24	117	385	25	142	6	612	56
	5	0	1	1	1	0	1	2	1	2	0	10	1
B20.2T	27	32	58	23	88	23	122	424	26	156	13	770	55
	2	4	1	0	1	0	1	1	0	1	1	8	1
B21.2T	19	29	52	21	80	23	129	428	25	145	11	733	55
	1	1	0	0	1	1	1	1	1	2	1	20	0
B24.2T	5	25	48	18	75	23	128	441	25	147	9	710	60
	2	2	1	0	2	1	0	3	1	5	1	59	1
B25.2T	12	23	50	20	78	23	122	422	23	138	12	760	54
	1	1	1	0	3	1	1	1	1	1	0	54	1
B26.2T	22	35	65	23	98	24	122	382	27	145	8	656	54
	2	1	1	0	4	0	0	1	1	3	0	30	1
B27.2T	9	23	44	18	73	22	115	423	26	152	10	646	53
	1	1	1	0	0	0	1	2	1	3	0	23	1

Table 11 -- continued

Sample	Cr	Co	Ni	Cu	Zn	Ga	Rb	Sr	Y	Zr	Nb	Ba	Pb
C1T	40	34	46	28	112	25	71	301	27	140	4	401	44
	3	1	1	1	4	0	0	1	0	1	1	19	0
C2T	37	43	53	28	114	25	60	330	23	142	3	455	46
	3	5	1	1	2	0	1	1	0	1	0	10	1
C3T	33	36	53	30	119	26	58	327	26	152	2	389	46
	1	2	1	0	3	1	1	5	1	6	1	69	1
C5T	37	33	57	29	112	25	67	306	28	141	5	442	45
	3	2	2	1	3	0	0	4	1	1	1	25	0
C6T	23	42	51	22	75	21	48	286	21	133	4	373	36
	1	3	1	0	1	1	1	2	1	2	1	11	1
C8T	41	31	49	29	119	25	71	310	30	158	5	391	40
	3	2	2	1	3	0	0	2	1	2	1	31	1
C12T	32	27	46	29	108	27	59	311	23	141	4	495	49
	3	5	3	1	5	2	1	1	1	4	0	42	1
C17T	29	36	55	24	96	26	60	304	23	151	3	423	43
	2	6	3	1	2	5	1	1	1	3	0	36	1
C20T	26	27	53	24	99	24	57	346	31	182	1	274	44
	2	3	2	0	2	0	1	2	1	0	0	4	1
C21T	32	34	53	26	116	24	60	271	27	148	4	356	40
	2	1	2	1	4	0	1	4	1	2	0	47	2
C24T	7	34	40	18	75	22	38	257	20	157	0	249	43
	1	3	2	1	2	1	0	4	0	2	---	18	1
C25T	10	29	42	21	83	22	49	280	27	168	0	156	44
	3	1	3	0	2	1	1	6	0	2	---	33	1
C26T	30	36	46	28	109	24	67	329	31	164	2	311	42
	1	3	3	1	1	0	1	1	0	4	0	27	1
C27T	15	32	45	21	82	22	50	287	24	158	1	261	41
	1	4	2	1	2	0	1	1	1	3	1	28	0

Table 12. Trace element analysis of the grab samples; concentrations are in PPM

Sample	Cr	Co	Ni	Cu	Zn	Ga	Rb	Sr	Y	Zr	Nb	Ba	Pb
RD-1	42	52	55	26	92	21	49	263	21	148	4	358	29
RD-2	61	46	67	37	113	24	69	381	19	147	10	721	34
PL-1	37	32	47	35	108	24	60	454	29	178	1	318	34
PL-2	44	47	53	29	101	22	66	356	26	154	0	343	40
OP-1	29	29	57	34	103	25	59	289	21	145	5	418	29
LB-8	83	65	63	41	197	30	143	202	20	111	13	859	38
R-6	20	42	47	22	77	20	39	274	20	169	1	294	34
A-1	34	40	55	25	86	22	45	295	22	165	2	330	39
SM-1	99	56	45	48	219	31	122	321	17	97	16	1059	40
C-6	26	50	51	32	111	24	53	266	12	149	4	650	50
WG-1	30	41	48	24	87	22	50	233	19	142	4	395	36
WM-1	23	44	50	23	82	21	46	217	23	153	2	267	33
LX-1	120	66	49	53	238	34	123	301	9	63	22	1453	44
BR-1	27	33	23	29	149	28	50	248	26	345	14	603	40
SR-6	49	50	55	32	113	23	70	316	26	145	7	472	34

APPENDIX E

DISCRIMINANT SCORES FROM THE MAJOR AND TRACE ELEMENT GROUPS

Table 13. Summary of major element discriminant analysis from samples plotted in Figure 15. Abbreviations: upper = upper bentonite, lower = lower bentonite, ash = middle ash

	upper vs ash	lower vs ash	upper vs lower
Element	Percent Contribution		
Na_2O	-1.95	17.85	5.89
MgO	-14.36	-68.16	37.65
Al_2O_3	-16.33	5.16	25.18
SiO_2	-1.47	1.54	4.10
P_2O_5	-1.90	4.61	63.46
K_2O	66.89	128.67	1.90
CaO	0.43	-6.10	-32.45
TiO_2	6.44	40.92	-5.22
MnO	-2.93	-9.25	0.51
Fe_2O_3	65.18	-15.25	-1.03

Summary of trace element discriminant analysis from samples plotted in Figures 13, and 14.

	upper vs ash	lower vs ash	upper vs lower
Element	Percent Contribution		
Cr	13.74	28.44	
Co	-5.78	5.08	
Ni	19.28	36.67	
Cu	24.40	-9.44	
Zn	37.39	44.69	
Ga	11.28	-9.76	
S	-0.30	4.31	
Rb	125.39	88.47	20.38
Sr	7.48	30.55	-21.01
Y	9.23	2.87	22.70
Zr	-22.15	-2.57	97.05
Nb	-62.48	18.11	0.91
Ba	63.67	-20.53	-22.37
Pb	-21.14	-16.89	2.35

Table 14. Summary of the major element discriminant analysis from the three analyzed ash samples

	B1.0 vs. B1.1	B1.0 vs. B1.2	B1.1 vs. B1.2
Element	Percent Contribution		
Na_2O	-6.34	65.51	56.48
MgO	4.16	13.09	-1.02
Al_2O_3	12.30	6.58	5.96
SiO_2	1.93	7.79	10.09
P_2O_5	26.35	14.80	3.45
K_2O	0.33	-8.36	-2.20
CaO	1.13	1.20	-2.06
TiO_2	0.00	-1.27	0.66
MnO	60.25	1.52	28.80
Fe_2O_3	-0.11	-0.87	-0.16

Summary of the trace element discriminant analysis from the three analyzed ash samples

	B1.0 vs. B1.1	B1.0 vs. B1.2	B1.1 vs. B1.2
Element	Percent Contribution		
Cr	-0.82	-0.98	0.35
Co	-0.03	0.05	20.93
Ni	25.64	17.37	20.57
Cu	23.50	26.62	5.16
Zn	47.84	54.24	22.56
Ga	-3.09	-5.29	2.10
S	6.96	7.99	20.33
Rb	2.53	20.44	-19.29
Sr	48.58	39.18	1.47
Y	92.83	1.31	62.96
Zr	34.45	1.92	42.48
Nb	40.80	22.03	104.55
Ba	-135.68	-0.15	-101.44
Pb	16.49	15.27	9.27

Table 15. Summary of the trace element discriminant analysis of trace element groups TR1 and TR2, and the grab samples plotted in Figure 20

	TR1 upper vs. grab	TR1 lower vs. grab
Element	Percent Contribution	
Cr	-63.51	-16.51
Co	42.82	53.04
Ni	-0.17	-4.70
Cu	135.80	109.89
Zn	47.05	-32.98
Ga	-61.99	-8.74

	TR2 grab vs. upper	TR2 grab vs. lower
Element	Percent Contribution	
Rb	-1.77	0.35
Sr	9.17	2.25
Y	-36.88	-22.98
Zr	0.00	25.79
Nb	-166.23	-157.05
Ba	255.63	206.03
Pb	40.08	45.60

APPENDIX F

ROTATED FACTOR LOADINGS FROM THE TRACE ELEMENT GROUP

Table 16. Summary of rotated factor loadings for the major, and trace, elements plotted in Figures 18, 19, and 22

Rotated Factor loadings from the major element group

Element	Factor 1	Factor 2
Na_2O	0.785	-0.306
MgO	-0.913	0.270
Al_2O_3	-0.784	-0.202
SiO_2	0.587	-0.424
P_2O_5	0.148	0.944
K_2O	0.915	0.180
CaO	0.134	0.835
TiO_2	-0.377	0.726
MnO	0.768	0.263
Fe_2O_3	-0.916	0.106

Rotated factor loadings from the trace element groups TR1, and TR2

Element	Factor 1	Factor 2
Cr	-0.090	0.941
Co	-0.223	0.430
Ni	0.550	0.514
Cu	-0.124	0.961
Zn	-0.241	0.857
Ga	0.159	0.623
Rb	0.938	-0.196
Sr	0.816	-0.258
Y	-0.208	0.415
Zr	-0.573	-0.044
Nb	0.955	-0.076
Ba	0.973	-0.158
Pb	0.752	-0.451

Table 16 -- continued

Rotated factor loadings from the combined trace element group, and the grab samples

Element	Factor 1	Factor 2
Cr	0.948	0.029
Co	0.785	-0.188
Ni	0.044	0.308
Cu	0.937	-0.008
Zn	0.934	0.045
Ga	0.798	0.250
Rb	0.181	0.927
Sr	-0.385	0.763
Y	-0.615	-0.114
Zr	-0.427	-0.357
Nb	0.518	0.745
Ba	0.547	0.803
Pb	-0.383	0.783

REFERENCES CITED

Abbott, P. L., and Smith, T. E., 1978, Trace-element composition of clasts in Eocene conglomerates, southern California and northwestern Mexico: Journal of Geology, v. 86, p. 753-762.

Andermann, G., and Kemp, J. W., 1958, Scattered x-rays as internal standards in x-ray emission spectroscopy: Analytical Chemistry, v. 30, p. 1306-1309.

Benson, W. E., 1954, Geology of the Knife River area, North Dakota: U.S. Geological Survey Open-file report, 323 p.

Bertin, E. P., 1975, Principles and practices of x-ray spectrometric analysis: New York, London, Plenum Press, 1079 p.

Blatt, Harvey, Middleton, G. V., and Murray, R. C., 1980, Origin of sedimentary rocks 2nd ed: San Francisco, Prentice Hall, 782 p.

Bluemle, J. P., 1977, Surface geology of North Dakota: North Dakota Geological Survey Miscellaneous Map 18, scale 1:2,500,000.

Borchardt, G. A., Harward, M. E., and Schmitt, R. A., 1971, Correlation of volcanic ash deposits by activation analysis of glass separates: Quaternary Research, v. 1, p. 247-260.

Bowles, F. A., Jack, R. N., and Carmichael, I. S. E., 1973, Investigation of deep-sea volcanic ash layers from equatorial Pacific cores: Geological Society of America Bulletin, v. 84, p. 2371-2388.

Brekke, D. W., 1979, Mineralogy and chemistry of clay-rich sediments in the contact zone of the Bullion Creek and Sentinel Butte Formations (Paleocene), Billings County, North Dakota: University of North Dakota Masters Thesis, 94 p.

Brown, R. W., 1948, Correlation of Sentinel Butte Shale in western North Dakota: American Association of Petroleum Geologists Bulletin, v. 32, p. 1265-1274.

Carlson, C. G., 1985, Geology of McKenzie County, North Dakota: North Dakota Geological Survey Bulletin 80, part 1, 48 p.

Clark, M. B., 1966, The stratigraphy of the Sperati Point quadrangle, McKenzie County, North Dakota: University of North Dakota, Masters Thesis, 108 p.

Criss, J. W., and Birks, L. S., 1968, Calculation methods for fluorescent x-ray spectrometry - empirical coefficients vs. fundamental parameters, Analytical Chemistry, v. 40, p. 1080-1086.

Davis, J. C., 1973, Statistics and data analysis in geology: New York, John Wiley and Sons, 550 p.

Fisher, S. P., 1953, Geology of west-central Mckenzie County North Dakota: North Dakota Geological Survey Report of Investigation 11, 2 sheets.

Floyd, P. A., and Winchester, J. A., 1978, Identification and discrimination of altered and metamorphosed volcanic rocks using imobile elements: Chemical Geology, v. 21, p. 291-306.

Forsman, N. F., 1982, A volcanic airfall marker bed in the Upper Fort Union Formation (Paleocene) of western North Dakota: Saskatchewan Geological Society Special Publication 6, p. 323-325.

-------, 1984, Durability and alteration of some Cretaceous and Paleocene pyroclastic glasses in North Dakota: Journal of Non-Crystalline Solids, v. 67, p. 449-461.

-------, 1985, Petrology of the Sentinel Butte Formation (Paleocene) North Dakota: University of North Dakota PhD. dissertation, 222p.

Forsman, N. F., and Karner, F.R., 1975, Preliminary evidence for the volcanic origin of bentonite in the Sentinel Butte Formation, North Dakota (abstract): North Dakota Academy of Science Proceedings, v. 29, pt. 1, p. 10.

Grim, R. E., 1953, Clay mineralogy: in Shrock, R. R., ed., New York, McGraw - Hill, 384 p.

Hahn, G. A., Rose, W. I., Jr., and Meyers, T., 1979, Geochemical correlation of genetically related rhyolitic ash-flow and air-fall ashes, central and western Guatemala and the equatorial Pacific: in Chapin, C. E., and Eleston, W. E. eds., Ash-flow tuffs: Geological Society of America Special Paper 180, p. 101-112.

Hanson, B. M., 1955, Geology of the Elkhorn Ranch area, Billings and Golden Valley Counties, North Dakota: North Dakota Geological Survey Report of Investigation 18, 1 plate.

Howorth, R., and Rankin, P. C., 1975, Multi-element characterization of glass shards from stratigraphically correlated rhyolitic tephra units: Chemical Geology, v. 15, p. 239-250.

Huff, W. D., 1983, Correlation of Middle Ordovician K-bentonites based on chemical fingerprinting: Journal of Geology, v. 91, p. 657-669.

Izett, G. A., Wilcox, R. E., Powers, H. A.,and Desborough, G. A., 1970, The Bishop Ash Bed, a Pleistocene marker bed in the western United States: Quaternary Research, v., p. 121-132.

Jack, R. N., and Carmichael, S. E., 1968, The chemical "fingerprinting" of acid volcanic rocks: California Division of Mines Special Report 100, p. 17-31.

Jacob, A. F., 1975, Criteria for differentiating the Tongue River and Sentinel Butte Formations (Paleocene), North Dakota: North Dakota Geological Survey Report of Investigation 53, 55 p.

Jacob, A. F., 1976, Geology of the Upper part of the Fort Union Group (Paleocene), Williston Basin, with reference to uranium: North Dakota Geological Survey Report of Investigation 58, 49 p.

Krumbein, W. C., and Graybill, F. A., 1965, An introduction to statistical models in geology: New York, N.Y., McGraw - Hill, 475 p.

Laird, W. M., 1956, Geology of the North Unit of Theodore Roosevelt National Park: North Dakota Geological Survey Bulletin, v. 23, p. 53-77.

Leake, B. E., Hendry, G. L., Kemp, A., Plant, A. G., Harrey, P. K., Wilson, J. R., Coats, J. S., Aucott, J. W., Lunel, T., and Howarth, R. J., 1968, The chemical analysis of rock powders by automatic x-ray fluorescence: in Chemical Geology, Amsterdam, Elsevier Pub. p. 7-86.

Leonard, A. G., 1908, The geology of southwestern North Dakota with special reference to coal: North Dakota Geological Survey Fifth Biennial Report, p. 29-114.

Leonard A. G., and Smith, C. D., 1909, The Sentinel Butte lignite field, North Dakota and Montana: United States Geological Survey Bulletin 341, p. 15-35.

Linares, J., Huertes, F., Lachica, M., and Reyes, E., 1973, Geochemistry of trace elements during the genesis of colored bentonites: Proceedings of the International Clay Conference, Madrid, 1972, p. 351-360.

Lindsey, D. A., 1975, The effect of sedimentation and diagenesis on trace element composition of water-laid tuff in the Keg Mountain area, Utah: U.S. Geological Survey Professional Paper 818-C, 35 p.

Lowe, D. J., 1986, Controls on the rates of weathering and clay mineral genesis in airfall tephras: a review and New Zealand case study: in Coleman, S. M., ed., Rates of Chemical Weathering of rocks and Minerals: Academic Press, p. 265 - 320.

Mack, M., and Speilberg, N., 1958, Statistical factors in x - ray intensity measurements: Spectrochemica Acta, v. 12, p. 169 - 178.

Martz, A. M., and Brown, F. H., 1981, Chemistry and mineralogy of some Plio-Pleistocene tuffs from the Shungra Formation, southwest Ethiopia: Quaternary Research, v. 16, p. 240 - 257.

Meldahl, E. G., 1956, The geology of the Grassy Butte area, Mckenzie County, North Dakota: North Dakota Geological Survey Report of Investigation 26, 1 sheet.

Metzger, C. F., 1969, Preliminary investigation of North Dakota bentonites for use in taconite production (abstract): North Dakota Academy of Science Proceedings, v. 21, p. 213-214.

Nesemeier, B. D., 1981, Stratigraphy and sedimentology of the Sentinel Butte Formation (Paleocene) near Lost Bridge, Dunn County, west-central North Dakota: University of North Dakota, Masters Thesis, 67 p.

Norrish K., and Hutton, J. T., 1969, An accurate x-ray spectrographic method for the analysis of a wide range of geologic samples: Geochemica et Cosmochimica Acta, v. 32, p. 431-453.

Randle, K., Goles, G. G., and Kittleman, L. R., 1971, Geochemical and petrological characterization of ash samples from Cascade Range volcanoes: Quaternary Research, v. 1, p. 261-282.

Richardson, D., and Ninkovich, D., 1976, The use of K_2O, Rb, Zr, and Y versus SiO_2 in volcanic ash layers of the eastern Mediterranean to trace their source: Geological Survey of America Bulletin, v. 87, p. 110-116.

Royse, C. F., Jr., 1967a, A stratigraphic and sedimentologic analysis of the Tongue River and Sentinel Butte Formations (Paleocene), Western North Dakota: unpublished PhD. dissertation, 312 p.

-------, 1967b, Tongue River - Sentinel Butte contact: North Dakota Geological Survey, Report of Investigation 45, 53 p.

-------, 1970, A sedimentologic analysis of the Tongue - River Sentinel Butte interval (Paleocene) of western North Dakota: Sedimentary Geology, v. 4, p. 19-80.

-------, 1972, The Tongue River and Sentinel Butte Formations (Paleocene) of western North Dakota: a review, in Ting, F. T. C., ed., Depositional environments of the lignite-bearing strata in western North Dakota, North Dakota Geological Survey Miscellaneous Series 50, p. 31-42.

Sarna-Wojcicki, A. M., Bowman, H. W., and Russel, P. C., 1979, Chemical correlation of some Late Cenozoic tuffs of northern and central California by neutron activation analysis of glass and comparison with x-ray fluorescence analysis: U.S. Geological Survey Professional Paper 1147, p. 1-15.

Schmid, R., 1981, Descriptive nomenclature and classification of pyroclastic deposits and fragments: Recommendations of the IUGS Subcommission on the systematics of igneous rocks: Geology, v. 9, p. 41-43.

Smith, R. E., and Nash, W. P., 1976, Chemical correlation of volcanic ash deposits in the Salt Lake Group, Utah, Idaho, and Nevada: Journal of Sedimentary Petrology, v. 46, p. 930-939.

Smith - Pope, R. A., 1975, Geochemistry of volcanic ash in the Salt Lake Group, Bonneville Basin, Utah, Idaho, and Nevada: University of Utah, Masters Thesis, 93 p.

Steiner, M. A., 1978, Petrology of sandstones from the Bullion Creek and Sentinel Butte Formations (Paleocene), Little Missouri Badlands, North Dakota: University of North Dakota Masters Thesis, 53 p.

Taggart, J. E., Lichte, F. E., and Walberg, J. S., 1981, Methods of analysis of samples using x-ray fluorescence and induction - coupled plasma spectroscopy, in Lipman, P. W., and Mullineaux, D. R., eds., The 1980 eruptions of Mount St. Helens, Washington: U.S. Geological Survey Professional Paper 1250, p. 683-687.

Taylor, J. K., 1985, Standard Reference Materials: Handbook for SRM users: National Bureau of Standards Special Publication 260 - 100, 85 p.

Tertian, R., and Claisse, F., 1982, Principles of quantitative x - ray fluorescence analysis: London, Heyden and Son Ltd., 385 p.

Wedephol, K. H., 1969, Handbook of Geochemistry: Berlin, Springer - Verlag, 442 p.

Williams, H., Turner, F. J., and Gilbert, C. M., 1982, Petrography: An introduction to the study of rocks in thin sections: San Fransisco, Freeman, 406 p.

Zielinski, R. A., 1985, Element mobility during alteration of a silicic ash to kaolinite - A study of tonstien: Sedimentology, v. 32, p. 567 -579.